

CSA GROUP™

STANDARDS RESEARCH

Galvanic Corrosion in Steel and Aluminum Bridges

November 2022

Authors

Jieying Zhang, Ph.D., P.Eng., National Research Council Canada

Nafiseh Ebrahimi, Ph.D., P.Eng., National Research Council Canada

Project Advisory Panel

Kris Mermigas, **MASc., P.Eng.,** Ministry of Transportation of Ontario

Paul King, **M.S., P.Eng.,** Rapid-Span Group

Scott Walbridge, **Ph.D., P.Eng.,** University of Waterloo

Sylvie Boulanger, **Ph.D.,** MTB Consulting

Jennifer Teague, **Ph.D.,** CSA Group

Mark Braiter, **B.Eng.,** MBA, CSA Group

Acknowledgments

The authors acknowledge the teamwork at NRC Construction Research Centre, especially Dr. Olga Naboka and Mr. B. Baldock for the experimental work. The authors appreciate the experimental support of the Surface Science Center of Western University, especially Ms. Katarina Albrechtas for conducting experiments and Dr. Sridhar Ramamurthy and Dr. Jamie Noel for technical exchanges. The authors are thankful to Mr. Éric Lévesque at Canam Ponts Canada Inc. for supplying materials, and Mr. Adam Macdonald at MTO and AMG Metals Inc. for supplying aluminum plates.

Financial Support

This research received support, in part, from the NRC's Climate Resilient Built Environment (CRBE) initiative funded by Infrastructure Canada.

Disclaimer

This work has been produced and is owned by the National Research Council Canada. It is designed to provide general information in regards to the subject matter covered. The views expressed in this publication are those of the authors. National Research Council Canada and Canadian Standards Association are not responsible for any loss or damage which might occur as a result of your reliance on, or use of, the content in this publication.
This report may not be reproduced in whole or in part without the written consent of the National Research Council Canada.

Copyright

©His Majesty the King in Right of Canada, as represented by the National Research Council Canada.

Table of Contents

Executive Summary 5

1 Introduction 6

1.1 Cost of Highway Bridge Corrosion 6

1.2 Galvanic Corrosion of Steel Bridges 7

2 Review of Galvanic Corrosion 7

2.1 Galvanic Corrosion Mechanism 7

2.1.1 Galvanic Corrosion Tendency and Rate 7

2.1.2 Galvanic Corrosion Series and Governing Factors 9

2.2 Galvanic Corrosion in Various Industries 10

2.2.1 Transportation 10

2.2.2 Piping Systems 11

2.2.3 Electronics, Batteries and Biomedical Implants 12

2.3 Galvanic Corrosion and Prevention in Bridge Design 13

2.3.1 Galvanic Corrosion Problem and Current Studies 13

2.3.2 AASHTO Guide Specification for Service Design of Highway Bridges 14

2.3.3 CSA S6:19, Canadian Highway Bridge Design Code 14

2.3.4 NASEM Guide Specification for Service Life Design of Highway Bridges 14

2.3.5 FHWA Steel Bridge Design Handbook for Corrosion Protection of Steel Bridges 15

2.3.6 European Design Guide for Use of Weathering Steel in Bridge Construction 15

2.4 Summary 15

3 Methods 16

3.1 Corrosion and Electrochemical cells 17

3.2 Measurement of Open-circuit Potential 18

3.3 Measurement of Linear Polarization Resistance 18

3.4 Potentiodynamic Polarization Experiment 19

3.5 Measurement of Galvanic Corrosion Current 19

3.6 Analysis of Microstructure Using Microscopy 20

3.7 Salt Spray Testing 20

4 Results 21
4.1 Open-circuit Potential 21
4.1.1 OCP and Effect of NaCl Concentration: Within Alloy Comparison 21
4.1.2 OCP in 1.5 wt% NaCl solution 25
4.1.3 Stainless Steel Washers 25
4.1.4 Patina Formation on Weathering Steel 25
4.2 Galvanic Corrosion Current 26
4.2.1 Validation of Measurement Setup 27
4.2.2 Galvanic Current of Coupling Structural Alloy/Bolt 27
4.3 Additional Corrosion Information and Visual Observation 30
4.3.1 LPR for Corrosion Resistance 30
4.3.2 PDP for Pitting Tendency 30
4.3.3 Microscopy Analysis 31
4.3.4 Bolted Plates in Salt Spray Test 33
5 Discussion 34
5.1 Development of Galvanic Series and Corrosion Tendency 34
5.2 Assessment of Galvanic Corrosion Rate 37
5.3 Galvanic Corrosion Assessment Process 40
5.4 Galvanic Corrosion Risk Mitigation 42
5.5 Application of This Study 42
6 Summary and Future Research Needs 43
6.1 Summary of Development 43
6.2 Application and Future Need 45
References 47
Appendix A Corrosion Damage Forms 53
Appendix B OCP Graphs in Various Salt Concentrations 55
Appendix C PDP Graphs in 1.5 wt.% NaCl solution 63

Executive Summary

Galvanic corrosion is one of the most prevalent corrosion problems of modern times, where dissimilar metals and alloys are routinely used in industrial applications. This report focuses on galvanic corrosion in bridge applications through a literature review, a comprehensive experimental study, advanced analysis, and the development of an evaluation tool, a guiding procedure, and a set of galvanic corrosion criteria. It aims to provide information and resources to bridge engineers to conduct a better assessment on galvanic corrosion in bridge design and management.

A galvanic series was developed that provides a systematic collection and comparison of the corrosion tendencies of bridge alloys. It has demonstrated that a significant galvanic corrosion tendency warrants attention, but also revealed that a seemly low tendency could lead to substantial galvanic corrosion between two actively corroding metals. These findings support the need of a method for further evaluation: a measurement of galvanic corrosion rate that assesses how fast the anodic alloy loses its mass. A set of criteria to interpret the magnitude of galvanic corrosion risk was established by considering both galvanic corrosion rate, and a new concept of a ratio that takes account of the galvanic corrosion rate in the context of a general corrosion rate (Gal/Corr), providing a consistent assessment for the alloys studied in this project. These advancements subsequently enabled the development of a three-step guiding procedure for assessing galvanic corrosion.

The experimental design and results provided the foundation on which 11 bridge alloys were studied by using quantitative electrochemical techniques, microstructural analysis, and visual inspection of samples tested in a salt-spray chamber. The results also support corrosion-mechanism-based mitigation strategies by countering the necessary conditions for galvanic corrosion to occur and considering the key factors that influence its magnitude; that is, how the assembly and configuration affect the cathode/anode surface area ratio and how an environment affects corrosivity. Another important finding was that the galvanic corrosion rate is not only governed by the driving force (potential difference) but also by individual corrosion behaviours of metals. Two actively corroding metals (e.g., weathering steel and a carbon steel bolt in a chloride-laden environment), despite having similar corrosion potentials, were found to produce a galvanic corrosion rate much higher than two less active metals having very different corrosion potentials (e.g., aluminum and stainless steel bolt).

While effectively comparing the galvanic corrosion resistance of paired bridge alloys, galvanic corrosion is clearly shown to be materials-environment-configuration specific. For example, the galvanic corrosion rate of A325 Type I carbon steel bolt coupled with weathering steel was found to be high in chloride-laden environments; however, it would be expected to be low in a chloride-free environment. In the future, developing a better understanding of the corrosion performance of bridge metals and alloys, and systematically examining them in a manner similar to their mechanical properties is recommended. This applies particularly to aluminum bridges. Although aluminum's corrosion potential indicates a high corrosion tendency, its actual corrosion rate can be low due to the protection from the corrosion products of aluminum oxides. It would be also beneficial to establish information about the individual corrosion properties of bridge alloys as a part of the alloys' complete characterization, including their interactions with exposure conditions, concerning especially weathering steel since its corrosion behaviour in chloride-laden environments is not fully understood. There is also a need to further develop risk assessment criteria to interpret galvanic corrosion. This study represents an initial effort based on existing data, an experimental study, and a newly developed concept of the Gal/Corr ratio that has put the evaluation of galvanic corrosion in a new perspective and will hopefully spur interest and promote further discussion and research.



"A 2019 Canadian Infrastructure Report Card indicates that 40% of bridges are in fair or poor condition primarily due to corrosion damage"

1 Introduction

Galvanic corrosion, a fundamental form of corrosion, is one of the most prevalent corrosion problems of modern times. Dissimilar metals and alloys are routinely used together in industrial applications, and thus extensive knowledge has been accumulated for many industrial alloys such as those used in the aerospace and automotive sectors. In the bridge community, galvanic corrosion principles have been applied, but only empirically and implicitly due to a lack of systematic information, knowledge, tools, guides, standards, and codes for mitigation and protection, particularly for high-strength bolts that transfer the critical loads of steel and aluminum bridge girders. Therefore, there is a need to improve the durability design of metallic bridges against galvanic corrosion.

1.1 Cost of Highway Bridge Corrosion

The 2002 U.S. Federal Highway Administration (FHWA) study, *Corrosion Costs and Preventive Strategies in the United States,* is a widely cited and influential benchmark document on the costs and control of corrosion [1]. It reveals an annual direct corrosion cost of about $276 billion – equivalent to approximately 3.1% of the U.S. Gross Domestic Product (GDP). A follow-up study by the National Association of Corrosion Engineers (NACE International[1]) updated the global cost to 3.4% of a country's GDP [2]. Contributing to the total corrosion cost is the annual direct cost of corrosion of highway bridges in the U.S., estimated at $8.3 billion and consisting of $3.8 billion to replace structurally deficient bridges over ten years. Canada's total direct annual cost of corrosion is estimated to be $51.9 billion, amounting to 2.98 percent of Canada's 2019 GDP [3]. The age profile of bridges in the US and Canada is similar, but Canada has a more corrosive environment due to the heavy use of de-icing salts on roads.

A 2019 Canadian Infrastructure Report Card indicates that 40% of bridges are in fair or poor condition primarily due to corrosion damage [4]. Atmospheric corrosion is the primary cause of steel bridge durability concerns. However, in all the modern engineering structures that frequently use mixed materials, other sources of corrosion risk can shorten this service life considerably.

The current corrosion protection design of bridges in Canada is prescribed by CSA S6:19, *Canadian Highway Bridge Design Code* (CHBDC) [5]. It provides a general description of exposure classes that are used to guide corrosion protection (i.e., whether to use a coating/metalizing system or weathering steel). However, it does not include a predictive function of corrosion performance over time, thus does not inform on alternative corrosion protection measures, such as using a thickness allowance to compensate for the corrosion loss over the long term.

1 NACE International is now a part of the Association for Materials Protection and Performance (AMPP).

1.2 Galvanic Corrosion of Steel Bridges

Although atmospheric corrosion has been studied globally and the resulting knowledge has been well implemented into steel bridge design, other forms of corrosion may raise durability concerns and cause damage to steel bridge components. In steel bridge construction, like in other modern engineering structures that routinely use mixed metals, the coupling of dissimilar metals introduces the risk of galvanic corrosion provided three conditions are met:

- they are in electrical contact;
- they are exposed to the same electrolyte; and
- their corrosion potential difference is more than 50 mV [6].

Galvanic corrosion can be of particular concern for steel bridge girders and fasteners. After installation, a steel bridge girder and its connection bolts are in direct electrical contact and exposed to the same electrolyte resulting from rain, melting ice and snow, or a thin water film from air condensation. Therefore, steel bridge girders and connection bolts of different metals can form a galvanic corrosion cell where the component with a more negative corrosion potential becomes the anode and corrodes preferentially [7]. High-strength bolts carry tension, shear, or both, and pre-tension may be present depending on the type and purpose of the connection [8]. Considering their relatively small diameter and critical load-bearing function, protecting the bolts from corrosion and cross-section loss is a significant part of high-strength bolt design.

2 Review of Galvanic Corrosion

This section presents a mechanistic introduction of galvanic corrosion, a review of its study and prevention in various industries, and the current state of practice in bridge durability design including what exists in codes, specifications and guidelines for its prevention. It aims to answer the following questions:

1. What is the mechanism of galvanic corrosion that needs to be addressed by the tools/methods/guides for risk identification?
2. What are the main factors of galvanic corrosion that need to be addressed in the development of prevention methods?
3. How do various industries study and manage galvanic corrosion risk?
4. What is the status of galvanic corrosion risk management in the bridge design community?
5. What needs to be done to prevent galvanic corrosion risk in steel and aluminum bridge assemblies?

2.1 Galvanic Corrosion Mechanism

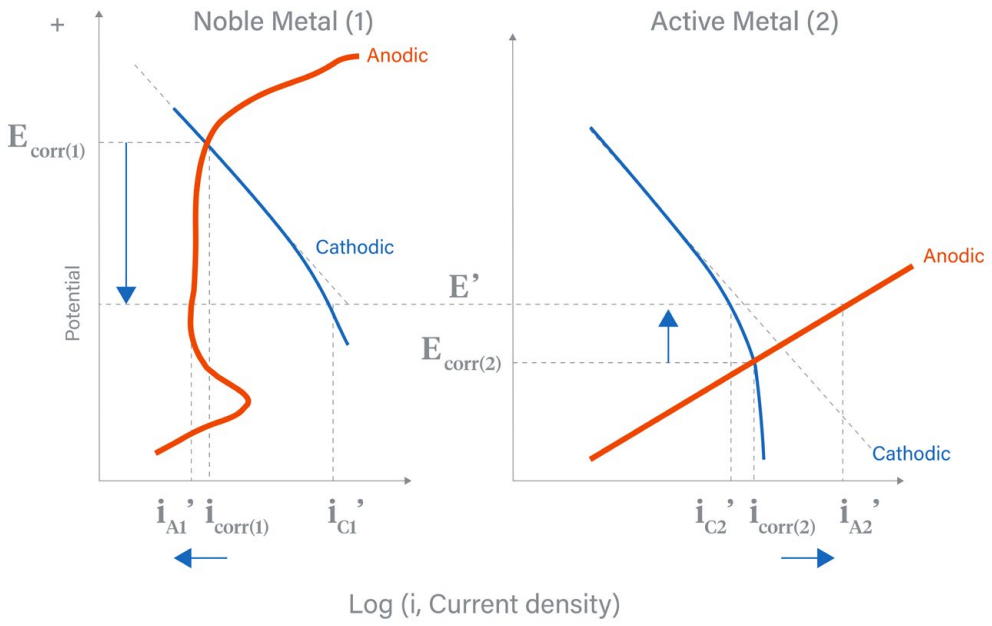
Galvanic corrosion is also often referred to as contact corrosion or bimetallic corrosion, for which three components are needed [7]. To make a galvanic corrosion cell, a metal/alloy and a less noble[2] metal/alloy are connected and immersed in an electrically conductive electrolyte such as a salt solution. It produces a current flowing between the two metals, which makes the less noble one dissolve/corrode faster, while the more noble metal is protected.

2.1.1 Galvanic Corrosion Tendency and Rate

The driving force for galvanic corrosion is the free corrosion potential (E_{corr}) difference between two metals. Figure 1 illustrates how this driving force works through the polarization curves when the two metals are electrically connected (or put in direct contact), showing the relationship of potential and corrosion current for the oxidation and reduction reactions. Starting from their respective free corrosion potential (E_{corr}) and corrosion rate (i_{corr}), the noble metal (electrode 1) has a much more positive potential ($E_{corr(1)}$) than that of the active metal ($E_{corr(2)}$) (electrode 2). When connected, they will shift towards a common potential (E').

2 The nobility of a metal relates to its resistance to corrosion. Thus, the more noble a metal is, the more resistant it is to corrosion.

Figure 1: Illustration of a galvanic corrosion cell formed between a noble metal (1) and an active metal (2): i = current density, A = anodic reaction, and C = cathodic reaction. Reproduced with permission from National Research Council Canada.



The two metals are polarized when the potential is changed; the active metal (2) is anodically polarized to a more positive potential E′ than its original E_{corr}; and the noble metal (1) is cathodically polarized to a more negative E′ than its E_{corr}. Their potential changes then induce changes in the oxidation and reduction reaction rates on both metals. Accordingly, the anodic reaction (metal dissolution) rate on the active metal (2) is increased from $i_{corr(2)}$ (the corrosion current before coupling) to i_{A2}', and its cathodic reaction rate is decreased from $i_{corr(2)}$ to i_{C2}'. The opposite occurs in the noble metal; its anodic dissolution is reduced from $i_{corr(1)}$ to i_{A1}'. and the cathodic reaction rate increases from $i_{corr(1)}$ to i_{C1}'.

The two-electrode system will have a new equilibrium at E′, and the currents from these reactions will follow the conservation of mass:

$$i_{C1}' + i_{C2}' = i_{A1}' + i_{A2}' \qquad (1)$$

In this process, the electrons are transferred from one electrode (anode) to the other (cathode), producing an electrical current flow in terms of the galvanic corrosion current i_{couple}:

$$i_{couple} = i_{C1}' - i_{A1}' = i_{A2}' - i_{C2}' \qquad (2)$$

The above representation in equations 1 and 2 assumes the electrolyte resistance is negligible, which is often the case in galvanic corrosion between bridge steel and its fasteners, or between two metal components immersed in rainwater or a condensation film with contaminants. In such a case, the two metals will reach the same potential E′.

Galvanic corrosion also co-exists with other forms of corrosion (see Appendix A), which can be referred to as general corrosion. Equation 2 and Figure 1 show three metal dissolving rates of the anodic metal before and after the formation of the galvanic corrosion cell:

- before galvanic corrosion, the general corrosion rate is i_{corr};
- with galvanic corrosion, the galvanic corrosion rate is i_{couple}, which can be measured externally;
- with galvanic corrosion, the total corrosion rate of the active metal is i_{A2}', which is higher than $i_{corr(2)}$, indicating corrosion acceleration by galvanic corrosion. This value can be slightly or significantly higher than i_{couple} depending on how much the metal is polarized from its original corrosion state.

Overall, a corrosion potential measurement can help to assess galvanic corrosion tendency, and a galvanic corrosion current measurement represents a quantitative method to assess the galvanic corrosion rate. Both are fundamental methods used to study galvanic corrosion and evaluate its risk in many engineering fields. Furthermore, galvanic corrosion co-exists with other corrosion forms, underscoring that a thorough understanding of corrosion risk is needed beyond just the galvanic corrosion for critical structures and components.

2.1.2 Galvanic Corrosion Series and Governing Factors

A galvanic series is an arrangement of metals and alloys in accordance with their actual and measured free corrosion potential in a given environment [9]. A galvanic series is typically presented for a seawater environment in corrosion engineering handbooks, and an example of a galvanic series in seawater is shown in Figure 2, which includes common construction metals and alloys. The relationships in the galvanic series can be a very useful guide for choosing metals to couple together. By consulting the series, material selection can be made so that metals with a minimal tendency to undergo a galvanic reaction are chosen.

Generally, metals located further apart within the series are most likely to undergo galvanic corrosion, which could lead to a high corrosion rate when combined.

In addition to their potential difference, many factors can play a role in the magnitude of galvanic corrosion between two coupled metals [9]:

Free Corrosion Potentials

The E_{corr} of coupled metals determines the intrinsic polarity of a galvanic couple (i.e., which is the anode and which is the cathode). Still, the extent of galvanic activity is not always related to the E_{corr} difference. For example, the galvanic corrosion of zinc (Zn) is higher when coupled with steel than with many other alloys such as nickel (Ni), copper (Cu), and titanium (Ti), although the potential difference between Zn and steel is much less than between Zn and Ni, Cu, or Ti [11]. In atmospheric galvanic corrosion, other factors such as reaction kinetics and the formation of corrosion products can also be essential in determining the galvanic corrosion rate. When the cathodic reaction is oxygen-diffusion limited, different galvanic corrosion rates of an anode can be explained by the oxygen diffusion rates through the oxide films. When diffusion is not the limiting process, the galvanic corrosion rate results from differences in the cathodic efficiency of oxygen reduction in the oxide scale on the cathode surface [12].

Figure 2: Galvanic series based on the data from LaQue [10]



Effect of Surface Area

The effect of the surface area of two coupled metals, often in terms of a cathodic to anodic area ratio, on galvanic corrosion depends on the type of control in the system. If the galvanic system is under cathodic control, variation in the anode area will have little effect on the total corrosion rate, but changes in the cathodic surface area would have a significant impact [9]. The opposite happens when the system is under anodic control [9]. The literature indicates that galvanic corrosion of zinc is mainly cathodically controlled [13].

Effect of Surface Condition

The surface of a metal in contact with an electrolyte is generally not "bare" but is covered with a surface layer. This can be an adsorption layer but is more often a solid film on the surface [9]. A corrosion product film may act as a physical barrier between the metal surface and the environment [9]. Oxide films often exhibit potentials that are very different from the base metals, and they determine the electrode position in a galvanic series [9]. Some stainless steel materials, such as SS316 in the galvanic series, demonstrate two distinct ranges of E_{corr}, with less noble values coming from the crevice corrosion that can occur with some surfaces and solutions.

Effect of Solution

Different electrolytes or solutions can create different potentials for a metal surface [9]. The conductivity of the electrolyte is an essential factor because it determines the distribution of galvanic corrosion across the anode surface. When conductivity is high, as in seawater, the galvanic corrosion of the anodic metal is distributed more uniformly across the surface [13].

Atmospheric Environment

Galvanic corrosion commonly occurs when building and structural materials are exposed to indoor and outdoor atmospheric environments [9]. Galvanic corrosion under atmospheric conditions is usually restricted to a narrow region of the anode metal near the bimetallic junction because of the high resistance of a thin-layer electrolyte formed by rain and water condensation. However, galvanic corrosion is most significant in saline environments, such as in a marine atmosphere or on bridges in Canada where de-icing salts are heavily used, because of the high conductivity of electrolytes in the presence of salts [9].

Galvanic corrosion can be costly. If materials with a good chance of forming a galvanic couple are used, corrosion damage will occur more rapidly. However, galvanic corrosion is preventable, and some basic rules can be followed to limit or prevent it from happening altogether. Galvanic corrosion can be mitigated by:

- avoiding contact between materials that have significant potential differences;
- making sure the area of the cathode is smaller than that of the anode;
- using cathodic protection, such as that provided by a sacrificial anode like zinc; or,
- using coatings that prevent the metals from coming into electrical contact [14].

2.2 Galvanic Corrosion in Various Industries

The widespread use of dissimilar metal combinations in modern industrial applications, including automobiles, aircraft, buildings and infrastructure, pipelines, electronics, batteries, and biomedical implants, has made galvanic corrosion a persistent and critical issue in corrosion engineering.

2.2.1 Transportation

Metals such as aluminum and magnesium are replacing low-carbon steel and cast iron in modern-day automobiles because the use of these materials dramatically reduces the weight of vehicles, thereby improving fuel efficiency [15]–[18]. Vehicles can be made of diverse metallic materials, such as aluminum engine blocks and suspension parts, steel car bodies, and aluminum dashboard poles [15]. This mixed metal model is also often used to make boats and aircraft as well, where titanium, copper, brass, stainless steel, carbon steel, and aluminum alloys are used in combination, and are consequently at risk of galvanic corrosion [19]–[21].

Galvanic corrosion of magnesium alloys coupled with other alloys, such as steel, is of particular interest

to the automotive and aircraft industries [22]–[25]. Their low density is ideal for weight reduction, and their mechanical and electrical properties are the main reasons for their wide use. Galvanic corrosion is, however, an ongoing concern as these alloys are routinely used in assemblies with steel components such as fasteners despite magnesium's low electrical potential in the galvanic corrosion series. This makes the magnesium alloys corrode preferentially when in electrical contact with other alloys such as steel.

Past studies have examined galvanic corrosion mechanisms to determine suitable fasteners for magnesium alloys [22]. Other studies, however, have also been published on how microstructure and alloy compositions correlate with the tendency and severity of galvanic corrosion occurrence [25]. These findings provide insight into the galvanic corrosion mechanism and, particularly, what needs to be considered in material development for steel bridge applications.

While galvanic corrosion can be assessed from basic principles and the corrosion properties of the coupled metals, galvanic corrosion testing is required to understand the in-situ risk, which may be higher than what is estimated based on uncoupled characteristics of the metals [25]. The need for a fast and reliable testing method is also essential because the cathodic alloy can influence galvanic corrosion of the anodic alloy [25]. Experiments have shown that steel was a poor cathode choice for magnesium while aluminum was the least damaging, and a greater distance between the cathode and anode reduced galvanic corrosion rate [23]. This implies that the surface of structural steel that is further away from the fasteners may contribute less to galvanic corrosion than the material immediately surrounding the fasteners.

Galvanic corrosion testing is an important consideration for steel bridge design; however, advanced tools and methods can also help improve the prediction of material performance for galvanic couples and to minimize corrosion damage under atmospheric conditions [26]. Data obtained from in-lab tests have been used as a guide for selecting corrosion-resistant materials and research has examined the use of electrochemical techniques to determine the galvanic series specific to materials used to make different types of cars, aircraft, and boats. Research techniques also include computational modelling [20] and salt spray tests [27].

Although using multiple materials in the design and construction of vehicles puts them at risk for galvanic corrosion, it is being successfully employed more and more. This is because galvanic corrosion prevention methods are also employed to limit unnecessary corrosion. Corrosion prevention methods include using e-coatings, organic coatings or other types of films to coat car body materials, which prevent them from coming into electrical contact with the dissimilar metals to which they are attached [28]–[31]. Another common galvanic corrosion prevention technique applied specifically in boats is using sacrificial anodes, which are commonly made out of zinc, aluminum or nickel [19]. An electrochemical technique that can be used to prevent galvanic corrosion is the anodization of the materials to form an insulating oxide film, which acts as a barrier to prevent a galvanic couple from forming [32].

2.2.2 Piping Systems

Corrosion damage due to dissimilar metals being in electrical contact is a pervasive problem in piping systems, and this is made worse by the extreme conditions to which the pipes are often exposed, such as drastic changes in solution pH, moving water, and high-salinity groundwater [33], [34]. In fact, galvanic corrosion is one of the primary forms of corrosion that leads to the degradation of pipes and represents a significant cause of nuisance or toxic substances such as iron or lead[3] entering drinking water supplies [35]-[39].

The risk of lead entering water supplies is not the only concern caused by the galvanic corrosion of piping systems. Galvanic corrosion can cause environmental disasters such as human waste and oil spills [40]–[42]. Corrosion damage also affects indoor piping systems. In a case examined by Shahin et al., a fire hydrant pipe failed for the second time due to galvanic corrosion

3 While lead pipes are now banned, it was common practice to fit copper pipes with lead connections when replacing old lead pipes, leading to subsequent galvanic corrosion at the connection site [35], [36].



"While galvanic corrosion can be assessed from basic principles and the corrosion properties of the coupled metals, galvanic corrosion testing is required to understand the in-situ risk, which may be higher than what is estimated based on uncoupled characteristics of the metals."

[43]. There can even be galvanic corrosion issues between the metal pipes and the oxide layers of the pipes. Song et al. studied galvanic coupling between carbon steel pipes and magnetite [44]. Magnetite is normally a protective oxide film, but the authors found that the rate of corrosion of these pipes increased because of the coupling interactions between magnetite and carbon steel [44].

Various prevention methods exist and are being developed to improve the safety and longevity of these multi-metal pipe systems. One of these is silicate-based inhibitor systems. This involves adding a silicon layer to the pipe to prevent it from coming into electrical contact with other metals in the system [39]. Other pipe corrosion prevention and detection techniques include periodic inspection and replacement of piping systems, cathodic protection [45], and barrier coatings [46]. All these techniques have been extensively tested and proven effective against galvanic corrosion. These corrosion prevention methods allow the selective use of mixed piping systems while minimizing costly repairs or dangerous failures [46].

2.2.3 Electronics, Batteries and Biomedical Implants

Electronics and lithium-based batteries can suffer reduced lifespan due to galvanic corrosion. Often, ultra-thin lithium foils are prepared on a copper substrate, and a metal-metal contact area is generated. The combination of these two metals in the presence of an electrolyte can lead to galvanic corrosion [47], [48]. Different ways of avoiding galvanic corrosion within batteries and electronics include using inorganic and organic corrosion inhibitors and coatings that prevent electrical contact between the dissimilar metals [49].

Galvanic corrosion is also a challenge for those developing medical implants as they are commonly made of mixed metal components consisting of stainless steel, nickel, and titanium alloys. Many studies have focused on how the environments within the human body impact the coupling of different implant alloys. For example, researchers have examined the corrosion of titanium and nickel alloys in dental implants using electrochemical techniques in environments that simulate the exposure conditions to help prevent premature failure [50]-[52].

Case studies have also been published on the early failure of medical implants that likely occurred due to galvanic corrosion [53], [54]. For example, a case showed that a knee replacement failed and required replacement after only seven years because of the galvanic corrosion of a titanium screw [53]. These studies demonstrate that galvanic corrosion between titanium and stainless steel is a real concern for medical implants. Using electrochemical and surface analysis techniques to observe corrosion processes between various types of metals used in implants is one approach to identifying whether metals might be at risk of failure due to galvanic corrosion when used together.

2.3 Galvanic Corrosion and Prevention in Bridge Design

2.3.1 Galvanic Corrosion Problem and Current Studies

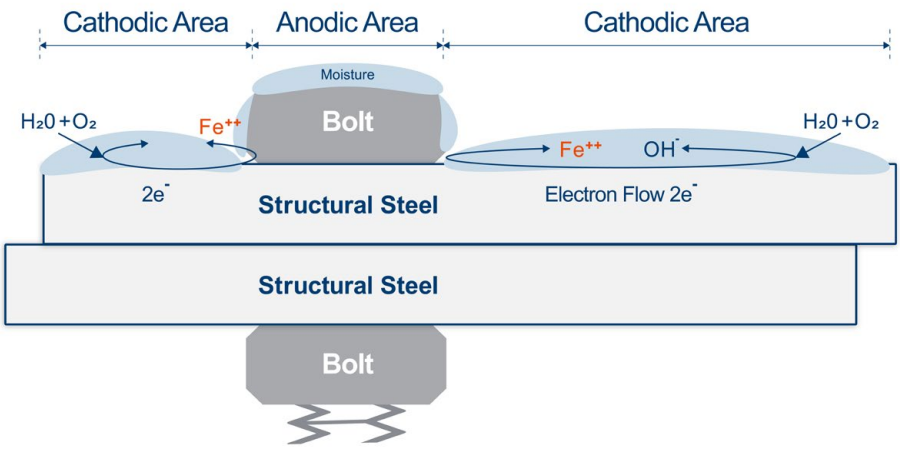
Corrosion by itself in steel and aluminum bridge assemblies is a prevalent and challenging problem. In the design of bridge components, corrosion is often considered in relation to the exposure environment. This environment can be concrete (pH of 12.5 and above), atmosphere, or immersed environments like soil, tidal, or marine settings [55]. Given this, the primary protection approach has been to isolate bridge metals and alloys from their environments, for example, by using a coating that can help eliminate one of the necessary conditions for corrosion to occur. Still, in many situations, the effectiveness of this strategy depends on the applicability, quality control, and degradation rate of the coating. It is important to fully understand the necessary conditions of different corrosion forms and to develop protection strategies to help eliminate them. Fontana and Green conducted a preliminary assessment of corrosion mechanisms in bridge applications (Appendix A), with galvanic corrosion being one of the corrosion forms [55].

As discussed in Section 2.1, galvanic corrosion can happen in all exposure conditions that involve a conductive electrolyte. In bridge applications, the most recognized occurrence of galvanic corrosion is seen between steel girders and their fasteners, which are often made from different alloys, or between two dissimilar metal plates in direct contact. Galvanic corrosion is found commonly on steel bridges where secondary structural components, such as handrails, aluminum light poles, or electrical conduits are in contact with steel, as well as on steel where mill-scale is exposed [56].

Often, engineering experience is relied upon for choosing proper bolt materials in the context of galvanic corrosion, in part because galvanic corrosion mechanism-based guidelines do not exist for steel or aluminum bridge design. Recent studies on the galvanic corrosion of steel bridges were initiated by constructing ASTM A1010 stainless steel bridges [57]-[62]. Figure 3 illustrates a galvanic corrosion cell that is formed between a steel plate and a bolt, where the galvanic corrosion cell is formed with the bolt serving as the anode and the steel plate serving as the cathode.

A previous study [60] demonstrated the need to directly measure the galvanic corrosion current to understand the galvanic corrosion rate between two metals and thus the mass loss rate of the anode. Salt spray methods have also been used in other studies to demonstrate that it can be difficult to identify corrosion risk using some type of metals in the absence of experimental methods [59].

Figure 3: A schematic of galvanic corrosion cell of steel girder and bolt. Reproduced with permission from National Research Council Canada.



2.3.2 AASHTO Guide Specification for Service Design of Highway Bridges

The American Association of State Highway and Transportation Official's (AASHTO) *Guide Specification for Service Life Design of Highway Bridges* identifies corrosion protection of steel bridges to be the most critical precaution to ensuring that the bridge service life is achieved [63]. However, only two options are offered for a corrosion protection plan: apply a protective coating system or use uncoated weathering steel.

The guide states that corrosion protection must start with an understanding of the available protection rather than with a comprehensive understanding of corrosion mechanisms of steel bridges and their components. Galvanic corrosion is not mentioned in this guide, nor is galvanic corrosion protection in accordance with the galvanic corrosion mechanism.

2.3.3 CSA S6:19, Canadian Highway Bridge Design Code

The CHBDC prescribes the corrosion protection requirements of steel bridges in different exposure conditions to the superstructure and other components [5]. This represents a sophisticated approach by acknowledging that the deterioration mechanism of corrosion is specific to the material and the environment. Three major exposure conditions are classified by the quantity of chlorides and pollutants in the atmosphere: no direct chloride, airborne chlorides or light industrial atmosphere, and heavy industrial atmosphere. Each condition includes three sub-conditions as well as a "marine" condition, to account for different moisture conditions. This guidance, however, relates to the protection of superstructure components against general corrosion rather than specific corrosion mechanisms such as galvanic corrosion. For example, the corrosion protection it prescribes includes primarily coating, metalizing, galvanizing, or using more corrosion-resistant weathering steel.

The CHBDC Commentary presents a more comprehensive discussion of five corrosion mechanisms associated with steel bridge corrosion, including galvanic corrosion [64]. While not all factors that determine galvanic corrosion rate are discussed, the effect of the cathode/anode area ratio on corrosion rate is explained in detail, as is the effect of distance between the anodic and cathodic areas.

The CHBDC's Commentary also offers detailed corrosion mechanisms and key factors. It is a good starting point for developing corrosion-performance-based protection guidelines. Further guidance to help design against galvanic corrosion is needed, including:

- a galvanic series for common steel and aluminum bridge alloys to assess the galvanic corrosion tendency; and
- a rapid and reliable method or process that quantifies the galvanic corrosion rate.

2.3.4 NASEM Guide Specification for Service Life Design of Highway Bridges

The development of this guide in support of a new AASHTO *Guide Specification for Service Life Design of Highway Bridges* provided a thorough review on steel bridge corrosion protection by coatings from multiple international standards, guides, international bridge design codes, and bridge design manuals [65].

Compared to the detailed documentation on the corrosion of concrete structures, the corrosion of steel bridges was covered to a much lesser extent, and the report included a simple discussion on coatings and detailing such as drainage. The corrosion mechanisms of steel components were not addressed, nor was galvanic corrosion mentioned in the report. The survey results from bridge engineers, however, have clearly identified corrosion as the most common problem regarding the durability of steel superstructures and steel foundation bridges and the second-most indicated durability problem for steel bearings.

It highlights the current practice in bridge design where corrosion of steel bridges is seen as a general durability issue, and that applying a coating or metalizing or using a particular steel type is expected to mitigate against all corrosion forms. A corrosion design guide of steel and aluminum bridges would provide better guidance based on corrosion-form-specific mechanisms.

2.3.5 FHWA Steel Bridge Design Handbook for Corrosion Protection of Steel Bridges

Compared to its previous version in 2012, the 2015 version of the FHWA's *Steel Bridge Design Handbook for Corrosion Protection of Steel Bridges* has made significant progress in at least two areas [66]:

1. Introducing the quantitative classification of environmental corrosivity, based on ISO 9223 [67], to improve the definition of the corrosion environment. This is important for the corrosion of weathering steels and the durability of the protective coatings.
2. Introducing the concept of galvanic corrosion that has arisen from the construction of more corrosion-resistant steel girders using A1010 steel.

The report recommends that the fasteners be more resistant to corrosion than the girder materials to avoid a large cathode/anode area ratio. However, the report does not provide information on evaluating corrosion resistance and quantifying the galvanic corrosion tendency and rate.

2.3.6 European Design Guide for Use of Weathering Steel in Bridge Construction

A recent guiding document developed by European Convention for Constructional Steelwork (ECCS) considers a number of European codes and standards to provide guidance for the durable and reliable use of weathering steel in bridges and other structures [68]. For corrosion considerations, it starts by classifying the exposure environments to the weathering steel using ISO 9223 [67]. It identifies that inland corrosion in Europe can be typically categorized as low corrosivity (C2 category of ISO 9223) or, in cases of exceptional pollution, medium corrosivity (C3). The corrosivity categories in coastal areas of Europe range between medium and very high (C3 to C5). Weathering steel is suggested to be unsuitable in the very high corrosivity category (C5) as well as in marine and marine/industrial environments (CX) without additional corrosion protection.

The guide also introduces a new concept of corrosion load, in analogy to mechanical loads, that the protection should be designed to resist. With the corrosion load being defined using the ISO 9223 atmospheric corrosivity, corrosion protection is addressed through a loss of thickness allowance over a target design life. Loss of thickness allowances are provided for five countries (Belgium, Germany, UK, France, and Spain) over a 100-year design life.

In addition to designing according to the corrosion load of the environment, the guide also considers corrosion protection structural detailing and connections in the construction of weathering steel bridges. The galvanic corrosion risk of bolting materials that connect weathering steel girders is considered, for which it states that:

1. Hot-dip galvanized bolting assemblies can be used to connect weathering steel with a zinc layer thick enough to withstand the galvanic corrosion attack before the protective patina is formed.
2. Preloaded bolting assemblies made of stainless steel can be used without galvanic corrosion risk.

The use of preloaded bolting assemblies made of stainless steel may need further examination. The use of stainless steel fasteners can lead to corrosion because some types of stainless steel bolts/washers are prone to pitting corrosion [60]. This reinforces the need for guidelines that consider alloy corrosion behaviors in bridge applications. This would not only be helpful in the evaluation of galvanic corrosion risk, but is also essential to capture the risks from other forms of corrosion.

2.4 Summary

In summary, this section has helped to answer the following questions:

1. What is the mechanism of galvanic corrosion that needs to be addressed by tools/methods/guides for steel bridges?

The potential difference between two metals drives the galvanic corrosion current, leading to accelerated corrosion of the anodic metal. Thus, measurement of corrosion potential will help to assess galvanic corrosion tendency, and the measurement of galvanic corrosion current represents a quantitative method to assess galvanic corrosion rate. Both are fundamental methods that are used to study galvanic corrosion and evaluate its risk in many engineering fields. Further,

galvanic corrosion co-exists with other corrosion forms, therefore a complete consideration of corrosion risk is needed beyond the galvanic corrosion risk for critical structures and components.

2. What are the main factors of galvanic corrosion that need to be addressed in the development of prevention methods?

A galvanic series is an arrangement of metals and alloys which are commonly used in practice in accordance with their actual and measured free corrosion potential in a given environment. It is often developed in seawater and presented in corrosion engineering handbooks. It is a very useful guide for choosing metals to join with a minimal tendency to undergo a galvanic reaction. Beside the potential difference, many factors play a role in the magnitude of galvanic corrosion between two coupled metals, including the surface area, surface condition, solution, and atmospheric environment, because they affect the galvanic corrosion kinetics in terms of its corrosion rate. Prevention methods should be developed by mitigating the effects of these governing factors.

3. How do various industries study galvanic corrosion to manage galvanic corrosion risk?

Galvanic corrosion is prevalent in automobiles, aircraft, pipelines, electronics, batteries, and biomedical implants. The two methods universally used for assessing galvanic corrosion rate in these applications are the corrosion potential (or a galvanic series) and galvanic corrosion current measurements. Computer modelling and surface science can assist in further understanding these mechanisms. The galvanic corrosion prevention methods used in these applications are derived from the fundamental galvanic corrosion mechanisms (e.g., the use of a coating that prevents electrical contact between dissimilar metals).

4. What is the status of galvanic corrosion risk management in the bridge design community?

The bridge community has recognized corrosion as the most common problem for the durability of steel superstructures and steel foundation bridges. Among the codes and guides reviewed, the CHBDC provides an environmental exposure-specific protection guide and the ECCS offers a quantitative approach for corrosion thickness allowances for weathering steel design under different environmental exposures. Despite these documents recognizing that corrosion is a material-environment-specific deterioration mechanism, the corrosion protection of steel bridges is most commonly addressed by applying a coating, metalizing, or using a particular steel type, without considering the specific mechanisms of different corrosion forms such as galvanic corrosion. The lack of corrosion-mechanism-specific design guidance may prevent adequate protection against various forms of corrosion.

5. What needs to be done to prevent galvanic corrosion in steel and aluminum bridge assemblies?

There is an acute need to establish guidelines that consider bridge alloy corrosion behavior for their application in bridges. A corrosion-based design component for steel and aluminum bridges would provide better guidance if based on the specific corrosion form at play. This would be helpful to assist in the evaluation of galvanic corrosion but would also be essential to capture the risks from other forms of corrosion.

The current study aims to develop guidance for galvanic corrosion in bridge design and management, addressing the following current gaps in knowledge:

- Identification of the galvanic corrosion risk between two bridge alloys. This can be accomplished by measuring corrosion potential or through the galvanic series of common bridge metals and alloys.
- Quantification of galvanic corrosion rate. This can be accomplished through the measurement of galvanic corrosion current.

3 Methods

The following experiments were conducted at the NRC Construction Corrosion Lab, and some replicate measurements were performed in a laboratory of Western University following the same procedure, using the same materials and corrosion cell setup under NRC supervision. The results observed at both laboratories were consistent and in agreement.

3.1 Corrosion and Electrochemical cells

Table 1 lists the 11 alloys considered in this study along with their specifications, including four bridge structural alloys, five bolt alloys, and two additional washer alloys. The alloys were machined into electrodes (corrosion samples) from carbon steel (CS, 350W), weathering steel (WS, 350AT), A1010 stainless steel (SS), carbon steel bolt (A325 Type I), galvanized steel (GS) bolt (A325 Type I galvanized), weathering steel bolt (A490 Type 3), B8M stainless steel bolt, B8SH stainless steel bolt, SS316L washer, and SS410 washer.

The alloys were used to build corrosion cells. A corrosion cell consists of a working electrode(s) (alloy sample under study), a reference electrode (RE) (saturated Calomel electrode, SCE), a counter electrode (CE) (platinum), and an electrolyte (solution) that represents the corrosion environment (Figure 4).

Each corrosion sample (electrode) had a 3-62 threaded hole in the back, where a metal rod was attached for the electrical connection with the corrosion or electrochemical cells. Before mounting the samples in epoxy, the face without the threading was ground to P1200 finish using silicon carbide (SiC) paper. Next, the electrodes were mounted in a Hysol® clear epoxy resin that was purged under vacuum. This was done to remove bubbles in the epoxy that may cause corrosion at the interface of epoxy and the sample, such as crevice corrosion. Once the metal samples were mounted, only a surface area of either 1 cm^2 or 10 cm^2 was exposed for the corrosion measurement.

Table 1: Alloys and their specifications used in this study.

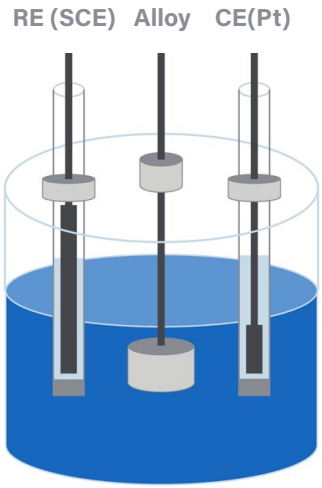
Number	Bridge structural alloy	Specification
1	Carbon steel, 350W	CSA G40.21-18 grade 350W [69] ASTM A572/A572M-12 Grade 50 [70]
2	Weathering steel, 350AT	CSA G40.21-18 Grade 350AT [69]
3	ASTM A1010, A1010	ASTM A1010-19 [71] ASTM A709/A709M-21 Grade 50 CR [72]
4	Aluminum, Al	Al 6061-T6 grade ASTM B209M/B209M-21a [73]
	Bolt alloy	**Specification**
5	Carbon steel bolt, A325 Type 1	ASTM F3125/F3125M-22 Grades A325 Type 1 [74]
6	Galvanized steel bolt, A325 Type 1 Galvanized	ASTM F3125/F3125M-22 Grades A325 Type 1-Galvanized [74]
7	Weathering steel bolt*, A490 Type 3	ASTM F3125 F3125/F3125M-22 Grades A490 Type 3 [74]
8	Stainless steel (SS) B8M bolt, SS316	ASTM A320/A320M-22 B8M (SS316), Class 2 [75]
9	Stainless steel B8SH bolt, SS304	ASTM A320/A320M-22 B8 (SS304) Class 2 [75]
	Additional stainless steel washers	**Specification**
10	Stainless steel washer, SS316L	ASTM A194/A194M-22 Grade 8M (SS316L) [76]
11	Stainless steel washer, SS410	ASTM A194/A194M-22 Grade 8 (SS410) [76]

*A490 Type 3 is rarely used in bridges in Canada. This type is added as a weathering steel bolt in this corrosion study.
A490 Type 3 and A325 Type 3 are both weathering steel of different strengths but similar chemical compositions under ASTM F3125.

Before each test, the electrode was ground to a P2500 finish, sonicated with methanol, rinsed with ultrapure water, and dried with argon gas. The electrode was then set up in a corrosion cell quickly to avoid the formation of oxides on the alloy surface from air exposure. The galvanized steel sample was not ground to keep the zinc layer intact.

Three solutions were prepared at different salt (NaCl) concentrations. All solutions were prepared with ASTM Type I water (ASTM D1193-06 2018) with a resistivity of 18.2 MΩ.cm. Experiments were performed in either 0.5 wt%, 1.5 wt% or 3.5 wt% NaCl solution using 99.0% reagent grade NaCl obtained from Thermo Fischer Scientific. The solutions were naturally aerated. The corrosion potentials were measured and reported in reference to SCE in this study. All experiments were done using a Solartron, model 1287 potentiostat. CorrWare software was used to manage the potentiostat, and CorrView software was used to analyze collected data (both from Scribner Associates).

Figure 4: Electrochemical cell for corrosion measurement; RE = reference electrode (SCE = saturated Calomel electrode), CE = counter electrode of platinum (Pt), Alloy = working electrode



3.2 Measurement of Open circuit Potential

The free corrosion potential[4] of a metal or an alloy (E_{corr}) is one of the most important corrosion properties and is indicative of the metal surface's activity and the corrosion environment's oxidizing power. E_{corr} can be measured in an open circuit with respect to a reference electrode. The value of E_{corr} of one metal/alloy is compared to that of another metal/alloy, providing an estimate of the galvanic corrosion tendency and identifying which metal will serve as the anode and corrode faster. The open-circuit potential (OCP) experiments were performed for 48 hours or until the corrosion potential reached a steady state.

The samples for OCP measurement were polished to better simulate when the de-icing or airborne salts are accumulated and render the patina unstable or cause it to flake off. As such, no patina was present on the surface for the corrosion potential measurements. However, the corrosion potential of weathering steel was also explored with a patina formation to better understand its behaviour in a chloride-free environment. For this purpose, an artificial patina was formed on weathering steel through accelerated wetting-drying cycles. The wetting immersion used a simulated chloride-free environment solution in 0.0001 M Na_2SO_4 solution for 30 minutes before drying in UV light for 2 hours [77]. The cycle was repeated for 40 days. The corrosion potentials of the four weathering samples were measured during the immersion periods.

3.3 Measurement of Linear Polarization Resistance

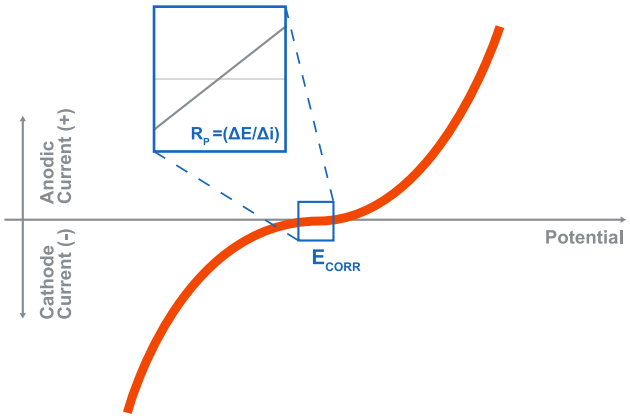
Linear polarization resistance (LPR) is a non-destructive electrochemical technique useful for measuring relative corrosion rates. An LPR measurement involves scanning the potential over a short voltage range (e.g., ± 5 to ±15 mV) from E_{corr} (or OCP) and measuring the current response. In this small region, the current-potential relationship is approximately linear (Figure 5) and so the reciprocal of the slope yields the polarization resistance, R_p, (in analogy to the elastic modulus of steel). R_p is a measure of the opposition of the electrochemical interface to the passage of current and, for a corrosion reaction, is inversely proportional to the corrosion rate (e.g., Jones [7]).

An LPR measurement was done at the end of each 48-hour E_{corr} measurement. From E_{corr}, the potential was polarized to E_{corr} ± 15 mV at a scan rate of 1 mV/s

4 Open-circuit potential (OCP) is used interchangeably with free corrosion potential or corrosion potential (E_{corr}).

for two cycles, and the current response was measured. LPR measurements were done to compare the corrosion resistance of the different bridge alloys. The greater the value of R_p, the lower the corrosion rate.

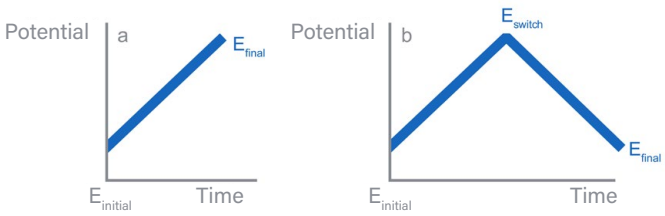
Figure 5: Potential, current and linear region E_{corr}. ΔE = change in potential, Δi = change in current.



3.4 Potentiodynamic Polarization Experiment

Potentiodynamic polarization (PDP) is an electrochemical technique in which an applied potential (E) is scanned, or imposed on the sample, and the current response is recorded. It is often scanned linearly with time from its initial free corrosion potential E_{corr}, which is denoted by $E_{initial}$ in Figure 6. At the same time, the current response is recorded. The measured current provides information on the electrochemical processes that can occur within the scanned potential range and a relative measure of their rates. Compared to LPR measurements, PDP measurements investigate potential-current response over an extensive range of applied potential, commonly ending with a final potential (E_{final}) beyond 1 V from $E_{initial}$.

Figure 6: A schematic of potential scan (a) and reverse (b) with time in potentiodynamic polarization



A forward anodic scan gives information on the formation and properties of oxide films on the surface (Figure 6a). In the reverse scan (6b), the current is recorded again as the potential is scanned back to $E_{initial}$. The current response during the reverse scan indicates whether the oxidations observed on the forward scan were reversible or irreversible. The data obtained from this test is often plotted as log (i) vs. E and referred to as a polarization curve. Polarization curves provide information on the behaviour of a given system as a function of potential and can identify regions of active, passive, and transpassive behaviours. Additional details regarding the oxide film breakdown behaviour can be obtained using cyclic measurements. This is especially useful for studying features of localized corrosion [7].

In this study, potentiodynamic polarization experiments were performed in naturally aerated 1.5 wt.% NaCl solution. An electrode was held at E_{corr} for one hour, followed by a potentiodynamic scan from -0.25 V (vs. E_{corr}) to more positive potentials at a scan rate of 1 mV/s. The scan was then reversed when the maximum current was reached. The nature of corrosion and the possibility of localized corrosion were investigated in these measurements.

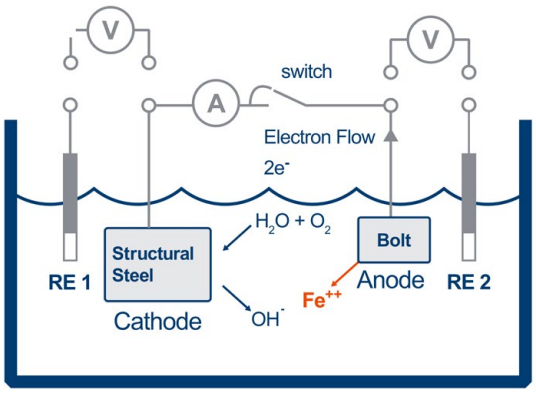
3.5 Measurement of Galvanic Corrosion Current

As discussed in Section 2.1.1, a galvanic corrosion current flows between the and the cathode in a galvanic cell. This can be measured in the lab by separating the two metals and connecting them through a zero-resistance ammeter (ZRA), creating direct electrical contact because the negligible electrical resistance enables the measurement of the current flow. This method measures the net current that passes from one metal to the other (I_{couple}), from which the galvanic corrosion density on the anode can be calculated by considering its surface area. The anodic galvanic corrosion current density represents the galvanic corrosion rate of the anode. The measured I_{couple} does not include all the ongoing oxidation and reduction reactions that occur on the surface of each of the metals. For this reason, it is important to note that a galvanic current can significantly underestimate the total corrosion rate of the anode if a substantial portion

of its oxidation is balanced by a reduction reaction on its surface, rather than on the coupled cathodic metal. Again, galvanic corrosion co-exists with other forms of corrosion, such as general corrosion or pitting corrosion [7].

The galvanic corrosion experimental setup illustrated schematically in Figure 7 follows the basic principles of ASTM G71-81:2019 [78], a structural alloy (e.g., A1010 steel) sample and a bolt sample are immersed in an electrolyte. Before coupling them with an open switch, the reference electrodes RE 1 and RE 2 can measure their E_{corr}. Once the two samples are connected when the switch closes, a ZRA starts to measure their galvanic corrosion current (I_{couple}). In this study, the coupled metals are between a structural alloy and a bolt material with an area ratio of 10:1 in a 1.5 wt% NaCl solution.

Figure 7: A schematic of the experimental setup for galvanic corrosion current measurement of structural steel (in the case of being a cathode) and bolt



3.6 Analysis of Microstructure Using Microscopy

The microstructure of an alloy can have a direct effect on the physical properties of the alloy and its corrosion performance. The most common influences of microstructure are grain size and the presence of phases and intermetallic compounds.

Samples from structural and bolt alloys were mounted and ground using silicon carbide papers down to P4000 grit size, followed by diamond polishing and a final polish with colloidal silica. Samples 350W, 350AT, and A490 were etched with 2% nital; B8M and B8SH were electrolytically etched in 60% nitric acid; A1010 was etched using glyceregia reagent (HCl/glycerol/HNO_3 mixture), and the aluminum sample was etched using Weck's reagent. The surface of the samples was imaged both in the as-polished condition and after etching.

Sample A325 Type I GS was not polished due to the presence of a zinc layer. This sample was monitored under a secondary electron microscope to measure the thickness of the zinc layer. A Hitachi SU5000 scanning electron microscope (SEM) with a Schottky field emission gun was used for imaging the galvanized zinc layer of the A325 bolts and their interface with the substrate carbon steel. The sample was made from the cross-section of the shank of an A325 bolt. Images and spectra were taken using Oxford Aztec software and X-Max 80 detector.

3.7 Salt Spray Testing

The salt spray test is one of the oldest corrosion test methods, and ASTM B117-19, *Standard Practice for Operating Salt Spray (Fog) Apparatus* [79] was first established in the 1930s. It has remained the most commonly used corrosion test, usually performed in contained and controlled environments, such as in a salt fog chamber [79]. The environment in a salt spray test can be set up with variations in temperature, pH level, salt concentration, and duration to accelerate the corrosion rate and facilitate the comparison of corrosion resistance in the study.

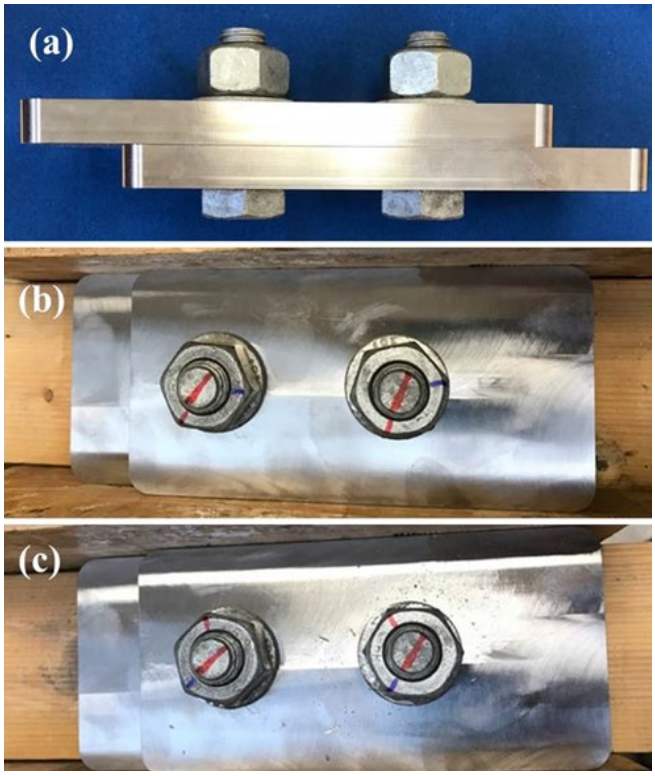
In addition to the electrochemical experimental program, the salt spray test was also conducted to validate the corrosion performance of the studied alloys. Table 2 shows a list of plates and bolts for salt-spray testing. To prepare the bolted samples for salt spray testing, selected structural steel plates were machined to 15 cm by 17 cm with a thickness of 1.4 cm. Two plates were then bolted together and were tightened to 1/3 of a turn after the initial fastening of the bolts, as shown in Figure 8. For the test, bolted plates were placed in a 5% salt spray and fog atmosphere for one month. The samples were visually inspected every seven days, with photographs taken to record the corrosion progress of the bolted plates.

This test was conducted for comparative purposes based on visual corrosion damage to help validate the corrosion resistance of the alloys under examination. After 28 days in the salt spray chamber, bolted samples of various bolt/plate samples were taken out for visual examination.

Table 2: List of plates and bolts in salt spray testing

Structure Steel Plate	Bolt
Carbon steel (350W)	A325 Type I CS, A490
Weathering steel (350AT)	A325 Type I CS, A325 Type I GS, B8M, B8SH
Aluminum	B8M, B8SH

Figure 8: (a) Bolted plates, (b) aligning bolts, and (c) tightening bolts to 1/3 turn.



4 Results

The results are presented to first consider galvanic corrosion tendency (thermodynamics), followed by galvanic corrosion current (kinetics), and finally corrosion behaviours of individual alloys and visual observations. In this way, information of increasing sophistication is presented:

- Open-circuit potentials (OCPs) indicate the corrosion tendency and their differences indicate the galvanic corrosion tendency between two alloys.
- Galvanic corrosion currents indicate the magnitude of damage with time on the anode of the coupled alloys.
- Corrosion rates and pitting tendency provide additional information on the corrosion properties of the individual alloys to help further understand their galvanic corrosion behaviours. Visual observation of the coupled alloys' corrosion and galvanic corrosion damage in the salt-spray chamber supplement already gathered information to validate the corrosion performance of the studied alloys.

4.1 Open-circuit Potential

4.1.1 OCP and Effect of NaCl Concentration: Within Alloy Comparison

OCP values (E_{corr}) of the structural alloys and bolt materials were measured at three different NaCl concentrations for 48 hours or until stabilization. Data plots are presented in Appendix B, with some presented in this section for illustration.

- B.1 presents OCP with time measured from two or three replicates of each alloy in the order of carbon steel, weathering steel, A1010 steel, aluminum, carbon steel bolt (A325 Type I), galvanized A325 Type I bolt, weathering steel bolt (A490 Type III), stainless steel bolt B8M, and stainless steel bolt B8 in the 0.5 wt% NaCl solution;
- B.2 presents these alloys in the 1.5 wt% NaCl solution; and
- Section B.3 presents results obtained in the 3.5 wt% NaCl solution.

The following observations were made for carbon steel and weathering steel:

- The OCPs of carbon steel were highly replicable and stabilized within 25 hours. The average values were 600 mV (see Figure 9), 650 mV, and 670 mV for the chloride concentrations of 0.5 wt%, 1.5 wt% and 3.5 wt%, respectively. OCPs in the three 1.5 wt% and 3.5 wt% NaCl solutions were similar, with a difference of about 20 mV.
- The OCPs of weathering steel were similar to those of carbon steel for the three NaCl solutions but tended to stabilize faster with time than carbon steel, particularly in the 0.5 wt% and 1.5 wt% NaCl solutions, where steady state was reached within 5 hours.
- In summary, carbon steel and weathering steel OCPs ranged from 600 mV to 700 mV, including both structural steel and bolts.

Figure 9: OCP vs. time of carbon steel 350W in 0.5 wt% NaCl solution; square, circle and triangle symbols are replicates 1, 2 and 3, respectively.

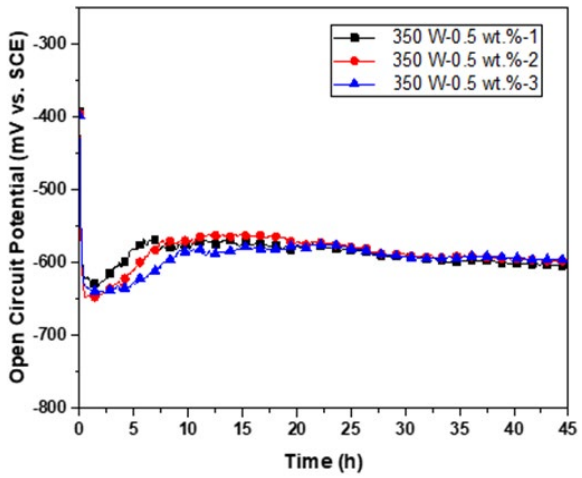


Table 3 presents the OCP values (E_{corr}), (rounded to the nearest ten millivolts for comparison due to the dynamic process of corrosion) of the structural alloys and bolt materials. Measurements represent at least two replicates at different NaCl concentrations for 48 hours or until stabilization. In comparison, A1010 steel demonstrated much more positive potentials, which were about -100 mV for all three concentrations of the NaCl solutions. This was expected because of its high chromium content (about 9-10%). Weathering steel has only about 0.4% chromium. However, A1010 steel samples also showed a tendency to develop crevice corrosion at their edges. Figures 10 and 11 reveal that when crevice corrosion occurs, the OCP can drop by 300 mV to about -400 mV. Therefore, the OCPs of A1010 steel demonstrated two values (potentials) in the tested salt solutions: -100 mV, and -400 mV in samples with crevice corrosion.

Figure 10: OCP vs. time of A1010 in 0.5 wt% NaCl solution; square, circle and triangle symbols are replicates 1, 2 and 3, respectively

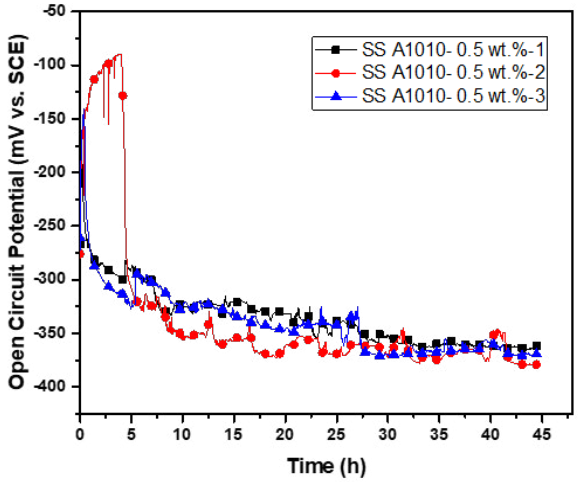


Figure 11: OCP vs. time of A1010 in 3.5 wt% NaCl solution; circle (passive), and square (creviced)

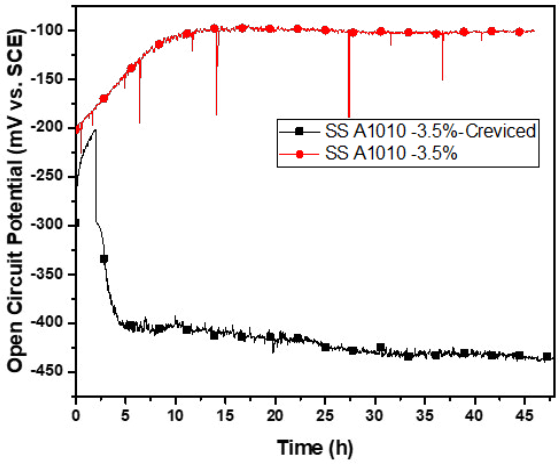


Table 3: OCP of structural alloys and bolt materials at three NaCl concentrations

NaCl Solution	0.5 wt%		1.5 wt%		3.5 wt%	
	OCP (mV)	Time to stabilization (h)	OCP (mV)	Time to stabilization (h)	OCP (mV)	Time to stabilization (h)
Bridge structural alloy						
Carbon Steel (350W)	-600	25	-650	25	-670	25
Weathering Steel (350AT)	-600	5	-650	5	-650	5
ASTM A1010*	-100 -400*	10 5	-100 -400*	10 10	-100 -440*	10 5
Aluminum (A1)	-780	3	-680	3	-700	3
Bolt Alloy						
Carbon steel (A325 Type I)	-620	15	-610	10	-680	8
Galvanized steel (A325 Type I)	-980	3	-1050	3	-1080	2
Weathering steel (A490 Type 3)	-600	4	-620	5	-650	10
Stainless steel (SS) B8M (SS316)	-50	15	-60	10	-100	15
Stainless steel B8SH (SS 304)	-150	5	-180	5	-200	10
Stainless steel washers						
SS 316L	-	-	-80	20	-	-
SS 410	-	-	-100	15	-	-

*OCP with pitting corrosion

The OCPs of aluminum were also measured with good repeatability. They stabilized quickly within 3 hours in the 0.5 wt% and 3.5 wt% NaCl solutions. The OCPs slightly decreased with increasing NaCl concentration and ranged from -700 mV to -650 mV in the tested solutions.

The following summarizes the OCP results of the four bridge structural alloys of carbon steel, weathering steel, A1010 steel, and aluminum:

- The OCP was observed to become negative with increasing the NaCl concentrations for all the alloys. This was expected, showing greater corrosion activity with increased chloride concentration. From 0.5 wt% to 3.5 wt%, the change in OCP was observed to be less than 100 mV. This is notable and in significant contrast to the effect of chlorides on the OCP of carbon steel rebar in concrete, which can drop by more than 500 mV when the chloride content increases.
- In a galvanic series, in order of decreasing nobility, A1010 steel would have two positions, -100 mV and -400 mV for crevice corrosion; carbon steel and weathering steel would range from -600 mV to -700 mV; and Aluminum -650 mV to -700 mV.

For the carbon steel bolt (A325 Type I), galvanized steel bolt, weathering steel bolt (A490 Type 3), stainless steel bolt B8M, and stainless steel bolt B8, their OCPs were observed as follows:

- The OCPs were highly repeatable and in a range expected for each material except for the B8SH bolt.
- Galvanized steel OCPs were around -1000 mV to -1060 mV at the three NaCl concentrations.
- Carbon steel and weathering steel bolts decreased from -600 mV to about -650 mV with increasing NaCl concentration.
- B8M bolts (SS 316) demonstrated the most positive (noble) OCPs, from -40 mV to -80 mV, with increasing NaCl concentration (Figure 12).
- B8SH bolts were the only samples where pitting corrosion occurred repeatedly. The pitting corrosion was visible on its surface, as shown in Figure 13. This also explains its oscillating OCPs with time, displaying dynamic pitting growth and re-passivation processes, as shown in Figure 14. They ranged from -60 mV to -180 mV. This type of bolt is thus not recommended for use in steel or aluminum bridges when salt exposure is expected.

Figure 12: OCP vs. time of B8M in 0.5 wt% NaCl solution; square, circle and triangle symbols are replicates 1, 2 and 3, respectively

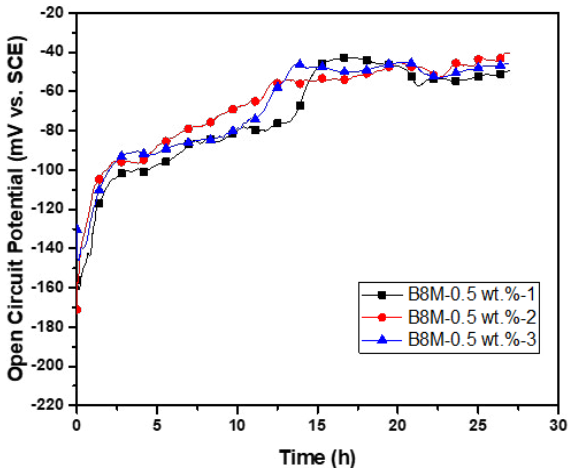


Figure 13: Visible pitting corrosion on B8SH surface after OCP measurements obtained from (a) Western University (b) NRC. The white resin (b) is an additional protective layer for inhibiting crevice corrosion.

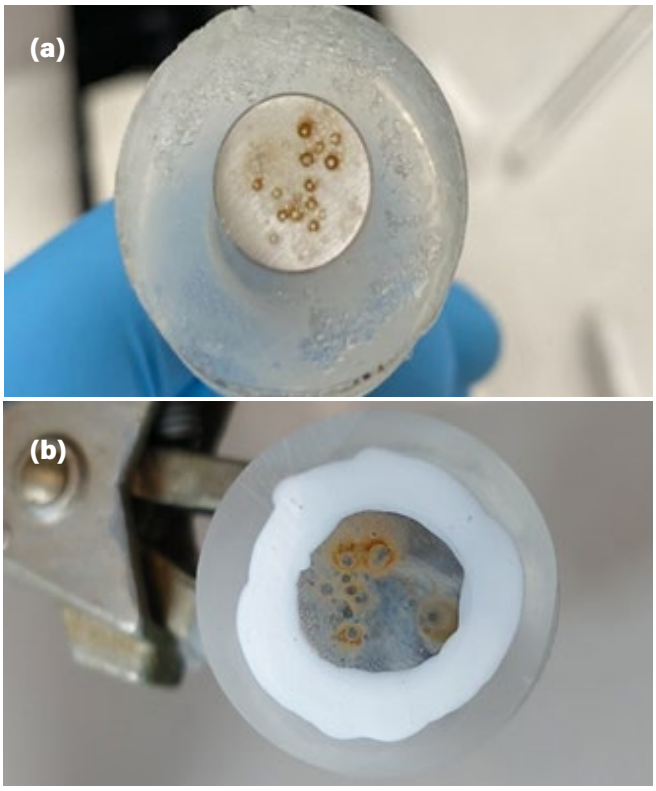
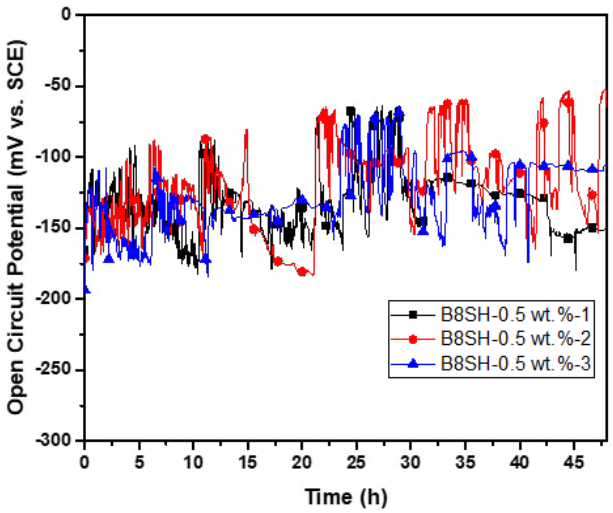


Figure 14: OCP vs. time of B8SH in 0.5 wt% NaCl solution; square, circle and triangle symbols are replicates 1, 2 and 3, respectively.



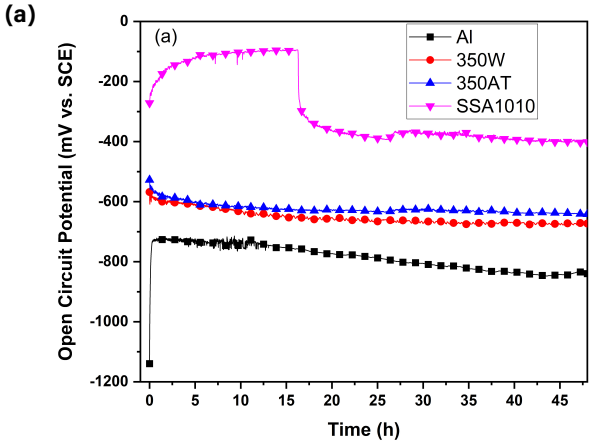
4.1.2 OCP in 1.5 wt% NaCl solution

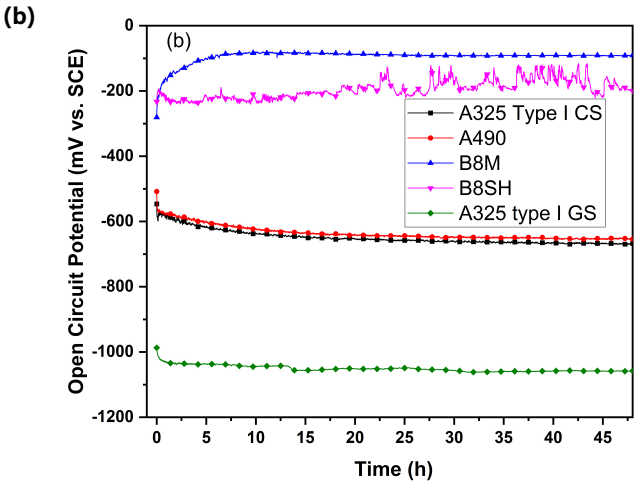
The OCPs of the alloys under study at three NaCl concentrations demonstrated relatively small differences in OCP within the alloy sample groups (within 100 mV). A comparison of among different alloy sample groups was explored using the 1.5 wt% NaCl solution. The 1.5 wt% NaCl concentration was also used for the LPR, PDP, and galvanic corrosion current measurements.

Figure 15 compares the OCPs of (a) the four bridge structural alloys tested and (b) the five bolt alloys. Given that a more positive OCP, in general, indicates higher corrosion resistance, A1010 had the most positive (noble) value among the structural alloys at -100 mV in a passive state and at -400 mV at crevice corrosion. The next favorable potentials were demonstrated by carbon steel and weathering steel, with very similar corrosion potentials of about -600 to -650 mV. Aluminum exhibited the least favorable corrosion potential of about -700 mV. The structural alloys demonstrate that they belong to three distinct corrosion potential groups.

In comparison, the bolt alloys also demonstrated three corrosion potential groups, but with a broader range of differences. B8M revealed the most positive corrosion potential of about -80 mV; carbon steel and weathering steel bolts had similar corrosion potentials (-600 to -650 mV), which were also almost identical to those of structural carbon steel and weathering steel. The galvanized steel bolt had the lowest corrosion potential of around -1000 mV, which was expected due to the surface zinc.

Figure 15: OCP vs. time of (a) structural alloys and (b) bolt materials in 1.5 wt% NaCl solution. Square is aluminum, circle is 350W, triangle is 350AT, inverted triangle is SS A1010





4.1.3 Stainless Steel Washers

Ideally, washers are made from the same alloy as bolts to avoid galvanic corrosion. In practice, they are sometimes reported or found to be different. The B8M (SS316) and B8SH bolts (SS304) ordered for this study came with SS316L and SS410 washers. Therefore, it was decided to conduct their OCP measurements to provide more information. The results are presented in Appendix B (Figures 52 and 53), obtained in the 1.5 wt% NaCl solution. The SS316L washer had a corrosion potential of about -50 mV, which was very similar to (but slightly more positive than) the B8M (SS316) bolt. The two materials, SS316 and SS316L, are almost identical in their compositions, except that SS316L has much less carbon. This is consistent with their corrosion potential measurements. The SS410 washers had a slightly more negative (more active) corrosion potential of about -100 mV than the SS316L washer. More research will be needed to understand better whether this washer tends to develop pitting corrosion, although no pitting corrosion was found in the current study.

4.1.4 Patina Formation on Weathering Steel

The corrosion potentials of the four weathering samples were found to rise from -400 mV to more positive (noble) values of -100 to -150 mV over time (Figure 16 (a)), which are much more positive than the -600 to -700 mV in the NaCl solutions as measured with the polished samples (Figure 16 (b)).

Figure 16: Corrosion potential (E_{corr} = OCP) with patina formation on weathering steel (a), and the polished weathering steel in presence of chloride (b). Square, circle, triangle and inverted triangle represent samples 1, 2, 3 and 4, respectively.

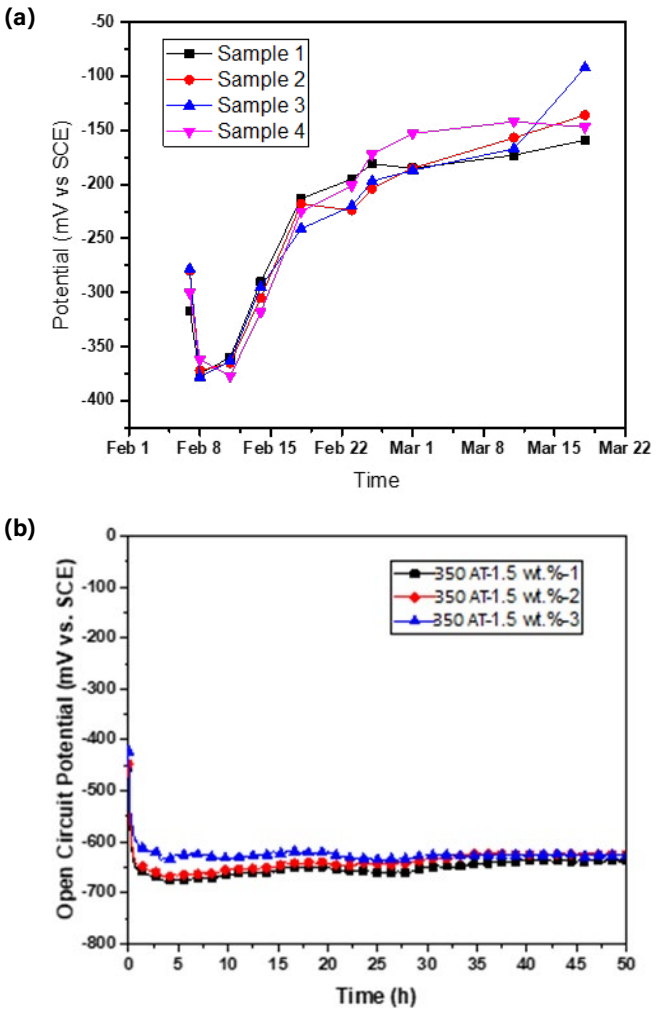
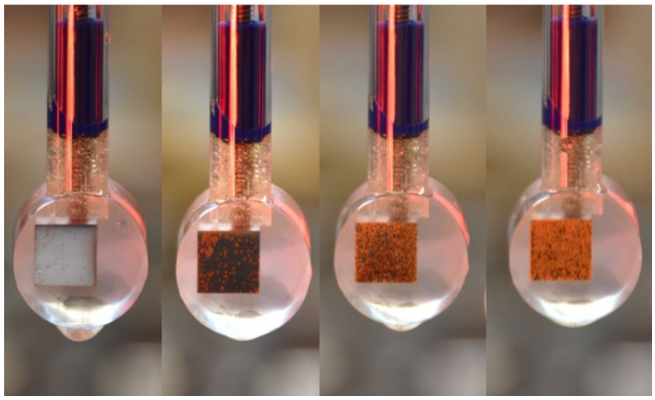


Figure 17 depicts the patina formation on 350AT weathering steel (from left to right); which thickened with time, the number of immersion cycles and drying under UV light. After 38 days, the patina may have also assumed its corrosion protection function because the corrosion potential began to stabilize, as shown in Figure 16(a). This should be further explored in future research to better understand the corrosion of weathering steel and the effect of chlorides. It should be noted that galvanic corrosion in the presence of NaCl is more relevant to studying the risk that causes the potential damage. Without chlorides, galvanic corrosion is less likely to occur, not only because the corrosion likelihood of each alloy in the galvanic couple is low but also because the electrical resistance of the electrolyte is high. The patina formed in the cycling test flaked off when the samples were exposed to the NaCl solutions, and the potential dropped to -600 mV.

Figure 17: Formation of patina on 350AT weathering steel over 38 days



4.2 Galvanic Corrosion Current

A galvanic current measured between two alloys bears two pieces of relevant information:

- the polarity of the current that determines which is the anode and which is the cathode; and
- the magnitude of the current, divided by the surface area of the anode, which determines the galvanic corrosion rate and how fast the anode will be damaged by corrosion.

The setup in this study and presentation are as follows:

1. A galvanic couple or pair comprising a structural alloy and a bolt. For example, a galvanic couple denoted by "350AT/A325 Type I GS" refers to structural weathering steel coupled with an A325 Type I galvanized steel bolt.
2. The polarity of a measured current is indicative of the anode. When the current is positive, the structural alloy is the anode; when the current is negative, the bolt alloy is the anode.
3. Since the structural alloy has a larger surface area than the bolt, the galvanic corrosion current density, currently divided by the surface of the anode, will be lower when the structural alloy is the anode and the polarity is positive.

4.2.1 Validation of Measurement Setup

The measurement of galvanic corrosion involves a very small current, therefore it is advisable to validate the measurement setup, including the corrosion cells, connection, and machine, to help ensure quality of the signal. This validation is accomplished by coupling the same two alloys as, in theory, there should be an oscillating galvanic corrosion current for active alloys or no galvanic current for passive alloys.

Figure 18 shows the galvanic current between the two galvanized steel samples that would be actively corroding in the 1.5 wt% NaCl solution. The galvanic current (i_{couple}) is observed to change with time back and forth, indicating that there is no absolute anode or cathode between the same two active samples. Figure 19 depicts the galvanic current between two A1010 steel samples that would be passive. The i_{couple} between the two samples is near zero and the pattern indicates it is close to the limit of the potentiostat in measuring the minimal current.

Figure 18: Coupling current between two galvanized samples

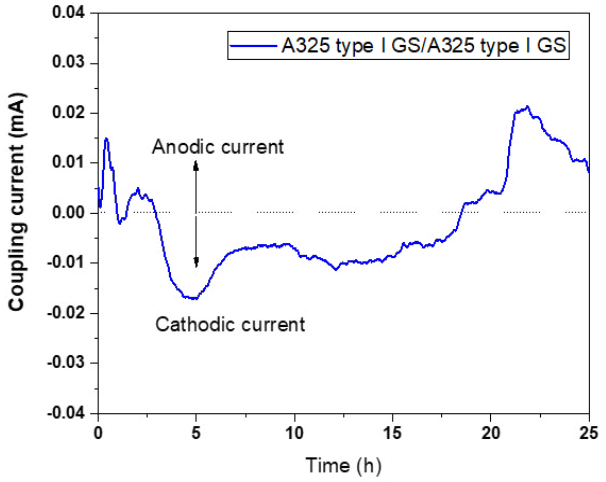
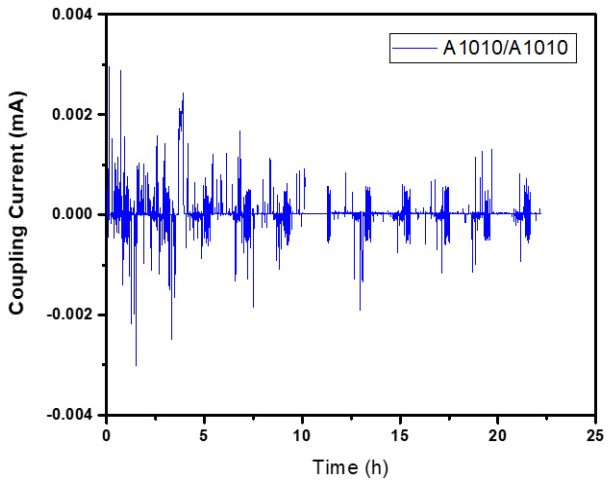


Figure 19: Coupling current between two A1010 samples.



4.2.2 Galvanic Current of Coupling Structural Alloy/Bolt

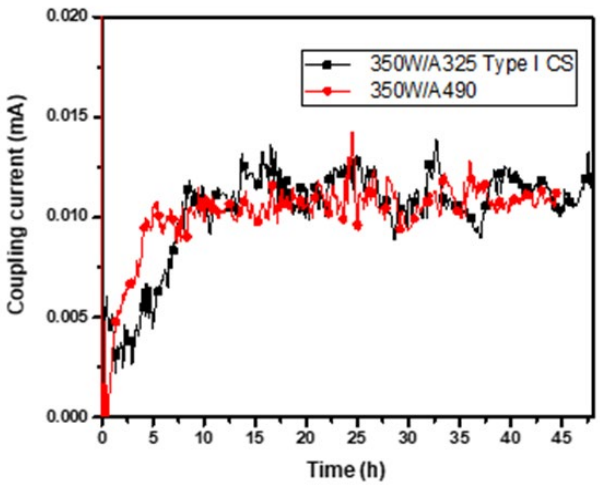
All galvanic coupling experiments were performed in the 1.5 wt% NaCl solution at NRC and Western University under NRC supervision. The current magnitudes of all the measured pairs were comparable and the current polarity was consistent between the data obtained by the two labs. A summary of the results at the end of the experiment is presented below in Table 4.

For the two pairs of 350W/A325 Type I CS and 350W/A490, structural carbon steel 350W was paired with carbon steel A325 Type I bolt and A490 weathering steel bolt, respectively, for galvanic corrosion measurement. The two pairs were chosen to validate the information derived from their similar corrosion potentials and to set reference values to understand other galvanic coupling pairs. This is because there are no existing criteria for interpreting galvanic corrosion. The results of the two reference pairs are presented in Figure 20. Both pairs display similar coupling currents around 12 µA, as averaged from the two experiments. The positive polarity of both currents indicates that 350W is the anode in both pairs and the anodic current density is about 1.2 µA/cm^2, which would be in a low corrosion rate category of the ISO 9223 [67].

Table 4: Galvanic corrosion current measured after 48 hours in 1.5 wt% NaCl solution (polarity: '+' means the structural alloy is the anode and '-' means the bolt is the anode; CS for carbon steel and GS for galvanized steel)

Coupled Number	Coupled Plate/Bolt	Western University (mA)	NRC (mA)
1	350W/A325 Type I CS	+0.019	+0.012
2	350W/A490	+0.025	+0.011
3	350AT/A325 Type I CS	-0.052	-0.071
4	350AT /A490	-0.022	-0.011
5	350AT /B8M	+0.021	+0.011
6	350AT /B8SH	+0.021	+0.010
7	350AT /A325 Type I GS	Start -0.910 End -0.022	Start -0.126 End -0.051
8	A1010/B8M	+0.0005	+0.0001
9	A1010/B8SH	+0.006	+0.002
	A1010/ A325 Type I GS		Start -0.783 End -0.215
10	Aluminum/ B8M		+0.014
11	Aluminum/ B8SH		+0.015

Figure 20: Galvanic current of 350W coupled with A490 and A325 Type I CS bolt. Square is 350W/A325 Type I CS, diamond is 350W/A490.

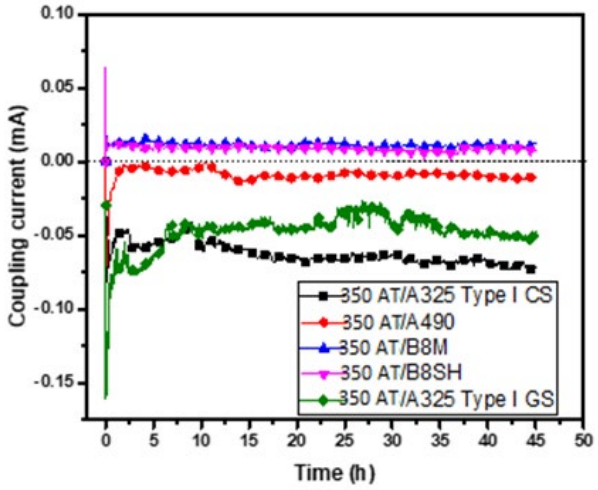


350AT weathering steel has been studied with a variety of bolts, and their galvanic corrosion currents are presented in Figure 21:

- Paired with B8M or B8SH, the galvanic current is about 11 µA. The bolts are protected against corrosion in contact with 350AT weathering steel.
- 350AT/A490 demonstrated negative values between -10 to -22 µA. The polarity, however, could change with time for this pair if monitored long enough because they are essentially the same materials undergoing active corrosion in the salt solution, as shown in Figure 18 for two galvanized steel samples.
- In the pair of 350AT/A325 Type I carbon steel, the current is about -60 µA, indicating the carbon steel bolt is the anode and is experiencing a higher corrosion rate than the aforementioned pairs.
- A325 Type I galvanized steel bolts produced even higher currents (122 µA) at the start of the experiment that over time declined to -51 µA. They showed rapid dissolution of the zinc layer on the bolt at the beginning and, with time, reached its carbon

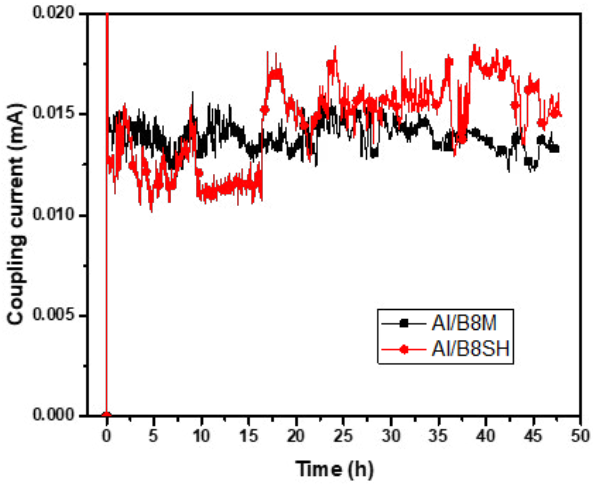
substrate. The current at the end of the experiment is comparable to that of the A325 carbon steel bolt, confirming the dissolution of zinc.

Figure 21: Galvanic current of 350AT coupled with A325 Type I CS (square) and GS (diamond), A490 (circle), B8M (triangle) and B8SH bolt (inverted diamond).



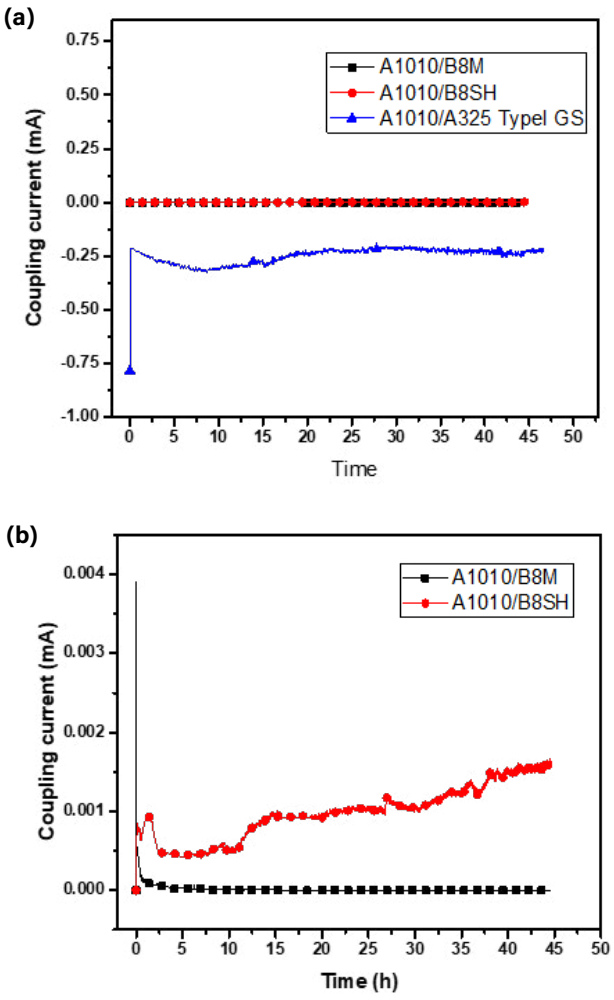
For aluminum paired with stainless steel bolts, as shown in Figure 22, both Al/B8M and Al/B8SH produced similar currents around 15 µA in positive polarity, similar to weathering steel paired with the two stainless steel bolts (12 µA).

Figure 22: Galvanic current of Al coupled with B8M (square) and B8SH (circle).



The galvanic corrosion of A1010 with B8M, B8SH, and A325 Type I galvanized steel are presented in Figure 23. Once again, the rapid dissolution of the zinc layer is observed by a negative current of -750 µA at the start of the experiment of A1010/A325 Type I galvanized steel. Over time this value lowers to -250 µA when the carbon steel substrate is reached. A1010/B8M and A1010/B8SH have negligible galvanic currents of about 0.5 µA, and 2 µA, respectively. A closer look in Figure 23 (b) at the two pairs revealed that the current B8SH was as low as 0.5 µA at the beginning of the experiment, but it increased over time to about 2 µA. This is likely due to localized corrosion in the B8SH bolt seen on its surface. With B8M, A1010/B8M generated the lowest current (about 0.5 µA) that remained stable throughout the experiment.

Figure 23: Galvanic current of A1010 bridge alloy coupled (a) A325 Type I GS (triangle), B8SH (circle) and B8M (square) and (b) with B8M (square) and B8SH (circle)

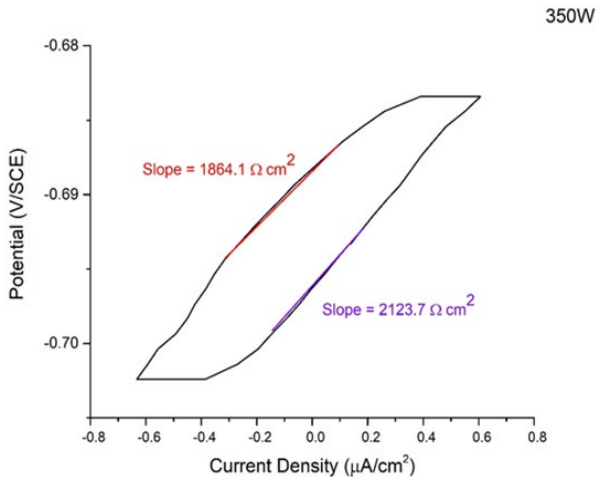


4.3 Additional Corrosion Information and Visual Observation

4.3.1 LPR for Corrosion Resistance

Corrosion resistance values were calculated by obtaining the slopes of the upper and lower halves of the LPR curve and averaging these values. An example graph (Figure 24) demonstrates the procedure for obtaining resistance values on 350W carbon steel, where an average of the slopes of forward and back scans was 1.98 KΩ cm^2. This is also used as a reference value to evaluate other studied alloys.

Figure 24: Potential vs. current density for 350W carbon steel in 1.5 wt% NaCl solution.



The polarization resistance data of bridge and bolt alloys in the study are summarized in Table 5, representing their individual corrosion resistance.

Table 5: Polarization resistance of the bridge and bolt alloys in 1.5 wt% NaCl solution

Alloy Type	Alloy Name	LPR (KΩ cm^2)
Bridge Body Alloy	350W	1.98
	350AT	1.52
	Al	394
	A1010	516
Bolt Alloy	A325 Type I CS	1.76
	A325 type I GS	0.56
	A490	2.2
	B8M	1410
	B8SH	88.6

The following observations are made from Table 5:

- Among all bridge structural materials, A1010 has the highest polarization resistance (516 kΩ.cm^2). This is expected since A1010 has about 9-10% chromium that protects it from corrosion. It is followed by aluminum, whose polarization resistance is as high as 394 kΩ.cm^2. Despite its much lower corrosion potential, aluminum oxides form on the surface in the presence of oxygen, which may block the progression of corrosion and result in a greater polarization resistance. 350W carbon steel and 350AT weathering steel show significantly lower polarization resistance, 1.98 and 1.52 kΩ.cm^2, respectively. This is expected from carbon steel. Weathering steel has some alloying elements in a low percentage (about 0.4% chromium) and is expected to have a higher corrosion resistance than carbon steel by forming an oxide layer. However, the patina is not stable in the presence of salt. Therefore, the polarization resistance of 350W and 350AT are similar in the measurements.
- Among bolt materials, B8M stainless steel has the highest corrosion resistance due to 19 wt% Cr and 8 wt% Ni and 2 wt% molybdenum (Mo) in its compositions. The B8SH alloy also has a high corrosion resistance (88.6 kΩ.cm^2), but it is about 15 times lower than B8M. Despite similar composition in the two stainless alloys, B8SH does not have Mo, which plays a significant role in passive film enhancement and the prevention of localized corrosion in chloride-laden environments.
- The galvanized A325 Type I bolt has the lowest corrosion resistance (0.56 kΩ.cm^2). The resistance measured here comes from the zinc layer's corrosion expected to have a low polarization resistance.
- Both A325 Type 1 carbon steel and A490 weathering steel bolts show similar polarization resistance values of 1.76 and 1.30 kΩ.cm^2. As discussed above, these two alloys are similar to the 350W and 350AT, respectively, confirming their similar polarization resistance values.

4.3.2 PDP for Pitting Tendency

Potentiodynamic polarization scans were performed in the 1.5 wt% NaCl solution. Figure 25 shows the PDPs of the 350W structural steel and the A325 Type I CS and A490 bolt alloy materials. Individual corrosion current

was estimated from the potentiodynamic polarization curves. From the curves, the individual corrosion rates were obtained for the studied bridge and bolt alloy materials, and their tendency to general/localized corrosion were investigated. The PDP performed on other alloys are presented in Appendix C and the results are presented in Table 6.

Figure 25: Polarization curves in 1.5 wt% NaCl solution for 350W carbon steel (square), A325 type 1 CS (circle), and A490 (triangle).

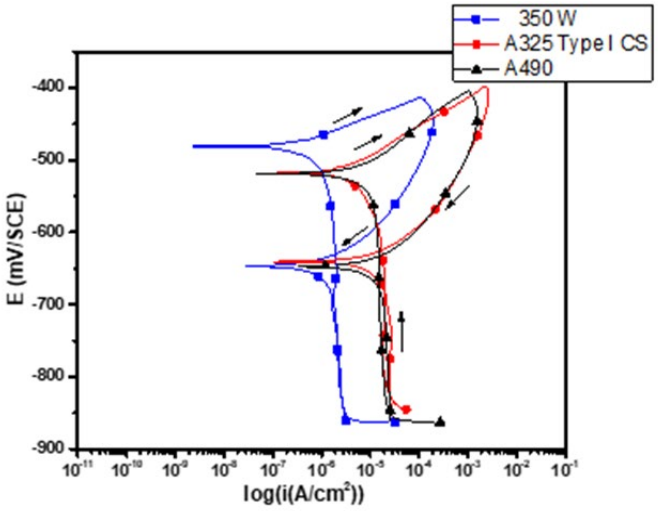


Table 6: Corrosion rate (i_{corr})of the bridge and bolt alloys in 1.5 wt% NaCl solution

Type	Alloy Name	i_{corr} (µA/cm²)	Nature of Corrosion
Bridge Structural Alloy	350W carbon steel	19	General
	350AT weathering steel	13	General
	Al	5	General
	A1010	3	Localized
Bolt Alloy	A325 Type I carbon steel	17	General
	A490 weathering steel	11	General
	A325 Type I galvanized steel	8.5	General
	B8M	0.12	Passive
	B8SH	0.17	Localized

The following observations were made from the results presented above:

- The potentiodynamic polarization is a valuable tool in identifying the nature of corrosion, as well as the individual corrosion rate.
- The bridge structural alloys of 350W and 350AT show general corrosion with relatively high corrosion rates of 19 and 13 µA/cm², respectively in the 1.5 wt% NaCl. They agree with the LPR data that showed both alloys had low and similar polarization resistance. The same trend is observed in bolt materials: A325 Type I carbon steel and A490 weathering steel have general corrosion with higher corrosion rates (17 and 11 µA/cm², respectively). A325 Type I galvanized bolts also show a relatively high corrosion rate of 8.5 µA/cm².
- Both Al and A1010 show lower corrosion rates of 3 and 5 µA/cm², respectively. When polarized, they exhibit a tendency for localized corrosion.
- B8M showed passive behaviour with negligible corrosion rates (0.12 µA/cm²), and the alloy remained passive during polarization, exerting high resistance to localized corrosion. While B8SH revealed a passive corrosion rate (0.17 µA/cm²), it was susceptible to localized corrosion as explained previously.

Recall that Al has as negative a corrosion potential as weathering steel and carbon steel in the salt solutions; Al has demonstrated much higher corrosion resistance with a lower corrosion rate. Therefore, Al has a significantly more negative corrosion potential than A1010, and yet they have comparable corrosion rates. These results demonstrate the importance of understanding the difference between corrosion thermodynamics and kinetics, as well as the corrosion behaviours of different metals.

4.3.3 Microscopy Analysis

4.3.3.1 Optical Microscopy

Figures 26 and 27 present the microstructural analyses of the studied bridge alloys obtained from optical microscopy.

Figure 26: Optical microscope images of etched surface of (a) 350W, (b) 350AT, (c) A1010 and (d) Al

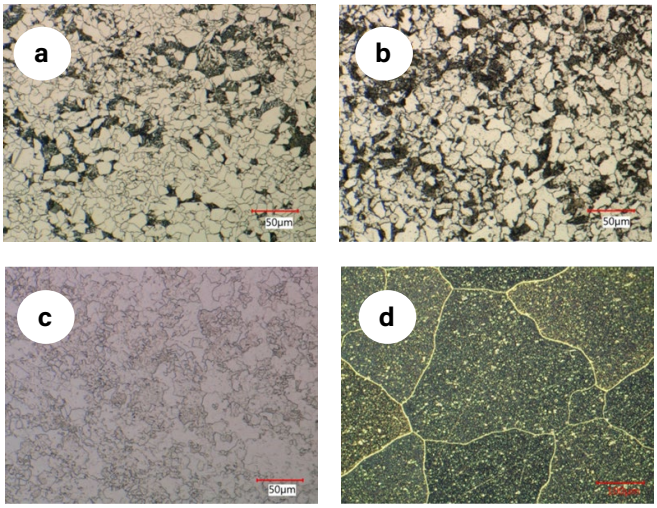
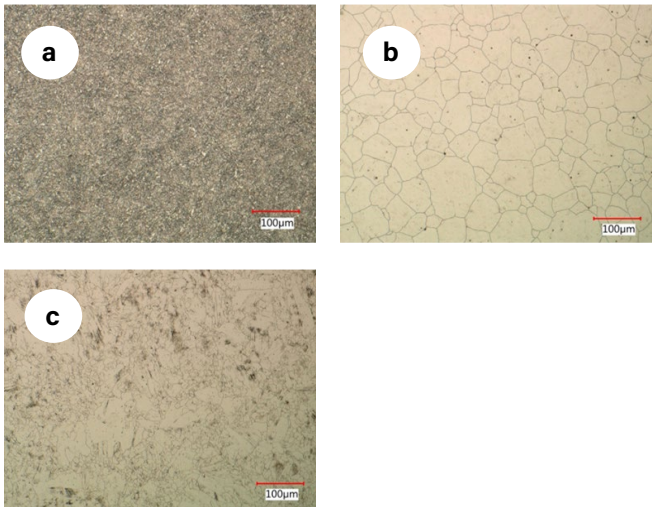


Figure 27: Optical microscope images of etched surface of (a) A490, (b) B8M, and (c) B8SH



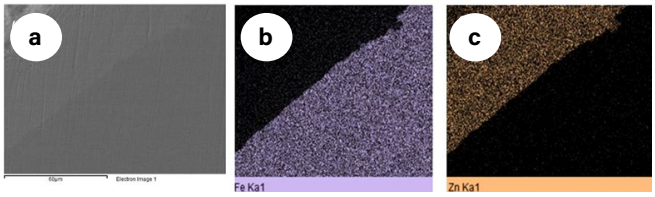
The optical microscope images of the etched surfaces (Figures 26 and 27) show different microstructures in these samples. Note that it is not possible to interpret the microstructures accurately without knowing the processing history of the samples. Based on the optical images of the etched surfaces, the microstructures of these samples are interpreted as follows:

- Sample 350W carbon steel appears to contain ferrite and pearlite. One can see Widmanstatten ferrite in some areas in this sample at higher magnifications.
- Sample 350AT weathering steel has a microstructure that appears to contain ferrite and pearlite. Some pearlitic bands in this sample are also detected.
- Sample A1010 steel appears to have two phases, a bright phase and a darker phase of ferrite and tempered martensite.
- Sample Al shows grain boundaries and secondary phase inside grains.
- Sample A490 appears to have a microstructure of probable and tempered martensite. The presence of a bainitic phase is also a possibility.
- Sample B8M shows a microstructure comprised of equiaxed grains, typically observed in austenitic stainless steels.
- Sample B8SH comprises grains of various sizes and a dark phase. There is a combination of some small and large grains in this sample. Without additional analysis and information on this sample's prior history/processing, it is difficult to identify the dark phase.

4.3.3.2 SEM imaging and EDS analysis of galvanized steel bolt

The Zn/Fe interface is visible by the SEM imaging in Figure 28(a). EDS mapping was performed on the same area to evaluate the sample's distribution of zinc and iron. Figure 28 (b) presents the iron map and Figure 28(c) highlights the distribution of zinc.

Figure 28: SEM image of Zn/Fe interface of zinc and steel in A325 galvanized bolts(a), EDS map showing Fe (b), and EDS map showing zinc (c).



To estimate the thickness of the zinc layer, a series of thickness measurements were performed on a sample taken from the shank of a galvanized A325 bolt. Figure 29 shows the SEM imaging of the sample with the thickness measurements, in which the difference in the contrast observed in the sample is

due to the difference in the atomic weight of Zn and Fe. This contrast in the image was used to estimate the thickness of the Zn layer. The measurements reveal that the thickness is not uniform around the sample, ranging from 57 µm to 166 µm. The Zn/Fe interface was also examined using an EDS line scan. The elemental count per second over 32 µm of the interface is shown in Figure 30. A clear drop in Fe concentration and a rise in Zn concentration is observed at the Zn/Fe interface in galvanized bolts. There are some traces of carbon and phosphor in the sample as well. The A325 bolt substrate is mainly iron (98.7 wt %) with slight traces of manganese and silicon. Moving toward the interface, traces of zinc appear.

Figure 29: Zinc layer thickness measurements in galvanized A325 Type I bolt.

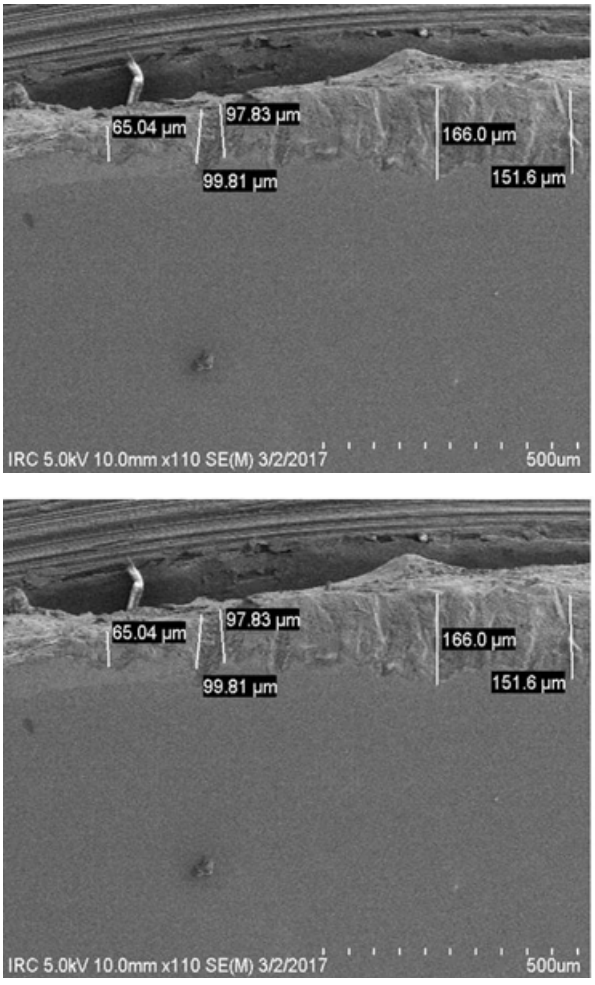
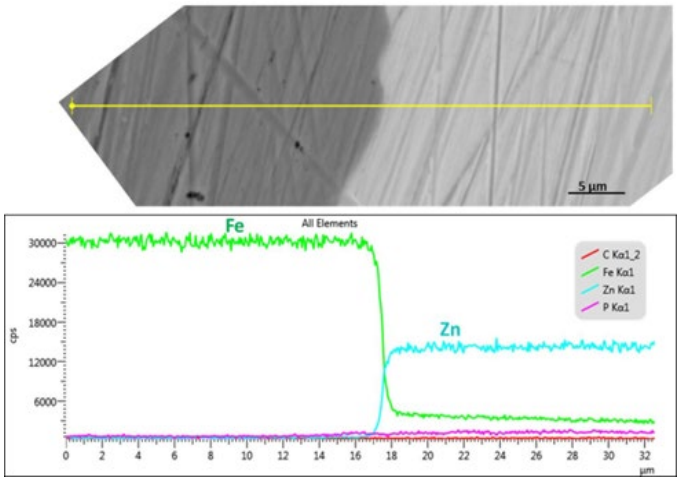


Figure 30: SEM imaging and EDS line scan of Zn/Fe interface, showing change in elemental concentration over 32 µm of interface.



4.3.4 Bolted Plates in Salt Spray Test

Figure 31 presents the corrosion progression of 350AT weathering steel plates bolted with A325 Type I, B8M, and B8SH bolts. As expected, the 350AT weathering steel plate was severely corroded. The A325 Type I carbon steel bolt showed general corrosion in contact with heavily corroded plates. Corrosion of the zinc layer was visible by the white zinc oxide on galvanized A325 Type I bolt. Both B8M and B8SH bolts showed almost no signs of corrosion (slight discoloration). Although the tests in the corrosion cell found B8SH to experience severe pitting corrosion, the salt spray test did not generate pitting corrosion. Further study is needed for B8SH.

Figure 32 presents the corrosion progression of 350AT weathering steel plates bolted with A325 Type I, B8M, and B8SH bolts. As expected, the 350AT weathering steel plate is severely corroded. A325 Type I carbon steel bolt shows general corrosion in contact with heavily corroded plates. Corrosion of the zinc layer is visible by the white zinc oxide on galvanized A325 Type I bolt. Both B8M and B8SH bolts show almost no signs of corrosion on the bolt (slight discoloration). Although the tests in the corrosion cell found B8SH to experience severe pitting corrosion, the salt spray test did not find it to have pitting corrosion yet. Further study is needed for B8SH.

Figure 33 presents the corrosion progression of B8M and B8SH bolts that connect two aluminum plates. Visual examinations show no sign of corrosion on bolts while aluminum is corroded at the bolt interface and plate. Once again, the results agree with the electrochemical prediction of aluminum being the anode. Our previous study using the same procedure showed that A1010 did not corrode in the salt spray chamber [59].

Figure 31: Bolted plates of 350W carbon steel after salt spray testing. 350W plate-A325 Type 1 carbon steel bolt (top), 350W plate-A490 bolt (bottom).



350W plate- A325 Type I carbon steel bolt



350W plate- A325 Type I carbon steel bolt



350W plate- A490 bolt



350W plate- A490 bolt

Figure 32: Bolted plates of 350AT weathering steel after salt spray testing. 350W plate-A325 Type 1 carbon steel bolt (top), 350AT plate-B8M bolt (middle), 350W plate-B8SH bolt (bottom).



350AT plate- A325 Type I galvanized bolt



350AT plate- A325 Type I galvanized bolt



350AT plate- A325 Type I carbon steel bolt



350AT plate- A325 Type I carbon steel bolt



350AT plate- B8M bolt



350AT plate- B8M bolt



350AT plate- B8SH bolt

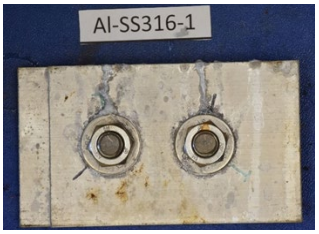


350AT plate- B8SH bolt

Figure 33: Bolted plates of aluminum after salt spray testing. Al plate-B8M (top), Al plate-B8SH bolt (bottom).



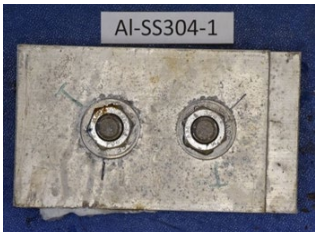
Al plate- B8M bolt



Al plate- B8M bolt



Al plate- B8SH bolt



Al plate- B8SH bolt

5 Discussion

5.1 Development of Galvanic Series and Corrosion Tendency

A galvanic series is a collection of engineering metals and alloys ordered according to measured free corrosion potentials (E_{corr}) in a given environment (mostly seawater). The position of an alloy in the series indicates its corrosion tendency relative to other alloys, indicating whether it is more or less noble (inert). The

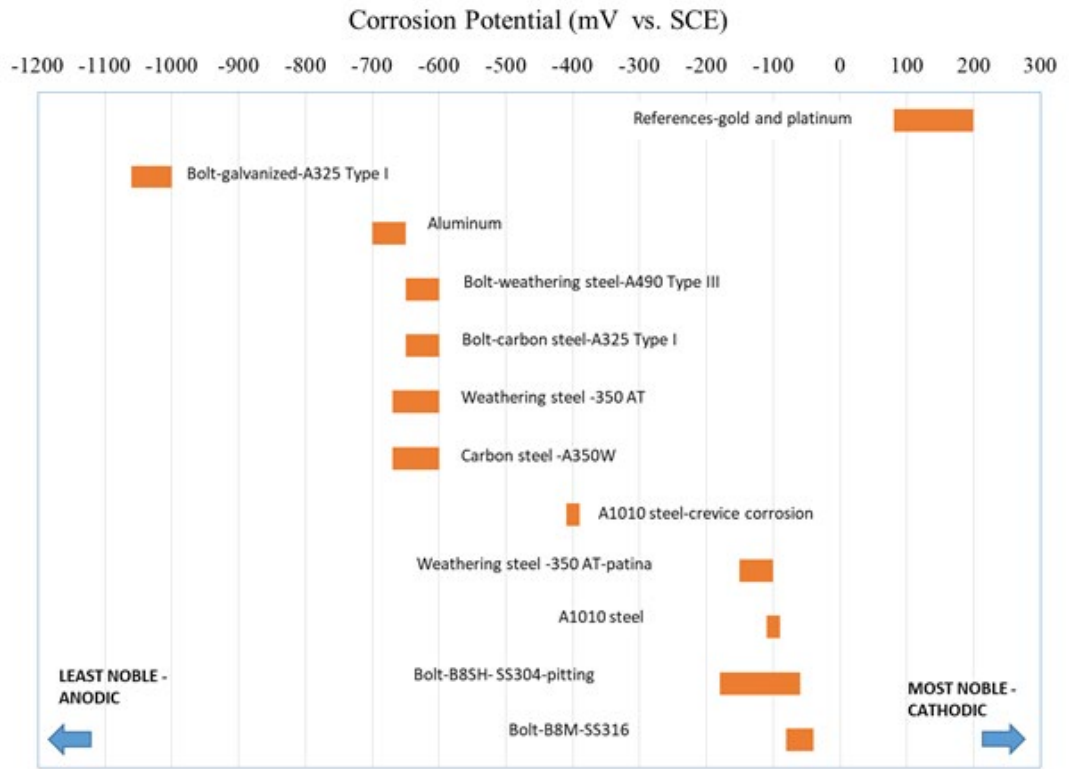
relationships of the alloys presented in a galvanic series, defined by their positions and difference in E_{corr}, are thus a handy guide for selecting two alloys with less tendency to undergo galvanic corrosion.

A galvanic series has been developed for the bridge alloys in this study and is presented in Figure 34. In this galvanic series, each entry of an alloy displays a range of corrosion potentials (E_{corr}) obtained in the NaCl solutions from 0.5 wt% to 3.5 wt%, simulating exposure environments defined by various chloride concentrations. The only exception is the "weathering steel-patina" entry which was developed in a solution free of salts. Appearing in the rightmost portion of the figure are gold and platinum (E_{corr} ranging from +80 mV to 200 mV in seawater) [7]. As expected, bridge structural alloys and bolt materials have more negative E_{corr} than gold and platinum (indicated by their left-side placement in the series), meaning that they are less noble and comparatively more active in corrosion tendency.

The galvanic series as presented in Figure 34 provides a systematic collection, ranking and comparison of the corrosion tendency of bridge alloys for the first time, revealing a categorization into four groups of the studied alloys according to their E_{corr}:

- **Group A.** The noblest group with the slightest tendency to corrode consists of stainless steel A1010, B8M, and B8SH, and their E_{corr} range from -200 mV to 0 mV.
  - Weathering steel 350AT in a salt-free environment with a well-formed patina, and other weathering steel such as ASTM A490 Type 3 bolts with a well-formed patina would be expected to fall into this group as well. This helps to emphasize that the corrosion behaviour of an alloy is not only a total property of the material and its composition but is determined by both material and environment exposure.
- **Group B.** The second group, to the left of Group A, is A1010 steel when crevice corrosion occurs, with E_{corr} being slightly higher than -400 mV. Thus, A1010 steel has two positions in the galvanic series. This phenomenon of having two positions in a galvanic

Figure 34: Galvanic series of bridge alloys of this study



series is commonly known for stainless steels because some steels tend to exhibit localized corrosion, especially in salt-laden environments. This also demonstrates that material in an environment (in terms of its chemistry) could have more than one corrosion behaviour due to the local (micro) conditions on the material surface caused by, for instance, differential aeration corrosion. This also shows that corrosion can be a highly dynamic process, explaining why corrosion current measurements of replicate samples could present with a range of values.

- **Group C.** The third group further left to the on the galvanic series has more negative E_{corr} in a range of -700 mV to -600 mV. It consists of carbon steel (both structural 350W and A325 Type I bolt), polished weathering steel (both structural 350AT and A490 Type 3 bolt), and aluminum. The aluminum alloys cover a wide range in the galvanic series from -700 to – 1000 mV when tested in seawater [7], however, our tests reveal a somewhat narrower range of 700 mV to -600 mV. The difference may come from the solutions.
- **Group D.** The least noble group is from zinc on A325 Type I galvanized bolt as expected, which was lower than -1000 mV. The negative E_{corr} range obtained in this study is consistent with zinc's well-known corrosion potentials. Still, it is important to note that its negative potential is part of the reason for its wide use, and it often serves as a sacrificial anode to protect other alloys through the galvanic corrosion process.

Table 7 presents the corrosion differences obtained between the bridge structural alloys and bolt materials from their corrosion potentials measured in the 1.5 wt% NaCl solution at the end of 48 hours to demonstrate the use of the galvanic series (or two measured potentials) for an estimation of the galvanic tendency.

Polarity: '+" means bolt alloy being the cathode, and '-" means bolt alloy being the anode. Dark grey*: Low tendency of galvanic corrosion by potential. Light grey†: Medium tendency of galvanic corrosion by potential. White‡: High tendency of galvanic corrosion by potential.

For the bridge alloys studied in the 1.5 wt% NaCl solutions (Table 7), three levels of galvanic corrosion tendency can be categorized according to the corrosion potential difference:

- **Low tendency by potential.** These are the galvanic pairs of alloys from the potential Group A (stainless steel) or Group C (weathering steel, carbon steel, and aluminum), presenting corrosion potential differences less than 50 mV, or slightly above 50 mV (i.e., 60 mV between aluminum and A325 Type I carbon steel bolt).
- **High tendency by potential.** Those pairings with corrosion potential differences from 200 mV to about 900 mV. These include: i) galvanized A325 Type I bolt (Group D) paired with the structural alloys in Group A, B, and C, and ii) Group B bolts (carbon steel and weathering steel) paired with the structural alloys in Group A (e.g., carbon steel A325 Type I bolt pairing with A1010 steel).

Table 7: Potential difference in 1.5% of NaCl solution to illustrate corrosion tendency

Bolt Material	Bridge Structural Alloy					
	Weathering Steel	Weathering Steel - Patina	Carbon Steel	A1010 Steel	A1010 Crevice	Aluminum
A325-Type I galvanized steel	-372‡	-850‡	-365‡	-913‡	-611‡	-349‡
A325-Type I carbon steel	17*	-461‡	24*	-524‡	-222‡	40*
A490 Type 3 Weathering steel	37*	-441‡	44*	-504‡	-202‡	60*
B8M SS316	587††	109††	594††	46*	348††	610††
B8SH SS304	517††	39*	524‡	-24*	278††	54††

- **Medium tendency by potential.** This category is made up of the corrosion potential differences from 278 mV to about 610 mV. It includes stainless steel bolts paired with non-stainless structural alloys in Group C. Including high corrosion potential differences as the "High tendency" category, the potentials in the medium tendency category have a different polarity. The positive polarity means that the structural steel is the anode, and the bolt/cathode is protected. This lowers the tendency of galvanic corrosion because the structural steel has a larger surface area in a galvanic coupling with the bolt.

The results represent a valuable tool that not only presents the corrosion potential of each alloy (structural and bolt) to estimate corrosion tendency but also illustrates the relative position and difference of the two alloys to estimate their galvanic corrosion tendency when coupled. Furthermore, it provides a valuable reference to guide the development of new alloys for bridge applications and underscores the importance of considering both mechanical performance and corrosion tendency, including galvanic corrosion, when doing so.

We used the corrosion potential difference to distinguish among the galvanic corrosion tendency of the low, medium, and high categories for the various structural-bolt alloy pairings. In estimating the galvanic process, we determined that the magnitude and the polarity of the corrosion potential difference can determine corrosion tendency level. The polarity determines which alloy functions as the anode. When a bolt becomes the anode in a galvanic corrosion cell, a higher failure risk emerges than when the structural steel assumes such role. Thus, it is recommended to use fastener material (including bolts, washers, and nuts) with a higher corrosion potential than the bridge structural steel. This may exclude galvanized steel bolts, though, as they are often used to take advantage of their sacrificial corrosion properties.

It is also worth noting that the galvanic corrosion tendency estimated by corrosion potential difference is a galvanic corrosion tendency (governed by thermodynamics) while the actual galvanic corrosion damage is controlled by galvanic corrosion current (corrosion kinetics) presented in the next section. This is because a high corrosion tendency does not always lead to a high corrosion rate. For example, the formation of an effective oxide layer (corrosion products) can significantly reduce the corrosion rate, and aluminum alloys are well known for having very negative corrosion potentials but could have a very low corrosion rate (or high corrosion resistance).

5.2 Assessment of Galvanic Corrosion Rate

This section describes the galvanic corrosion coupling currents of the alloy pairs (structural and bolt) and the galvanic corrosion risk in terms of corrosion damage rate, which is presented in Table 8.

As previously discussed, there is no existing knowledge that guides the assessment of the magnitude of galvanic corrosion. We selected two structural steel/bolt pairs, 350W structural carbon steel with two respective bolts materials, A325 Type I carbon steel and A490 weathering steel, as the reference pairs in this study to compare the magnitude of galvanic corrosion of other galvanic couples. In both pairs, the anodes were the samples of 350W structural carbon steel (10 cm^2), demonstrated by the positive polarity of the current. The resulting anodic current densities were 1.2 μA/cm2 and 1.1 μA/cm^2. These galvanic corrosion densities will cause the anode (carbon steel) to lose its steel more rapidly under a general corrosion rate of 19 μA/cm^2. The galvanic current densities of 1.2 μA/cm^2, and 1.1 μA/cm^2, less than 10% of its general corrosion rate prior to galvanic coupling in the same environment, would be considered under the low corrosion category, thus presenting low galvanic corrosion rate.

For the 350AT weathering steel/A325 Type I carbon steel pair, the measured coupling current was 71 μA, and given the negative polarity, the bolt served as the corroding anode with a coupling current density of 71 μA/cm^2. This represents accelerated corrosion for the carbon steel bolt since its corrosion current was 17 μA/cm^2 before connecting with 350AT. Galvanic corrosion accelerated its corrosion rate by more than four times and imparted it with a very high galvanic corrosion rate.

We further analyzed the galvanic corrosion rate (galvanic current density on the anode, μA/cm^2) compared with an anodic alloy's general corrosion

Table 8: Evaluation of galvanic corrosion current density measured in 1.5 wt% NaCl solution

Coupled Structural Alloy/Bolt	Anode (Surface Area)	M: Galvanic Corrosion Rate Galvanic Corrosion Level (based on ISO 9223)	N: Individual Corrosion Rate without Galvanic Coupling (μA/cm²)	Galvanic Corrosion/ Corrosion Ratio (M/N) Galvanic Tendency Level
350W/A325 Type I CS	350W (10cm²)	1.2 μA/cm² Reference: Low	Plate: 19 μA/cm²	0.06 Low
			Bolt: 17 μA/cm²	—
350W/A490	350W (10 cm²)	1.1 μA/cm² Reference: low	Plate: 19 μA/cm²	0.06 Low
			Bolt: 11 μA/cm²	—
350AT/A325 Type I carbon steel	A325 Type I-CS (1 cm²)	71 μA/cm² Very high	Plate: 13 μA/cm²	—
			Bolt: 17 μA/cm²	4.17 Very high
350AT/B8M	350AT (10 cm²)	1.1 μA/cm² low	Plate: 13 μA/cm²	0.08 Low
			Bolt: 0.12 μA/cm²	—
350AT/B8SH	350AT (10 cm²)	1.0 μA/cm² low	Plate: 13 μA/cm²	0.08 Low
			Bolt: 0.17 μA/cm²	—
350AT/A325 Type I Galvanized	A325 Type I-GS (1 cm²)	51 μA/cm² Very high	Plate: 13 μA/cm²	—
			Bolt: 8.5 μA/cm²	6.00 Very high
A1010/B8M	A1010 (10 cm²)	0.01 μA/cm² Negligible	Plate: 3 μA/cm²	0.003 Negligible
			Bolt: 0.12 μA/cm²	—
A1010/B8SH	A1010 (10 cm²)	0.02 μA/cm² Negligible	Plate: 3 μA/cm²	0.006 Negligible
			Bolt: 0.17 μA/cm²	—
A1010/A325 Type I GS	A325 Type I-GS (1 cm²)	End 215 μA/cm² Extreme	Plate: 3 μA/cm²	-
			Bolt: 8.5 μA/cm²	25.29 Extreme
Aluminum/B8M	Aluminum (10 cm²)	1.4 μA/cm² low	Plate: 5 μA/cm²	0.28 Low
			Bolt: 0.12 μA/cm²	—
Aluminum/B8SH	Aluminum (10 cm²)	1.5 μA/cm² low	Plate: 5 μA/cm²	0.30 Low
			Bolt: 0.17 μA/cm²	—

rate observed prior to galvanic coupling. For the two reference pairs, the ratio of the galvanic corrosion rate to the general corrosion rate (Gal/Corr) was found to be 0.06 (Table 9). This is less than 10% of the general corrosion rate that would occur without coupling and is rated as low galvanic risk, consistent with the previous rating of the galvanic corrosion rate by itself. Other pairs were evaluated for both the galvanic corrosion rate and the ratio with the general rate, giving rise to four distinct groups in terms of galvanic corrosion current density:

- **Negligible.** Stainless steel A1010 (the anode) with B8M and B8SH has galvanic corrosion current densities of 0.01 μA/cm², about one order of magnitude lower than the reference pairs. The galvanic corrosion rate is thus negligible in comparison with general corrosion.
The Gal/Corr ratios were less than 0.01, or 1%, indicating a low enough galvanic corrosion risk to be rated as negligible.

- **Low.** When the stainless steel bolts were paired with the structural 350AT weathering steel (the anode) or aluminum (the anode), the galvanic corrosion current densities ranged from 0.2 to 1.5 μA/cm^2, on the same level of low as the reference pairs. The Gal/Corr ratios were all less than 0.5, meaning that the galvanic corrosion rate was lower than half of the general corrosion rate of the anodic alloy. The galvanic corrosion tendency was thus also rated to be low.
- **Very High.** When the structural 350AT weathering steel was paired with the A325 bolts (Type I carbon steel or Type I galvanized steel), the galvanic corrosion current densities ranged from 51 to 71 μA/cm^2, more than one order of magnitude higher than the reference pairs and indicating very high rate in comparison. The Gal/Corr ratios, 4.17 and 6.00, were greater than 2, meaning that the galvanic corrosion rate was more than double the general corrosion rate of the anodic alloy. The galvanic corrosion tendency is thus rated very high.

  The results of these two pairs warrant further examination because the estimated galvanic tendency would be low if only looking at their corrosion potentials (Table 7). Despite their similar corrosion potentials, in chloride-laden environments, they corrode rapidly and exhibit a high corrosion tendency. In such a case, a small polarization can also result in a significant galvanic corrosion current.

  These two pairs clearly illustrate that bridge alloy individual corrosion behaviors/properties need to be characterized, encompassing the alloy properties interacting with their exposure conditions. Such information then should be made available to the bridge community. The data will assist in evaluating a particular corrosion mechanism. More importantly, it will provide bridge engineers with a comprehensive corrosion evaluation of the selected metals and alloys and facilitate general corrosion tendency evaluation.

- **Extreme.** The pair of A1010 steel with the galvanized A325 Type I bolt showcased an extreme case, which confirms a prediction from their large corrosion potential difference. Their galvanic corrosion rates reduced over time, from the initial 783 to 215 μA/cm^2 at the end of the monitoring period, which was more than two orders of magnitude higher than the reference pairs. The Gal/Corr ratio was as high as 25, and the galvanic corrosion tendency was thus also rated to be extreme.

Given this analysis, a large corrosion potential difference could indicate a higher galvanic corrosion tendency, which should lead to further investigation, particularly for critical applications. Conversely, a seemingly minor corrosion potential difference that indicates a lower galvanic corrosion tendency could also lead to a large galvanic corrosion rate depending on the alloy's individual corrosion behavior in the specific environment. In the future, it would be beneficial to establish individual corrosion behaviors/properties of bridge alloys as part of their interactions with exposure conditions.

It bears repeating that the extreme level of galvanic corrosion current found on the galvanized steel bolt signifies high corrosion rate. It is, in fact, this well-known attribute that is exploited, whereby the zinc layer undergoes galvanic corrosion to form a galvanic corrosion cell, protecting metals in contact. Hence, not all galvanic corrosion is "bad." This research is focused on presenting the galvanic corrosion risk in terms of its magnitude, including how to evaluate it.

The above analysis also confirms the need to establish criteria to interpret galvanic corrosion. Provisional galvanic corrosion criteria are presented in Table 9, which are based on both the galvanic corrosion rate (the metal loss rate caused by the current flow from one metal to the other) and the newly introduced Gal/Corr ratio (developed to enable comparison of the galvanic corrosion metal loss rate with the metal loss rate without the galvanic corrosion in the same environment). For example, the Gal/Corr ratio can provide a sense of how "bad" the affected area is compared to the area unaffected by galvanic corrosion that is further away from the metal contact. Note an area unaffected by galvanic corrosion could still undergo a "bad" general corrosion by itself.

This setup of galvanic corrosion criteria was an initial inquiry, and further study is needed to develop comprehensive assessment criteria. More data are required, evident by the criteria categories ("medium"

and "high" tendency), which currently lack example alloy pairs. In addition, longer-term corrosion damage from laboratory and field studies should be obtained to correlate current densities for improvement. Despite this, our experimental design allowed us to observe diverse galvanic corrosion densities, which enabled the development of the preliminary criteria that can serve as the basis for further development and discussion.

5.3 Galvanic Corrosion Assessment Process

Both corrosion potential and corrosion magnitude function were used as a tool for conducting galvanic corrosion assessment by using information of increasing sophistication, as illustrated in Figure 35:

- Step 1: Assess galvanic corrosion risk of the coupled metals and alloys based on the information drawn from engineering experience, literature, or guiding documents, including codes and standards.
- Step 2: Assess galvanic corrosion risk (tendency) based on their corrosion potentials from an existing galvanic series or corrosion potential measurements.
- Step 3: Measure the galvanic corrosion current and assess the magnitude of galvanic corrosion. For critical structures, a general corrosion rate is recommended for a more comprehensive risk assessment using the galvanic corrosion risk criteria (Table 9).

In this process, Step 1 defines the exposure condition, materials, and configuration for a galvanic corrosion scenario in the specific application. The exposure condition should be similar to previously observed conditions to ensure a valid comparison. Step 2 obtains the corrosion potentials and differences to assess the galvanic corrosion tendency. The additional information on individual corrosion performance, e.g., corrosion rates and pitting tendency (Section 4.3), are helpful for further assessment. Step 3 measures and quantitatively assesses the damage rate of galvanic corrosion. This step is highly recommended if galvanic corrosion occurs between an unfamiliar pair of metals and alloys that would be used in a critical bridge component.

This process is further demonstrated by the following analysis of some galvanic corrosion cells obtained under this study that best illustrate the assessing steps. Comparing the two couples of 350AT/A325 carbon steel bolt and 350AT/B8M (Table 10), the analysis is done whereby each step is based on both new information and that derived from the previous step so that understanding of the scenario improves and the basis for decision-making is updated:

- **Step 1.** This step could be done through a literature review.
- **Step 2.** From the galvanic series developed in this study, the corrosion potential differences or their positions are less than 50 mV apart for 350AT/A325 carbon steel and 587 mV for 350AT/B8M. Their potential differences were measured to be -16 mV and 587 mV, respectively. Both would help to deduce easily that 350AT/B8M would have a much greater galvanic tendency without knowing their individual corrosion properties.

Table 9: Galvanic corrosion rate evaluation and criteria.

Gal/Corr ratio	Galvanic corrosion rate/general corrosion rate	Galvanic corrosion
<0.01	Less than 1%	Negligible
0.01 to 0.5	1% to 50%	Low
0.5 to 1	50% to at par	Medium
1 to 2	Up to double	High
2 to 10	Up to 10 times	Very High
> 10	Higher than 10 times	Extreme

*Gal/Corr ratio: ratio of a galvanic corrosion rate to a general corrosion rate.

- **Step 3.** Despite the large galvanic corrosion tendency of 350AT/B8M, the galvanic corrosion rate is negligible (1.1 μA/cm^2). In contrast, despite the minimal potential difference of 350AT/A325 carbon steel, the galvanic corrosion rate on the A325 carbon steel anode is very high, at 71 μA/cm^2.

The procedure's application in the galvanic corrosion assessment of the two pairs clearly tracks the advancing decision process with more sophisticated information input: i) From Step 1, no assessment of their galvanic corrosion risks can be obtained; ii) From Step 2, an evaluation is that 350AT/B8M would have a higher galvanic corrosion risk than 350AT/A325 carbon steel bolt; and iii) From Step 3, the assessment is upgraded to reflect that 350AT/A325 has a much higher galvanic corrosion rate than 350AT/B8M.

The conclusion is that the galvanic corrosion risk is much higher in 350AT/A325 than in 350AT/B8M, opposite to the initial assessment from Step 2. The negligible galvanic corrosion rate of 350AT/B8M can be explained by the fact that the SS316 of B8M remains passive and acts as a poor cathode [80]; the very high galvanic corrosion rate of 350AT/A325 comes from the metals corroding rapidly in the 1.5 wt% NaCl solution where a small amount of polarization may increase the corrosion rate significantly.

For critical load bearing or load transfer components of bridges suspected of galvanic corrosion risk, the proposed three-step procedure in a severe environment is recommended for durability and safety. Equally important is a comprehensive understanding of corrosion for individual bridge alloys. This helps to understand further galvanic corrosion, such as the 350AT/B8M pair, which possesses a significant galvanic corrosion tendency but has a negligible galvanic corrosion rate. Galvanic corrosion co-exists with other forms of corrosion. The study of the B8SH bolt confirms this. When paired with weathering steel, 350AT or A1010, the galvanic corrosion risk is low. Unfortunately, this type of bolt may tend to have pitting corrosion and is therefore not recommended to use on bridges. Thus, its galvanic corrosion may not be a risk, but its corrosion behavior can be a valid risk to avoid. This has demonstrated that in actual practice, the corrosion risk needs to be evaluated comprehensively by considering the corrosion forms relevant to steel and aluminum bridges.

Figure 35: A three-step galvanic corrosion risk assessment process.

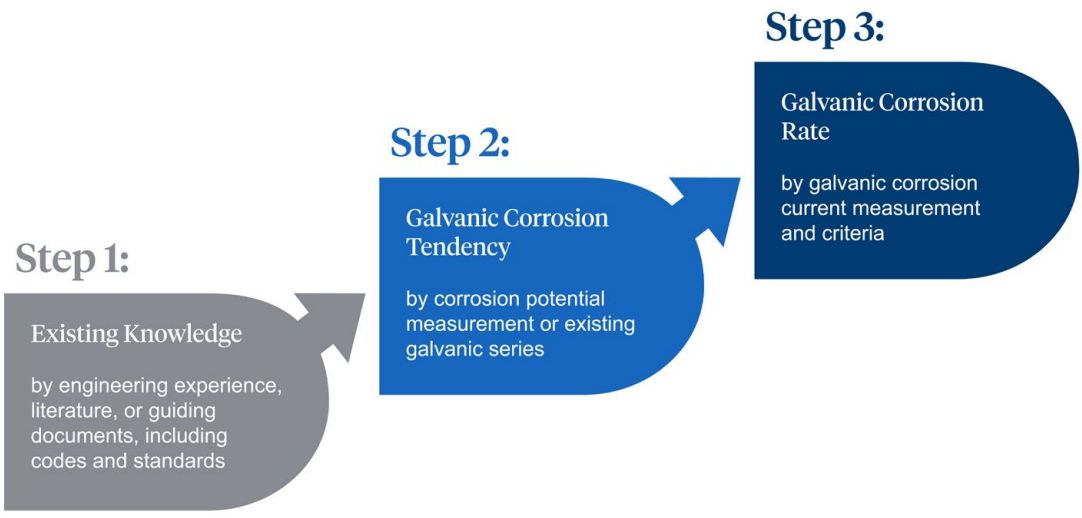


Table 10: A summary of galvanic corrosion of two pairs in 1.5 wt% NaCl solution.

	Galvanic Corrosion	A325 Type I Carbon Steel Bolt	Stainless Steel B8M Bolt
350AT Weathering Steel	Corrosion potential difference	-16 mV	587 mV
	Galvanic current	-0.071 mA	+0.011 mA
	Anode	A325 Type I	350AT
	Anodic current density	71 μA/cm²	1.1 μA/cm²

5.4 Galvanic Corrosion Risk Mitigation

The experimental results from the comprehensive experimental design and analysis have enabled the development of a galvanic series, a set of procedures for galvanic corrosion evaluation, and a set of evaluation criteria for galvanic corrosion assessment, and naturally, they also render an illustration of galvanic corrosion mitigation principles, which are summarized in Table 11.

Countering the first two necessary conditions for galvanic corrosion to occur, both electrical insulation and painting can achieve the electrical isolation and removal of the electrolyte's contact with metals. These approaches are out of the scope of this study. Contending with the third necessary condition, avoiding a corrosion potential different higher than 50 mV can help. This, however, presents a challenge when mixed metals are used routinely in engineering applications, including bridges, and a more feasible solution is to conduct a risk assessment of the candidate metals.

Among the three key factors that control the magnitude of galvanic corrosion, this study has illustrated that using higher corrosion resistant metals, avoiding large cathode/anode surface ratios by not choosing a bolt that would be the anode to bridge structural alloys, and reducing the salt content on bridges can be effective in lowering galvanic corrosion risk.

5.5 Application of This Study

As mentioned earlier, it is well known that corrosion is a material-environmental-specific deterioration mechanism. Galvanic corrosion can be even more complicated because it involves two materials and is environment-assembly-configuration specific. The assembly and configuration directly affect the cathode/anode surface area ratio, which is a key factor in galvanic corrosion. The environment influences the corrosivity of the electrolyte and is another critical factor. While the results from this study can be employed as mitigation strategies, this study's survey of the galvanic risk of specific pairs should not be used in direct applications without considering the actual environment, assembly, and configuration.

This is because the magnitude of galvanic corrosion presented in this study was from salt-laden environments that simulate the corrosive settings where a bridge would develop corrosion that requires protection and prevention. The classification scheme herein effectively compares alloy pair resistance to galvanic corrosion. For example, the galvanic corrosion risk found on the A325 Type I carbon steel bolt coupled with 350AT weathering steel was very high relative to other pairs studied in a chloride-laden environment.

Although this study focuses on galvanic corrosion for bridge structural alloys and bolt materials, the galvanic corrosion risk assessment tool and guide developed here apply to other configurations in bridge applications. For these other configurations, the same process would be followed: i) understand the environment; ii) examine the metal types in contact; and iii) understand the respective surface areas effective for galvanic corrosion.

Table 11: Galvanic corrosion mitigation for bridge applications.

	Corrosion Mechanisms	Mitigation Measures	Example in this study
Necessary Conditions	In electrical contact	Electrical isolation	N/A E.g., insulating oxide films and material insert
	Exposed to the same electrolyte	Removal of electrolyte or electrolyte's contact with metals	N/A E.g., painting
	Corrosion potential difference is more than 50 mV.	Avoiding materials having large corrosion potential differences or evaluating the risk	Risk evaluation by the three-step procedure in Section 4.6
Key Factors	Individual metal corrosion resistance	Use of metal having great corrosion resistance without pitting tendency	Stainless steel 316 B8M bolts have negligible galvanic corrosion risk
	Cathode/anode area ratio	Avoiding bolt being the anode	A325 Type I carbon steel bolt, the anode to a weathering steel bridge, has a high galvanic corrosion risk.
	Corrosivity of electrolyte	Avoid certain material pairs in a de–icing salt environment	Corrosion potential is significantly higher in the weathering steel sample with accelerated patina formation than in the salt solutions in Section 4.1

6 Summary and Future Research Needs

6.1 Summary of Development

Section 2 presented a mechanistic introduction of galvanic corrosion, a review of its study and prevention in various industries, and the current state of practice (via codes, standards and specifications) in bridge durability design. It explained that corrosion potential and galvanic corrosion current measurements are two fundamental methods for conducting galvanic corrosion risk assessment in engineering fields. A galvanic series is a useful guide for choosing metals to couple with a minimal tendency to undergo a galvanic reaction. Beside the potential difference, many factors play a role in the magnitude of galvanic corrosion between two coupled metals, including the surface area, surface condition, solution, and atmospheric environment because they affect the galvanic corrosion kinetics in terms of its corrosion rate. Many of these principles were demonstrated throughout this study and serve as the basis for developing prevention and mitigation strategies.

Section 2 described more explicitly for the first time how galvanic corrosion co-exists with other corrosion forms, implying that a complete understanding of corrosion risk is needed for critical structures and components beyond simply the galvanic corrosion rate. This was further confirmed in the experimental study, particularly by with the B8SH bolt that developed pitting corrosion in a galvanic cell. The bridge community has recognized corrosion as the most common problem for the durability of steel superstructure and steel foundation bridges. Nonetheless, the lack of corrosion-mechanism-specific design guidance hinders adequate protection against various forms of corrosion by addressing their specific mechanisms.

Section 3 described the comprehensive experimental program in which 11 bridge alloys were studied in solutions at three NaCl concentrations from 0.5 wt%, 1.5 wt%, and 3.5 wt%. A combination of several quantitative electrochemical techniques was used to explore the galvanic corrosion cells and individual corrosion behaviours of the alloys. Galvanic corrosion tendency (thermodynamics) and galvanic corrosion magnitude (corrosion kinetics) were measured.



"In bridge applications, if a bolt functions as the anode in the galvanic corrosion cell, the risk can be greater than when the structural steel serves as the anode because of the bolt's much smaller surface area."

Corrosion rate and passive-active behaviors of individual alloys were also measured to deepen the understanding of their galvanic corrosion, followed by the visual inspection of samples tested in a salt-spray chamber for validation.

In Section 4, the corrosion properties of the alloys, in corrosion resistance and corrosion rate, were presented in addition to the corrosion potentials and galvanic current measured on the studied alloys. Despite its negative corrosion potential, which is well known and confirmed in this study, aluminum demonstrated much higher corrosion resistance and low corrosion rate compared to weathering steel or carbon steel because aluminum oxides form on the surface and slow down corrosion progression.

These results led to better understanding the difference between corrosion thermodynamics and kinetics and metal corrosion behaviours.

Through the experimental study (Section 3) and advanced analysis (Section 4), an evaluation tool of a galvanic series, guiding procedure, and set of galvanic corrosion criteria for bridge researchers and engineers were developed with the aim of conducting better assessment of galvanic corrosion tendency.

A galvanic series was developed (Section 5.1) that provides a systematic collection and comparison of corrosion tendencies of bridge alloys for the first time. It is a powerful tool for presenting corrosion potentials in an orderly manner, which facilitates estimating galvanic corrosion tendency between two bridge alloys. This can help establish reference values to guide the development of new alloys for bridge applications and remind designers that both mechanical performance and corrosion, including the galvanic corrosion risk with existing bridge alloys, should be considered.

From the galvanic series, this study further demonstrated a significant corrosion potential difference could be used to predict a higher risk. However, a small difference indicating a lower galvanic corrosion tendency could lead to substantial galvanic corrosion for two metals, both actively corroding. Thus, a further evaluation method was developed using the actual galvanic corrosion current measurement (Section 5.2). In bridge applications, if a bolt functions as the anode in the galvanic corrosion cell, the risk can be greater than when the structural steel serves as the anode because of the bolt's much smaller surface area. Such analysis also called for a set of galvanic corrosion criteria to interpret galvanic corrosion risk for the first time in bridge applications. It was set up by considering both the galvanic corrosion rate and the concept of Gal/Corr ratio, which considers galvanic corrosion rate in the context of a general corrosion rate in the same environment. The corrosion rate and Gal/Corr ratio provided consistent assessment parameters for the alloys studied in this project. Being a preliminary effort, it has put the evaluation of galvanic risk in a new perspective and will hopefully encourage interest, discussion, and future collaboration among the bridge community.

These findings subsequently enabled the development of a procedure for galvanic corrosion assessment (section 5.3). The process consists of three steps that use information of increasing sophistication: 1) use of existing knowledge and experience, including guides, codes, and standards, 2) use of the galvanic series tool or corrosion potential measurements to obtain corrosion potentials, and 3) use of galvanic corrosion current measurements. The application of the guiding procedure has been demonstrated successfully using two examples in which the decision-making process was shown to improve with more information input, and how incomplete use of the process could mislead the conclusion.

6.2 Application and Future Need

This study was designed to apply galvanic corrosion mechanisms and key factors to better understand the galvanic corrosion risk in steel and aluminum bridges. The developed galvanic series of bridge alloys, a set of procedures, and a set of evaluation criteria for galvanic corrosion evaluation can be directly used in bridge applications.

The results of this study can also be employed as a mitigation strategy, for example, by considering how the assembly and configuration affect the cathode/anode surface area ratio and how an environment affects the corrosivity. Among the three key factors that control the magnitude of galvanic corrosion, this study has illustrated that using higher corrosion resistant metals, avoiding large cathode/anode surface ratios by not choosing a bolt that would be the anode to bridge structural alloys, and reducing the salt content on bridges can be effective in lowering galvanic corrosion risk.

It should be noted that galvanic corrosion caused by the galvanized layer of zinc is often used to protect the metals in contact. Hence, not all galvanic corrosion is “bad.” It is also important to mention that although this study presents the galvanic corrosion studied on bridge structural alloys and bolt materials, the galvanic corrosion assessment by the developed tool and guide, and ensuing mitigation strategy, applies to other configurations in bridge applications.

The magnitude of galvanic corrosion presented in this study was from salt-laden environments that simulate the corrosive environments where a bridge would experience corrosion risks that require protection and prevention. It provides an effective comparison of the pairs’ resistance to galvanic corrosion. However, this study has also shown that galvanic corrosion is materials-environment-configuration specific. Therefore, the galvanic risk of specific pairs should not be used in direct applications without considering the actual environment, assembly, and configurations. For example, the galvanic corrosion risk of A325 Type I carbon steel bolt coupled with 350AT weathering steel was very high relative to other pairs studied in the chloride-laden environment. In a chloride-free environment, however, it would be expected to be low. Experimental exploration of galvanic corrosion in absence of chloride needs to be studied in the future.

This study also demonstrated that galvanic corrosion rate is not only governed by the driving force of a corrosion potential difference but also determined by the corrosion performance of the metals. For example, two actively corroding metals (weathering steel and carbon steel bolt) with similar corrosion potentials were found to produce a much higher galvanic corrosion rate than two metals (aluminum and stainless steel bolt) with very different corrosion potentials. Thus, the developed procedure that includes a galvanic corrosion current measurement should be used for critical applications in corrosive environments. It also suggests that each metal's corrosion performance for bridge applications should be better and systematically understood in the same way their mechanical properties typically are for bridge applications.

Going forward, it would be beneficial to include information about individual corrosion behaviors/properties of bridge alloys with the properties of these alloys interacting with their exposure conditions. This will not only assist in evaluating corrosion mechanisms encountered in bridge applications but, more importantly, provide bridge engineers with more complete corrosion information about the alloys they are likely to use. This particularly applies to weathering steel because its corrosion

behaviour in salt-laden environments is not fully understood. Despite such an incomplete picture of its corrosion properties, about half of Canada's steel bridges (many of which are subject to de-icing salts) are constructed with weathering steel.

There is also a need to further develop the risk assessment criteria to interpret galvanic corrosion. This study represents an initial attempt based on existing data, lab analysis of typical bridge specimens, and introducing the new concept of a Gal/Corr ratio. The Gal/Corr ratio considers the galvanic corrosion rate in the context of general corrosion in the same environment, providing a consistent assessment of the alloys studied in this project. Although a preliminary effort, the work described herein puts the evaluation of galvanic risk in a newperspective that will hopefully stimulate discussion, collaboration, and further research.

References

[1] G. Koch, M. Brongers, N. Thompson, Y. Virmani, and J. Payer, "Corrosion cost and preventive strategies in the United States," Federal Highway Administration, Washington, DC, Report No. FHWA-RD-01-156, 2002. Accessed: Oct. 26, 2022. [Online]. Available: https://rosap.ntl.bts.gov/view/dot/39217

[2] G. Jacobson, "NACE International's IMPACT breaks new ground in the study of corrosion management," *Summer Bridge on Issues at the Technology/Policy Interface, The Bridge,* vol. 46, no. 2, Summer 2016. Accessed: Oct 26, 2022. [Online]. Available: https://www.nae.edu/File.aspx?id=155268

[3] Shipilov, S.A. "What Corrosion Costs Canada: Or, Can We Afford to Ignore Corrosion?" in Materials Development and Performance of Sulphur Capture Plants, eds. C. Barry, P. Wanjara, Montreal, Quebec, Canada: Canadian Institute of Mining, Metallurgy, and Petroleum, 2009, pp. 55-76.

[4] BluePlan Engineering, "The Canadian infrastructure report card. Monitoring the state of Canada's core public infrastructure," The Canadian Infrastructure Report Card, Ottawa, ON, 2019. Accessed: Oct 26, 2022. [Online]. Available: http://canadianinfrastructure.ca/downloads/canadian-infrastructure-report-card-2019.pdf

[5] *Canadian highway bridge design code,* CSA S6-19, Canadian Standards Association Group, Toronto, ON, 2019.

[6] F. Mansfeld, "Area relationships in galvanic corrosion," Corrosion vol. 27, no. 10, pp. 436–442, 1971. https://doi.org/10.5006/0010-9312-27.10.436

[7] D.A. Jones, *Principles and Prevention of Corrosion.* New York, NY: Macmillan Publishing Company, 1992.

[8] G. L. Kulak, "High strength bolting for Canadian Engineers," Canadian Institute of Steel Construction, Willowdale, ON, 2005. Accessed: Oct 27, 2022. [Online]. Available: http://kormitpars.com/images/bolt/HighStrengthBolting-canadian_engineers.pdf

[9] H. Uhlig and R. Revie, *Corrosion and Corrosion Control,* 3rd ed. New York, NY: Wiley-Interscience, 1985.

[10] F. LaQue, Marine corrosion: *Causes and prevention.* Malabar, FL: Krieger Publishing Company, 1975.

[11] F. Mansfeld, D. H. Hengtenerg, and J. v Kenkel, "Galvanic corrosion of Al alloys I. Effect of dissimilar metal," Corrosion, vol. 30, no. 10, pp. 343–353, 1974, doi: 10.5006/0010-9312-30.10.343.

[12] F. Mansfeld and J. Kenkel, "Electrochemical measurements of time-of-wetness and atmospheric corrosion rates," *Corrosion,* vol. 33, no. 1, pp. 13–16, 1977, doi: 10.5006/0010-9312-33.1.13.

[13] F. Mansfeld and J. Kenkel, "Galvanic corrosion of Al alloys — II. Effect of solution composition," *Corrosion,* vol. 15, no. 3, pp. 183–198, 1975, doi: 10.1016/S0010-938X(75)80008-4.

[14] E. Ghali and M. Elboujdaini, *Corrosion Prevention and Protection: Practical Solutions.* New York, NY: John Wiley & Sons, 2007.

[15] M. Hagarová, J. Brezinová, G. Baranová, J. Viňáš, and P. Maruschak, "Degradation of components in cars due to bimetallic corrosion," *Materials,* vol. 14, no. 12, 2021, doi: 10.3390/ma14123323. [Online]. Available: https://www.ncbi.nlm.nih.gov/pmc/articles/PMC8235354/pdf/materials-14-03323.pdf

[16] A. Chami, R. Benabbou, M. Taleb, Z. Rais, and M. E. Haji, "Analysis of survey data on corrosion in the automotive industry," *Mater Today Proc,* vol. 45, no. 8, pp. 7636–7642, 2021, doi: 10.1016/j.matpr.2021.03.113.

[17] A. Taub, E. Moor, A. Luo, D. K. Matlock, J. G. Speer, and U. Vaidya, "Materials for automotive lightweighting," *Annu Rev Mater Res,* vol. 49, pp. 327–359, 2019, doi: 10.1146/annurev-matsci-070218-010134.

[18] H. Schreckenberger, M. Papke, and S. Eisenberg, *The magnesium hatchback of the 3-liter car: Processing and corrosion protection,* SAE Transactions, v. 109, pp. 606–612, 2000. Accessed: Oct 26, 2022. [Online] Available: http://www.jstor.org/stable/44643882

[19] C. Nejneru, C. Savin, M. C. Perju, D. D. Burduhos-Nergis, M. Costea, and C. Bejinariu, "Studies on galvanic corrosion of metallic materials in marine medium," *IOP Conf Ser Mater Sci Eng,* vol. 572, p. 012106, 2019, doi: 10.1088/1757-899X/572/1/012106. [Online]. Available: https://iopscience.iop.org/article/10.1088/1757-899X/572/1/012106/pdf

[20] R. Adey, A. Peratta, J. Baynham, and T. Curtin, "Predicting cumulative galvanic corrosion damage in aircraft structures," in *NACE International Corrosion Conference Proceedings,* Houston, TX, 2019, Paper no. 13292, pp. 14.

[21] J. R. Xavier, "Galvanic corrosion of copper/titanium in aircraft structures using a cyclic wet/dry corrosion test in marine environment by EIS and SECM techniques," *SN Appl Sci,* vol. 2, no. 8, pp. 1–10, 2020, doi: 10.1007/s42452-020-3145-x. [Online]. Available: https://link.springer.com/content/pdf/10.1007/s42452-020-3145-x.pdf

[22] J. Skar, "Corrosion and corrosion prevention of magnesium alloys," *Materials and Corrosion,* vol. 50, no. 1, pp. 2–6, 1999, https://doi.org/10.1002/(SICI)1521-4176(199901)50:1<2::AID-MACO2>3.0.CO;2-N.

[23] G. Song, G. Johannesson, S. Hapugoda, and D. StJohn, "Galvanic corrosion of magnesium alloy AZ91D in contact with an Aluminum alloy, steel and zinc," *Corros Sci,* vol. 46, no. 4, pp. 955–977, 2004. https://doi.org/10.1016/S0010-938X(03)00190-2

[24] J. Jia, A. Atrens, G. Song, and T. Muster, "Simulation of galvanic corrosion of magnesium coupled to a steel fastener in NaCl solution," Materials and Corrosion, vol. 56, no. 7, pp. 468–474, 2005. https://doi.org/10.1002/maco.200403855

[25] J. Janiec-Anwar, "Galvanic corrosion of magnesium alloys," (Doctoral Thesis), University of Manchester, Manchester, UK, Manchester, UK, 2014. [Online]. Available: https://www.research.manchester.ac.uk/portal/files/102592751/FULL_TEXT.PDF

[26] P. Kramer, T. Curtin, M. Merrill, M. Kim, F. Friedersdorf, R. Adey., "Atmospheric corrosion measurements to improve understanding of galvanic corrosion of aircraft," in *NACE International Corrosion Conference Proceedings,* Phoenix, AZ, USA, April 15-19, 2018, Paper no. NACE-2018-10968. pp. 11.

[27] J. Jun, Y. C. Lim, Y. Li, C. D. Warren, and Z. Feng, "Mitigation of galvanic corrosion in bolted joint of AZ31B and carbon fiber-reinforced composite using polymer insulation," *Materials, vol*. 14, no. 7, p. 1670, 2021, doi: 10.3390/ma14071670. [Online]. Available: http://dx.doi.org/10.3390/ma14071670

[28] S. S. Wang and G. S. Frankel, "Fundamental study of corrosion-preventive compounds: part III—soft films," *Corrosion Engineering Science and Technology,* vol. 55, no. 6, pp. 497–505, 2020, doi: 10.1080/1478422X.2020.1745356.

[29] J. M. Beigay and D. R. Zaremski, "Aluminum striped stainless trim for prevention of auto body galvanic corrosion," *SAE Transactions,* vol. 81, pp. 1772–1780, 1972, doi: 10.4271/720515. http://www.jstor.org/stable/44722837.

[30] Z. Feng, G. L. Song, Y. Xu, D. Zheng, and X. Chen, "Micro-galvanic corrosion during formation of epoxy coating," *Prog Org Coat,* vol. 147, p. 105799, 2020, doi: 10.1016/j.porgcoat.2020.105799.

[31] U.C. Kumru, S. Erserin, O. Tekelioğlu, and U. Üzel, "The effect of corrosion on the mechanical behavior of the dissimilar material joints (aluminum – steel) using the friction stir spot welding method," *J Mater Electron Devices,* vol. 1, no. 1, pp. 1–6, 2020. [Online]. Available: http://dergi-fytronix.com/index.php/jmed/article/view/54

[32] T. Kosaba, I. Muto, and Y. Sugawara, "Effect of anodizing on galvanic corrosion resistance of Al coupled to Fe or type 430 stainless steel in diluted synthetic seawater," *Corros Sci,* vol. 179, p. 109145, 2021, doi: 10.1016/j.corsci.2020.109145.

[33] A. K. Halder, M. Manna, A. Chakraborty, and A. N. Bhagat, "Analysis of early failure of galvanised borewell pipe," *Eng Fail Anal,* vol. 133, p. 105957, 2022, doi: 10.1016/j.engfailanal.2021.105957.

[34] D. A. Yeshanew, M. G. Jiru, H. G. Lemu, and M. A. Tolcha, "Internal corrosion damage mechanisms of the underground water pipelines," *Advances in Science and Technology Research Journal,* vol. 16, no. 3, pp. 111–123, 2022, doi: 10.12913/22998624/149369. [Online]. Available: http://www.astrj.com/pdf-149369-75647?filename=Internal%20Corrosion%20Damage.pdf

[35] H. Zhang *et al.,* "Review on corrosion and corrosion scale formation upon unlined cast iron pipes in drinking water," *Journal of Environmental Sciences,* vol. 117, pp. 173–189, 2022, doi: 10.1016/j.jes.2022.04.024.

[36] L. Chang, J. H. W. Lee, and Y. S. Fung, "Prediction of lead leaching from galvanic corrosion of lead-containing components in copper pipe drinking water supply systems," *J Hazard Mater,* vol. 436, p. 129169, 2022. [Online]. Available: https://www.sciencedirect.com/science/article/abs/pii/S1001074222001966#preview-section-introduction

[37] L. Chang, J. H. Lee, and Y. S. Fung, "Prediction of lead leaching from galvanic corrosion in drinking water supply systems," *J Hazard Mater,* 2022, doi: 10.2139/ssrn.4034392.

[38] D. Q. Ng, J. K. Lin, and Y. P. Lin, "Lead release in drinking water resulting from galvanic corrosion in three-metal systems consisting of lead, copper and stainless steel," *J Hazard Mater,* vol. 398, p. 122936, 2020, doi: 10.1016/j.jhazmat.2020.122936.

[39] B. Li, B. F. Trueman, M. S. Rahman, and G. A. Gagnon, "Controlling lead release due to uniform and galvanic corrosion — An evaluation of silicate-based inhibitors," *J Hazard Mater,* vol. 407, p. 124707, 2021, doi: 10.1016/j.jhazmat.2020.124707.

[40] M. Wasim and M. B. Djukic, "External corrosion of oil and gas pipelines: A review of failure mechanisms and predictive preventions," *J Nat Gas Sci Eng,* vol. 100, p. 104467, 2022, doi: 10.1016/j.jngse.2022.104467. [Online]. Available: https://www.sciencedirect.com/science/article/abs/pii/S1875510022000580

[41] O. S. I. Fayomi, I. G. Akande, and S. Odigie, "Economic impact of corrosion in oil sectors and prevention: An overview," *J Phys Conf Ser,* vol. 1378, p. 022037, 2019, doi: 10.1088/1742-6596/1378/2/022037. [Online]. Available: https://iopscience.iop.org/article/10.1088/1742-6596/1378/2/022037/pdf

[42] B. Tansel and K. Zhang, "Effects of saltwater intrusion and sea level rise on aging and corrosion rates of iron pipes in water distribution and wastewater collection systems in coastal areas," *J Environ Manage*, vol. 315, p. 115153, 2022, doi: 10.1016/j.jenvman.2022.115153.

[43] D. S. Shahin, W. Khalifa, and L. Z. Mohamed, "Failure analysis of firefighting pipe: Case study," *Journal of Failure Analysis and Prevention*, vol. 22, pp. 1135–1143, 2022, doi: 10.1007/s11668-022-01397-7.

[44] G. D. Song, S. H. Jeon, Y. H. Son, J. G. Kim, and D. H. Hur, "Galvanic effect of magnetite on the corrosion behavior of carbon steel in deaerated alkaline solutions under flowing conditions," *Corros Sci,* vol. 131, pp. 71–80, 2018, doi: 10.1016/j.corsci.2017.10.017.

[45] Q. Sun and M. Dai, "Study on corrosion simulation and anti-corrosion of marine B10 seawater pipe system," in *2nd International Conference on Mechanical, Electronics, and Electrical and Automation Control (METMES 2022),* 2022, vol. December, p. 122441A. doi: 10.1117/12.2634871.

[46] D. A. Shifler, H. P. Hack, and D. Melton, "New techniques for galvanic corrosion in piping systems," in *Proceedings of the Corrosion/ 98 research topical Symposia,* San Diego, CA, USA, Mar. 22-27 1998, Paper number NACE-98706

[47] A. Kolesnikov *et al.,* "Galvanic corrosion of lithium-powder-based electrodes," *Adv Energy Mater,* vol. 10, p. 2000017, 2020, doi: 10.1002/aenm.202000017. [Online]. Available: https://onlinelibrary.wiley.com/doi/epdf/10.1002/aenm.202000017

[48] J. F. Dohmann *et al.*, "Galvanic couples in ionic liquid-based electrolyte systems for lithium metal batteries—An overlooked cause of galvanic corrosion?," *Adv Energy Mater,* vol. 11, no. 24, p. 2101021, 2021, doi: 10.1002/aenm.202101021. [Online]. Available: https://onlinelibrary.wiley.com/doi/epdf/10.1002/aenm.202101021

[49] B. Tan, L. Guo, D. Yin, T. Ma, S. Zhang, and C. Wang, "Environmentally sustainable corrosion inhibitors used for electronics industry," in *Environmentally Sustainable Corrosion Inhibitors,* Amsterdam, Netherlands: Elsevier Inc., 2022, pp. 359–381. doi: 10.1016/B978-0-323-85405-4.00007-0.

[50] C. D. Reis Barros, J. C. Rocha, B. F. Braz, R. E. Santelli, and J. A. Cunha Ponciano Gomes, "Galvanic corrosion of Ti6Al4V coupled with NiCr as a dental implant alloy in fluoride solutions," *Int J Electrochem Sci,* vol. 15, no. 1, pp. 394–411, 2019, doi: 10.20964/2020.01.07. [Online]. Available: http://www.electrochemsci.org/papers/vol15/150100394.pdf

[51] M. Cortada, L. Giner, S. Costa, F. J. Gil, D. Rodriguez, and J. A. Planell, "Galvanic corrosion behavior of titanium implants coupled to dental alloys," *J Mater Sci Mater Med,* vol. 11, pp. 287–293, 2000, doi: 10.1023/A:1008905229522.

[52] N. M. Taher and A. S. A. Jabab, "Galvanic corrosion behavior of implant suprastructure dental alloys," *Dental Materials,* vol. 19, no. 1, pp. 54–59, 2003, doi: 10.1016/S0109-5641(02)00008-8.

[53] M. J. M. Zee, B. C. van Bemmel, and J. J. A. M. van Raay, "Massive osteolysis due to galvanic corrosion after total knee arthroplasty: a rare cause for early revision?," *J Surg Case Rep,* vol. 2020, no. 2, pp. 1–3, 2020, doi: 10.1093/jscr/rjaa002.

[54] H. Serhan, M. Slivka, T. Albert, and S. D. Kwak, "Is galvanic corrosion between titanium alloy and stainless steel spinal implants a clinical concern?," *Spine Journal,* vol. 4, no. 4, pp. P379-387, 2004, doi: 10.1016/j.spinee.2003.12.004.

[55] M. Fontana and N. Greene, *Corrosion Engineering.* New York, NY: McGraw Hill, 1967.

[56] J. Kulicki, Z. Prucz, D. Sorgenfrei, D. Meritz, and W. Young, "Guidelines for Evaluating Corrosion Effects in Existing Steel Bridges". Transportation Research Board, Washington, DC, , Report No. 333, 1990. Accessed: October 26, 2022. [Online]. Available: https://onlinepubs.trb.org/onlinepubs/nchrp/nchrp_rpt_333.pdf

[57] M. A. Grubb, K. E. Wilson, C. D. White, and W. N. Nickas, "Load and resistance factor design (LRFD) for highway bridge superstructures, Reference manual," Federal Highway Administration, Washington, DC, Publication No. FHWA-NHI-15-047, 2015 Accessed: October 26, 2022. [Online]. Available: https://www.fhwa.dot.gov/bridge/pubs/nhi15047.pdf

[58] M. Hebdon and I. Groshek. (2018). Accelerated corrosion testing of ASTM A1010 stainless steel. Presented at World Steel Bridge Symposium. [Online]. Available: https://www.aisc.org/globalassets/nsba/conference-proceedings/2018/2018-wsbs-final-paper---groshek.pdf

[59] J. Zhang and N. Ebrahimi, "Corrosion risk of using stainless steel bolts for A1010 steel bridge girders," *J Bridge Eng,* vol. 26, no. 2, p. 06020001, Feb. 2021, doi: 10.1061/(asce)be.1943-5592.0001659.

[60] J. Zhang, N. Ebrahimi, and D. Lai, "Galvanic corrosion risk of using galvanized A325 bolts in corrosion-resistant steel bridges," *J Bridge Eng,* vol. 24, no. 6, p. 06019001, Jun. 2019, doi: 10.1061/(asce)be.1943-5592.0001395.

[61] I. G. Groshek, "Corrosion behavior of ASTM A1010 stainless steel for applications in bridge components," M. S. Thesis, Civ Eng, Virginia Tech, Blacksburg, VA, 2017. [Online]. Available: https://vtechworks.lib.vt.edu/bitstream/handle/10919/78191/Groshek_IG_T_2017.pdf?sequence=1

[62] Y. Virmani, "Improved corrosion-resistant steel for highway bridge construction knowledge-based design", Federal Highway Administration, Washington, DC, Report No. FHWA HRT-09-053. 2009. Accessed: Oct. 27, 2022. [Online]. Available: https://www.fhwa.dot.gov/publications/research/infrastructure/structures/09053/09053.pdf

[63] *Guide specification for service life design of highway bridges,* American Association of State Highway and Transportation Officials, Washington, D.C., 2020. [Online]. file:///C:/Users/jteague/Downloads/HBSLD-1_TableOfContents%20(3).pdf

[64] *Commentary on CSA S6:19, Canadian highway bridge design code,* CSA S6.1:19, Canadian Standards Association, Toronto, ON, 2019.

[65] T. Murphy, J. Kulicki, F. Moon, A-M. Langlois, N. Samtani, *Guide Specification for Service Life Design of Highway Bridges,* National Academies Press, Washington, D.C., 2020. [Online]. Available: https://nap.nationalacademies.org/booksearch.php?record_id=25672&term=publish

[66] R. Kogler, "Steel Bridge Design Handbook: Corrosion Protection of Steel Bridges", Federal Highway Association, Washington, DC, Report No. FHWA-HIF-16-002 - Vol. 19, :2015. Accessed: Oct. 27, 2022. [Online]. Available: https://rosap.ntl.bts.gov/view/dot/42715/dot_42715_DS1.pdf

[67] *Corrosion of metals and alloys - corrosivity of atmospheres - classification, determination and estimation,* ISO 9223:2012, International Organization of Standardization, Geneva, Switzerland, 2012.

[68] D. Ungermann and P. Hatke, "European design guide for the use of weathering steel in bridge construction," European Convention for Constructional Steelwork, Brussels, Belgium, vol. 143, 2021. Accessed: October 26, 2022. [Online]. Available: https://www.steelconstruct.com/wp-content/uploads/ECCS-Design-Guide-Weathering-Steel-Bridges.pdf

[69] *General requirements for rolled or welded structural quality steel / Structural quality steel,* G40.20-13/G40.21-13 (R2018), Canadian Standards Association Group, Toronto, ON, 2013.

[70] *Standard specification for high-strength low-alloy columbium-vanadium structural steel,* ASTM A572/A572M-12, American Society for Testing and Materials International, West Conshohocken, PA, 2012.

[71] *Standard specification for higher-strength martensitic stainless steel plate, sheet, and strip,* ASTM A1010/A1010M-13, American Society for Testing and Materials International, West Conshohocken, PA, 2013 (Reapproved 2018).

[72] *Standard specification for structural steel for bridges,* ASTM A709/A709M-21, American Society for Testing and Materials International, West Conshohocken, PA, 2021.

[73] *Standard specification for aluminum and aluminum-alloy sheet and plate,* ASTM B209/B209M-21A, American Society for Testing and Materials International, West Conshohocken, PA, 2021.

[74] *Standard specification for high strength structural bolts and assemblies, steel and alloy steel, heat treated, inch dimensions 120 ksi and 150 ksi minimum tensile strength, and metric dimensions 830 MPa and 1040 MPa minimum tensile strength,* ASTM F3125/F3125M-22, American Society for Testing and Materials International, West Conshohocken, PA, 2022.

[75] *Standard specification for alloy-steel and stainless steel bolting for low-temperature service,* ASTM A320/A320M-22, American Society for Testing and Materials International, West Conshohocken, PA, 2022.

[76] *Standard specification for carbon steel, alloy steel, and stainless steel nuts for bolts for high pressure or high temperature service, or both,* ASTM A194/A194M-22, American Society for Testing and Materials International, West Conshohocken, PA, 2022.

[77] P. Montoya, T. Marín, A. Echavarría, and J. A. Calderón, "Influence of anion and pH on the electrochemical co-deposition and transformation of iron oxy hydroxide," *Int. J. Electrochem. Sci.,* vol. 8, No. 12, pp. 12566–12579, 2013. [Online]. Available: http://www.electrochemsci.org/papers/vol8/81212566.pdf

[78] *Standard guide for conducting and evaluating galvanic corrosion tests in electrolytes,* ASTM G71-81, American Society for Testing and Materials International, West Conshohocken, PA, 1981 (Reapproved 2019).

[79] *Standard practice for cyclic salt fog/UV exposure of painted metal, (alternating exposures in a for/dry cabinet and a UV/condensation cabinet),* ASTM D5894-21, American Society for Testing and Materials International, West Conshohocken, PA, 2021.

[80] S. Qian and J. Zhang, "Theoretical and experimental study of microcell and macrocell corrosion in patch repair," *Cem Concr Compos,* vol. 28, pp. 685–695, 2006. https://doi.org/10.1016/j.cemconcomp.2006.05.010

Appendix A – Corrosion Damage Forms

The mitigation of corrosion should start by identifying corrosion damage forms as they may derive from distinctive environmental exposures, metal arrangements, and corrosion mechanisms. Since uniform corrosion or general corrosion is the most commonly visible corrosion damage in terms of rusting and tarnishing, coating the whole metal surface becomes one of the most common protection methods. However, corrosion damage comes in many forms which can result in cracking failures or loss of strength or ductility [9]. Coating may not be the most cost-effective approach for all forms of corrosion in the long service of bridges (75 years or longer).

Among many corrosion damage forms that have been identified with time and advances in corrosion engineering, the widest acceptance of corrosion damage categories can found in Fontana and Green's classic corrosion engineering textbook [55] which includes eight major groups: uniform/general corrosion, galvanic/bimetallic corrosion, pitting corrosion, crevice corrosion, intergranular corrosion (welding), selective leaching/parting, erosion corrosion, and stress corrosion (e.g., hydrogen stress cracking). Fontana and Green [55] had a preliminary assessment of corrosion mechanisms in terms of bridge applications. At least four of the eight corrosion damage forms are associated with bridge corrosion: uniform/general corrosion, crevice corrosion, galvanic corrosion, and pitting corrosion. A less obvious corrosion form can also occur in bridges with severe consequences: stress corrosion cracking.

Table A-1: Corrosion damage mechanism and association to bridge applications [55]

Corrosion Damage Form	Mechanisms/Damage	Related to Bridge Corrosion
Uniform Attack	Metal loss	Thickness loss to cross-section reduction that decreases load capacity
Galvanic Corrosion	Corrosion of the less corrosion-resistant metal is usually increased, and attack of the more resistant material is decreased.	Prevalent to bridge components and systems when different metals are in electrical contact, such as steel girders and fasteners, and different type of rebar in concrete.
Crevice Corrosion	This attack is usually associated with small volumes of stagnant solution caused by holes, gasket surfaces, lap joints, surface deposits, and crevices under bolt and rivet heads.	At small gaps and openings from differences in thickness, alignment, unsealed portion, such as the edge of overlapping of metal sheets; under bolts and rivet heads; or under physically damaged paint or any defects on the paint film.
Pitting	Pitting is one of the most destructive and insidious forms of corrosion. It causes equipment to fail because of perforation with only a small percent weight loss of the entire structure. It is often difficult to detect pits because of their small size and because the pits are usually covered with corrosion products. In addition, it isn't easy to measure quantitatively and compare the extent of pitting because of the varying depths and numbers of pits that may occur under identical conditions. Pitting is also difficult to predict by laboratory tests.	Steel cable; prestressing tendons; under deposit from bird nests and excrement. The damage could be catastrophic, but systematic field data and reports are not found. Further study is needed.

Intergranular Corrosion	Impurities can cause intergranular corrosion at the grain boundaries, enrichment of one of the alloying elements, or depletion of one of these elements in the grain-boundary areas. Small amounts of iron in aluminum, wherein the solubility of iron is low, have been shown to segregate in the grain boundaries and cause intergranular corrosion. It has been demonstrated that based on surface tension considerations, the zinc content of brass is higher at the grain boundaries. Depleting chromium in the grain-boundary regions results in intergranular corrosion of stainless steel.	
Selective Leaching	Selective leaching is the removal of one element from a solid alloy by corrosion processes.	
Erosion Corrosion	Erosion corrosion is characterized in appearance by grooves, gullies, waves, rounded holes, and valleys and usually exhibits a directional pattern. In many cases, failures because of erosion-corrosion occur relatively quickly. They are mainly unexpected because evaluation corrosion tests were run under static conditions or because the erosion effects were not considered.	Erosion corrosion could happen in steel piling when the flowing stream carries particulate matter.
Stress-corrosion Cracking	This cracking phenomenon has serious consequences since it can occur at stresses within the range of typical design stress.	It requires the presence of a high-stress level relative to the yield strength and could happen to deteriorated prestressing tendons. Further study is needed.

Appendix B – OCP Graphs in Various Salt Concentrations

Results of OCP measurements in various NaCl concentrations of 0.5, 1.5 and 3.5 wt.% for different alloy samples are presented.

B.1 0.5 wt% NaCl solution

Figure 36: OCP vs. time of 350W in 0.5 wt% NaCl solution; square, circle and triangle symbols are replicates 1, 2 and 3, respectively.

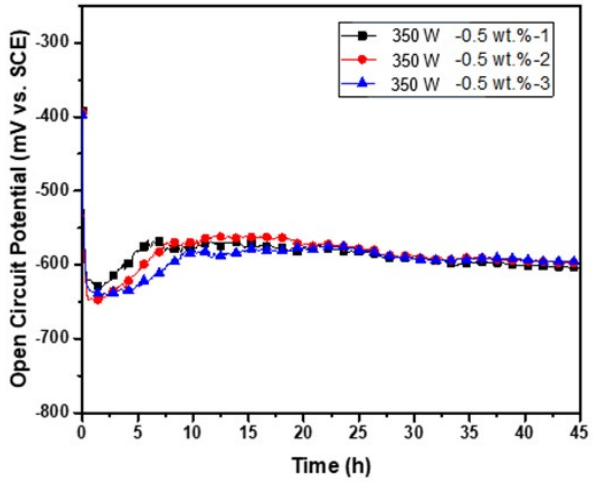


Figure 37: OCP vs. time of weathering steel (350AT) in 0.5 wt% NaCl solution; square, circle and triangle symbols are replicates 1, 2 and 3, respectively.

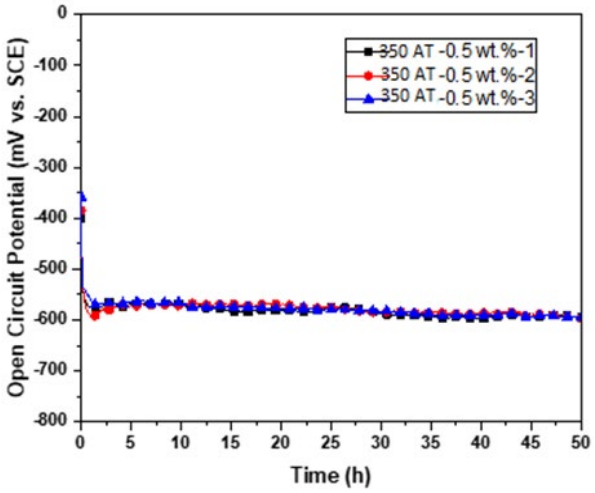


Figure 38: OCP vs. time of A1010 in 0.5 wt% NaCl solution square, circle and triangle symbols are replicates 1, 2 and 3, respectively.

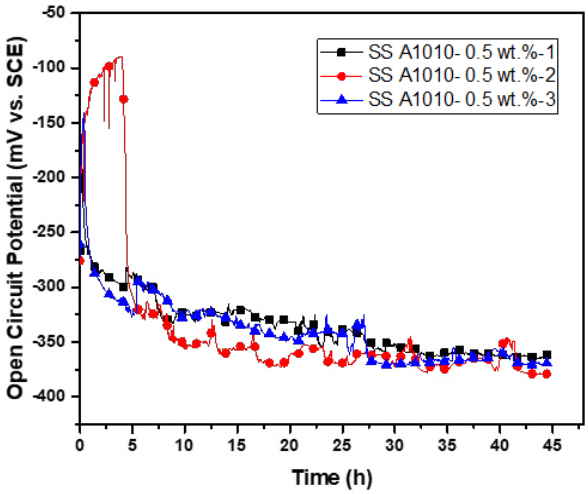


Figure 39: OCP vs. time of aluminum (Al) in 0.5 wt% NaCl solution; square, circle and triangle symbols are replicates 1, 2 and 3, respectively.

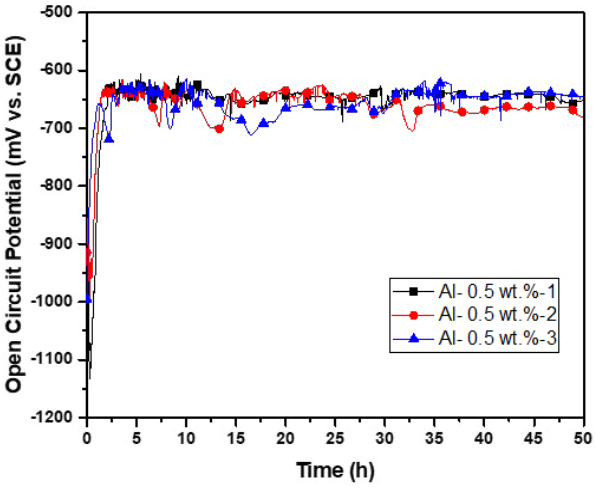


Figure 40: OCP vs. time of A325 Type I carbon steel (CS) in 0.5 wt% NaCl solution; square, circle and triangle symbols are replicates 1, 2 and 3, respectively.

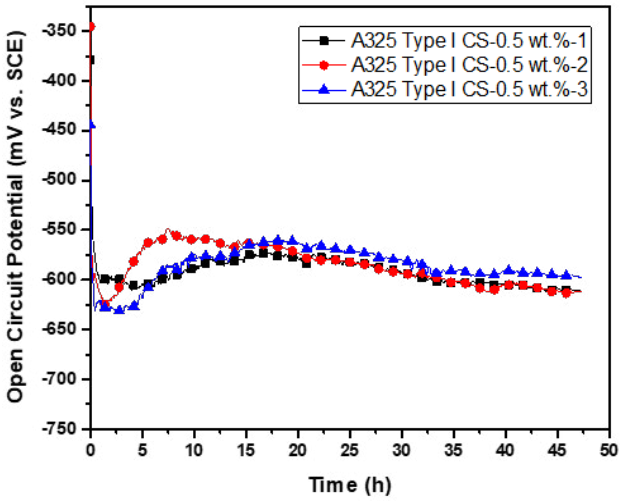


Figure 41: Potential vs. time of A325 Type I galvanized bolt in 0.5 wt% NaCl solution square, circle and triangle symbols are replicates 1, 2 and 3, respectively.

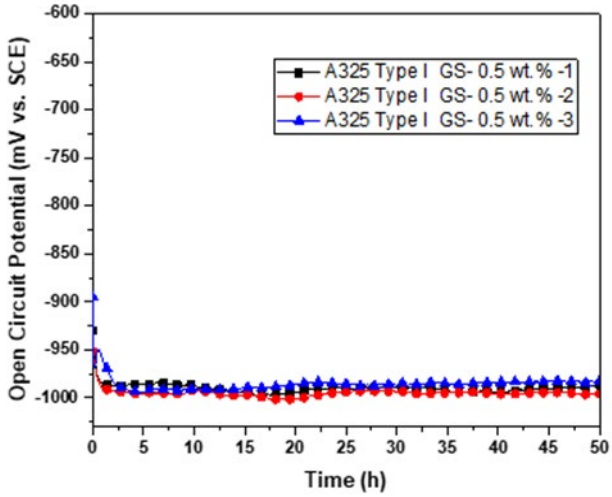


Figure 42: Potential vs. time of A490 in 0.5 wt% NaCl solution; square, circle and triangle symbols are replicates 1, 2 and 3, respectively.

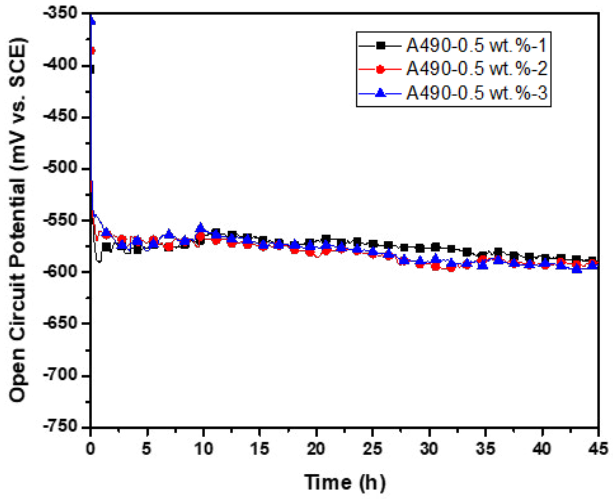
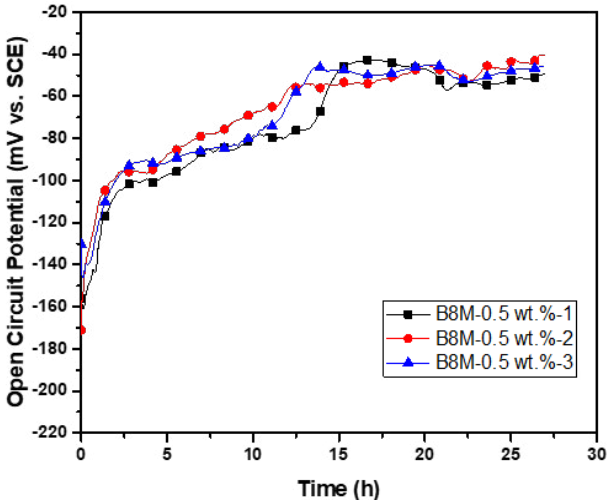


Figure 43: Potential vs. time of B8M in 0.5 wt% NaCl solution; square, circle and triangle symbols are replicates 1, 2 and 3, respectively.



B.2 1.5 wt% NaCl solution

Figure 44: Potential vs. time of B8SH in 0.5 wt% NaCl solution; square, circle and triangle symbols are replicates 1, 2 and 3, respectively.

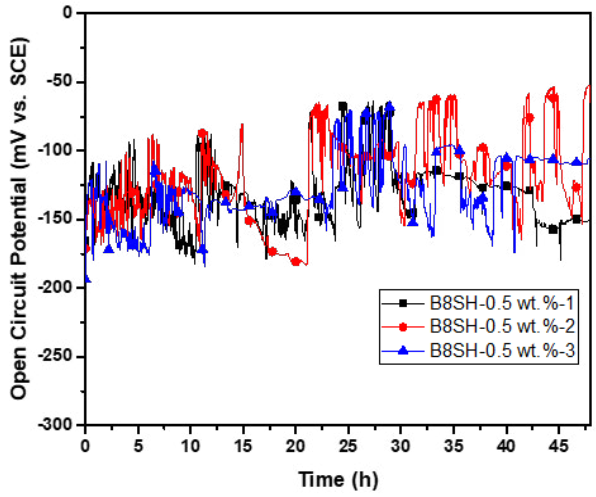


Figure 45: OCP vs. time of 350W in 1.5 wt% NaCl solution; square, circle and triangle symbols are replicates 1, 2 and 3, respectively.

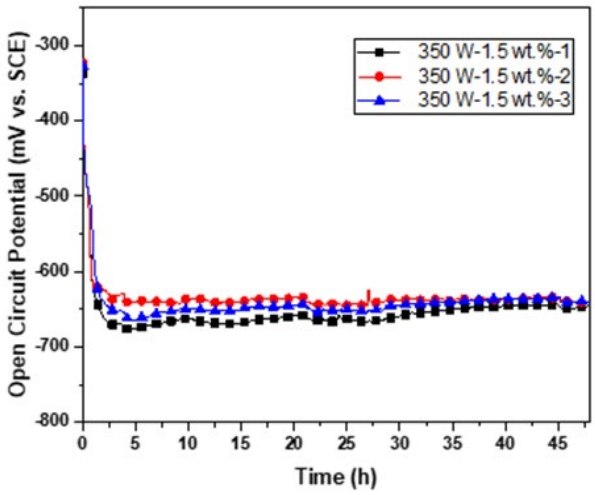


Figure 46: OCP vs. time of weathering steel 350AT in 1.5 wt% NaCl solution; square, circle and triangle symbols are replicates 1, 2 and 3, respectively.

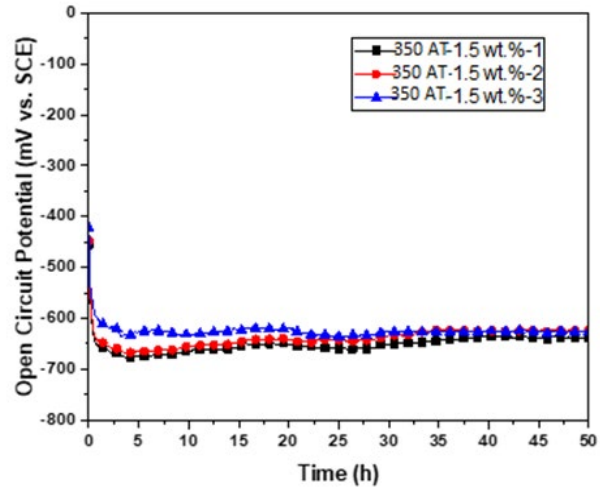


Figure 47: OCP vs. time of A1010 in 1.5 wt% NaCl solution; square, circle and triangle symbols are replicates 1, 2 and 3, respectively.

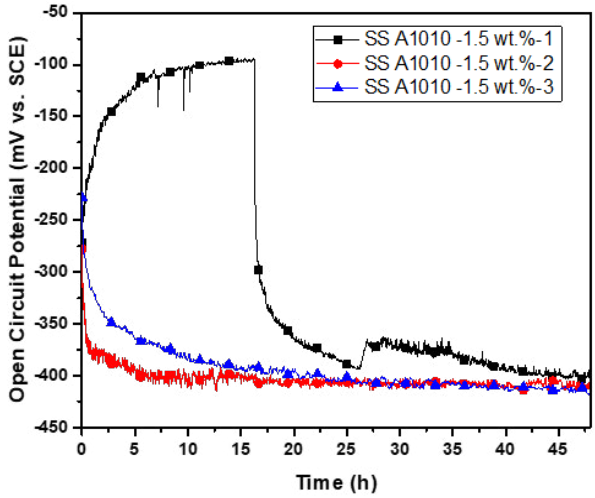


Figure 48: OCP vs. time of aluminum (Al) in 1.5 wt% NaCl solution; square, circle and triangle symbols are replicates 1, 2 and 3, respectively.

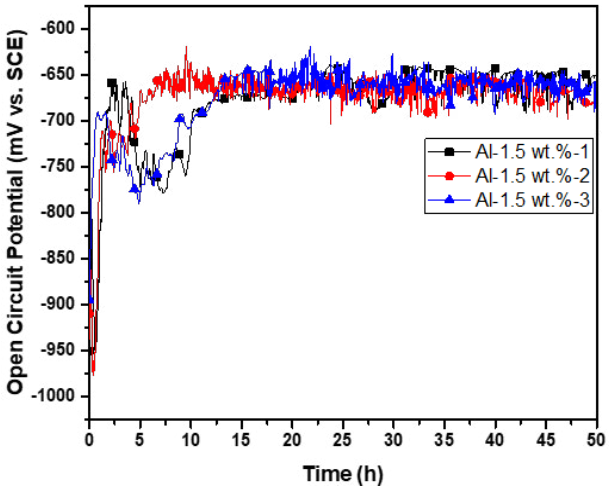


Figure 49: OCP vs. time of A325 Type I carbon steel (CS) in 1.5 wt% NaCl solution; square, circle and triangle symbols are replicates 1, 2 and 3, respectively.

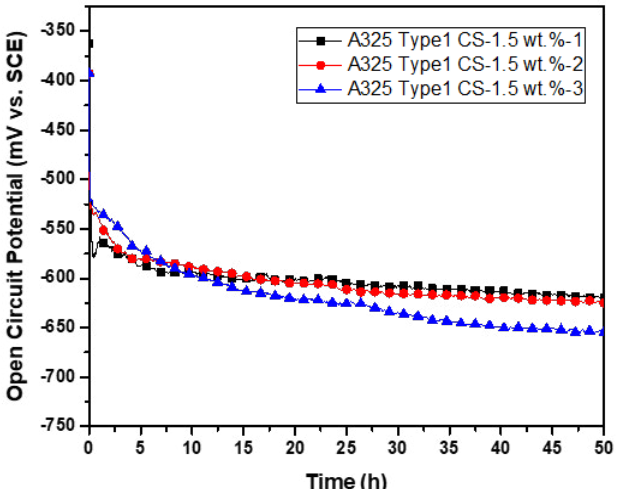


Figure 50: OCP vs. time of A325 Type I galvanized bolt in 1.5 wt% NaCl solution; square, circle and triangle symbols are replicates 1, 2 and 3, respectively.

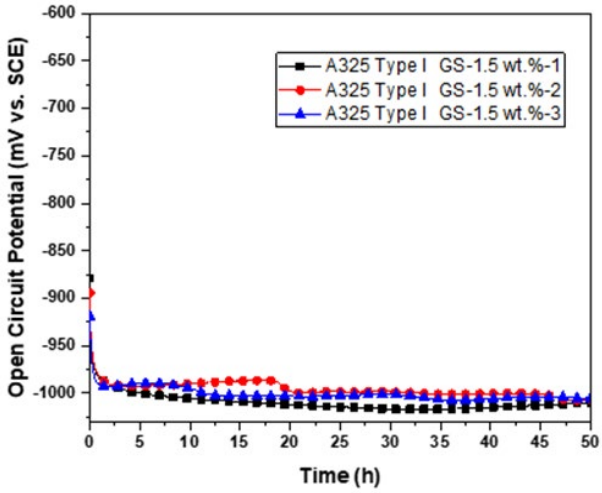


Figure 51: OCP vs. time of A490 in 1.5 wt% NaCl solution; square, circle and triangle symbols are replicates 1, 2 and 3, respectively.

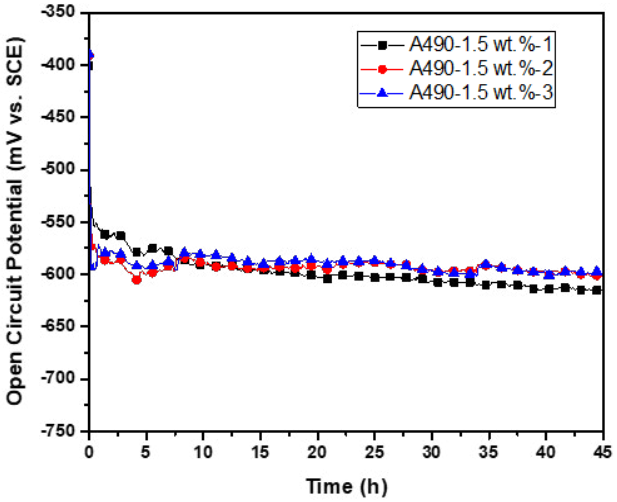


Figure 52: OCP vs. time of B8M in 1.5 wt% NaCl solution; square, circle and triangle symbols are replicates 1, 2 and 3, respectively.

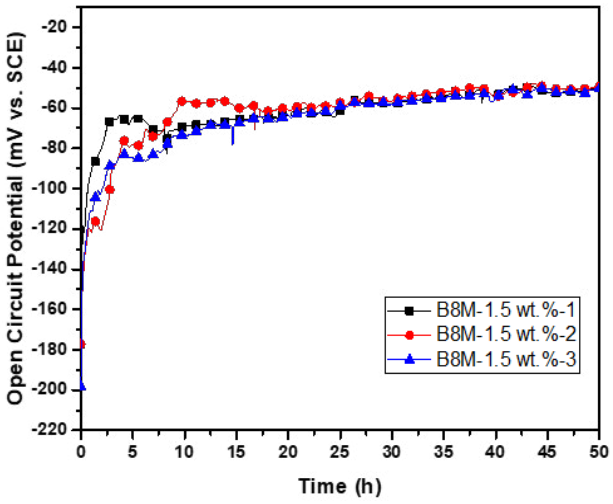


Figure 53: Potential vs, Time of SS316L washer in 1.5 wt% NaCl solution; square, circle and triangle symbols are replicates 1, 2 and 3, respectively.

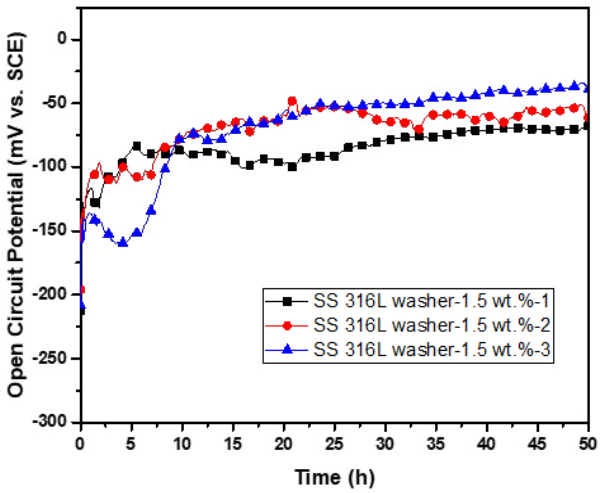


Figure 54: Potential vs. time of SS410 washer in 1.5 wt% NaCl solution; square, circle and triangle symbols are replicates 1, 2 and 3, respectively.

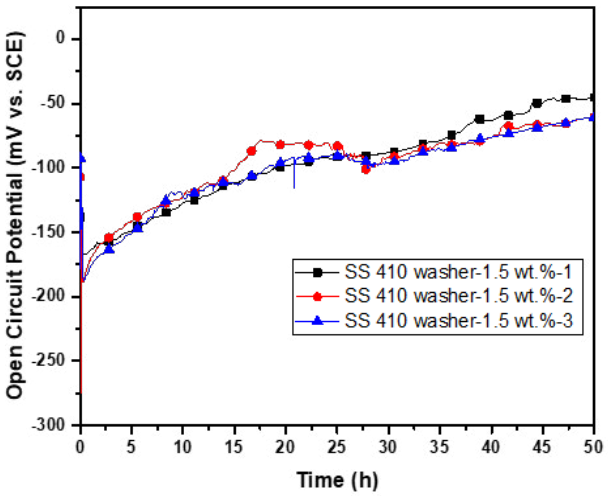
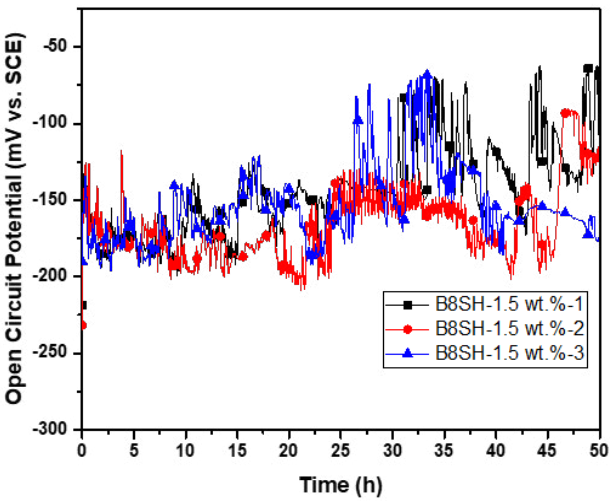


Figure 55: Potential vs. time of B8SH in 1.5 wt% NaCl solution; square, circle and triangle symbols are replicates 1, 2 and 3, respectively.



B.3 3.5 wt% NaCl solution

Figure 56: OCP vs. time of 350W in 3.5 wt% NaCl solution; square, circle and triangle symbols are replicates 1, 2 and 3, respectively.

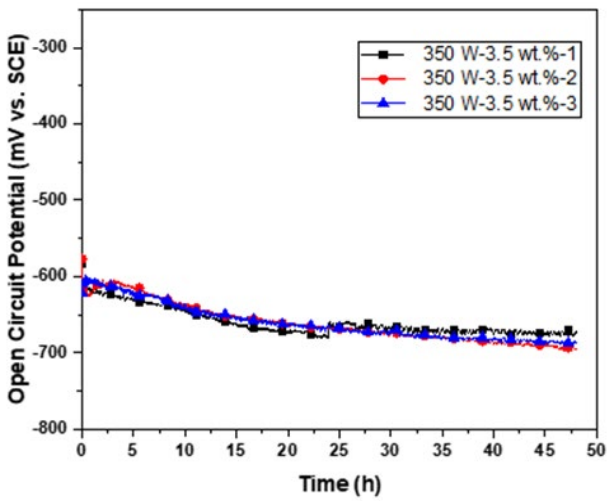


Figure 57: OCP vs. time of weathering steel in 3.5 wt% NaCl solution; square and circle symbols are replicates 1, 2 respectively.

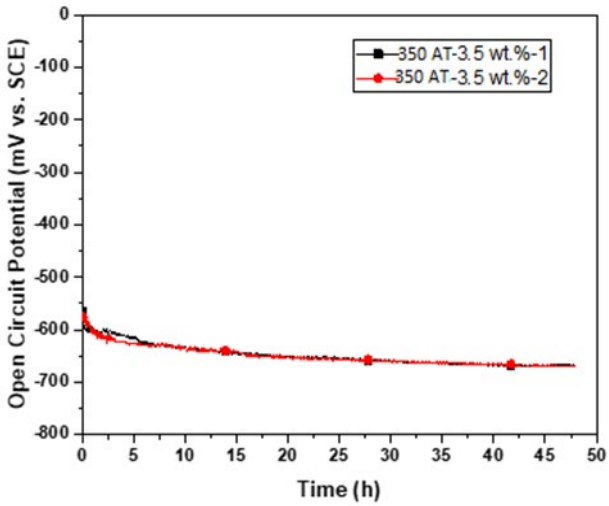


Figure 58: OCP vs. time of A1010 in 3.5 wt% NaCl solution; square and circle symbols are presenting creviced and passive potentials respectively.

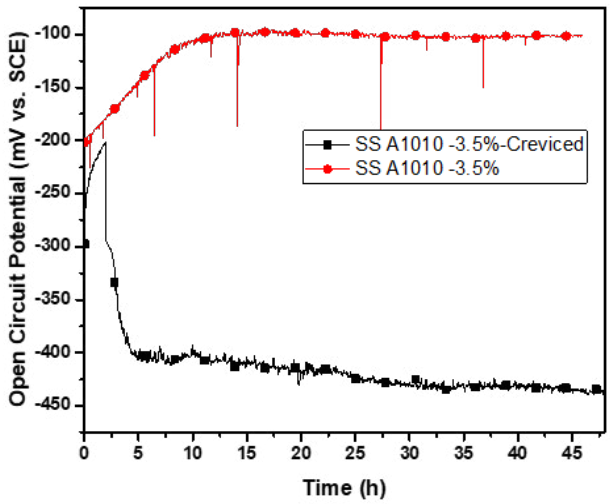


Figure 59: OCP vs. time of aluminum (Al) in 3.5 wt% NaCl solution; square and circle symbols are replicates 1, 2 respectively.

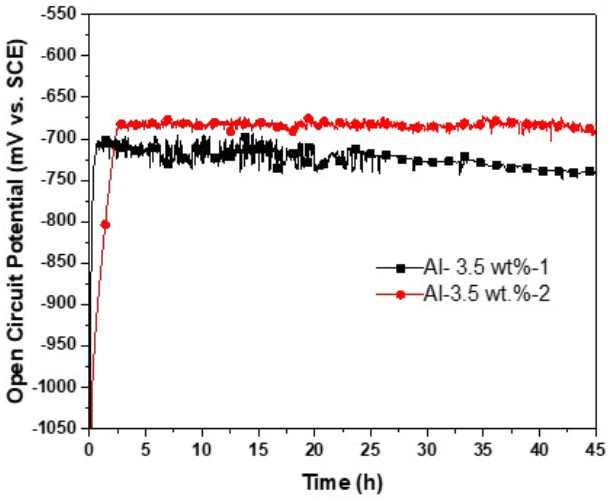


Figure 60: OCP vs. time of A325 Type I carbon steel in 3.5 wt% NaCl solution; square and circle symbols are replicates 1, 2 respectively.

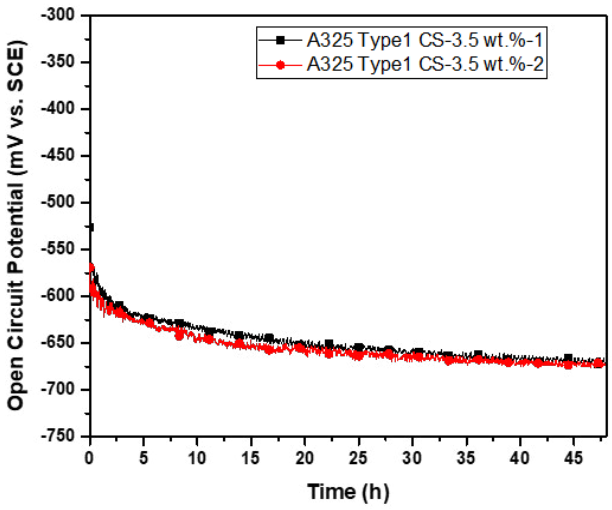


Figure 61: OCP vs. time of A325 Type I galvanized bolt in 3.5 wt% NaCl solution; square and circle symbols are replicates 1, 2 respectively.

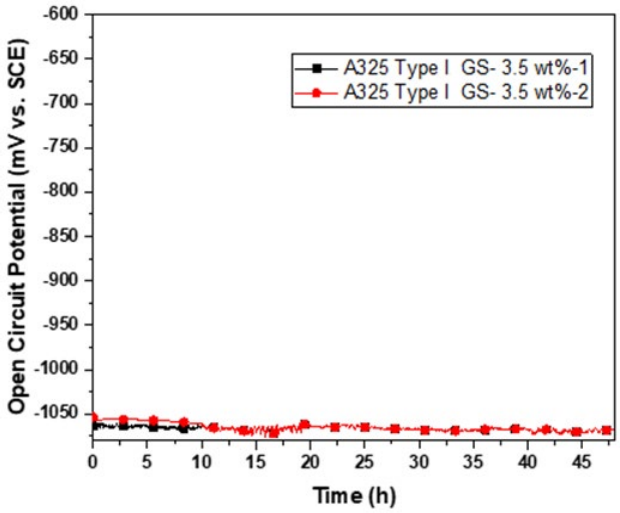


Figure 62: OCP vs. time of A490 in 3.5 wt% NaCl solution; square and circle symbols are replicates 1, 2 respectively.

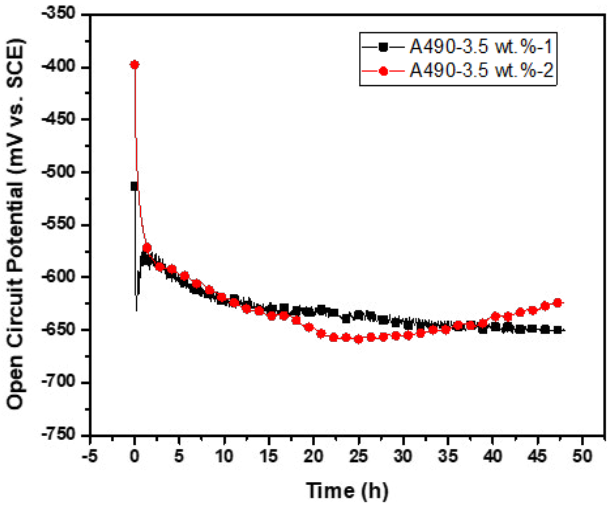


Figure 63: OCP vs. time of B8M in 3.5 wt% NaCl solution red; square and circle symbols are replicates 1, 2 respectively.

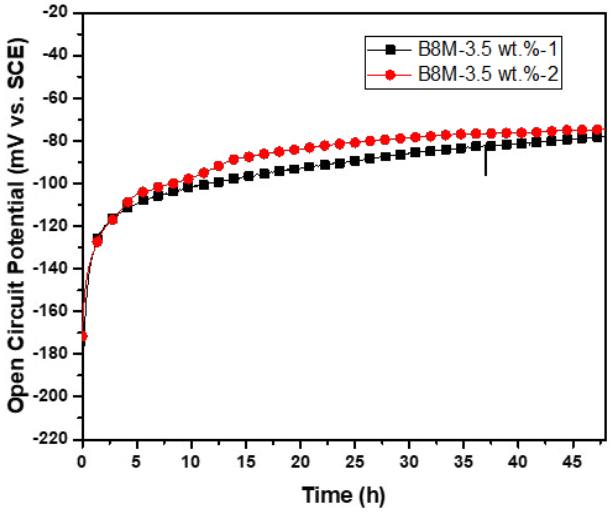
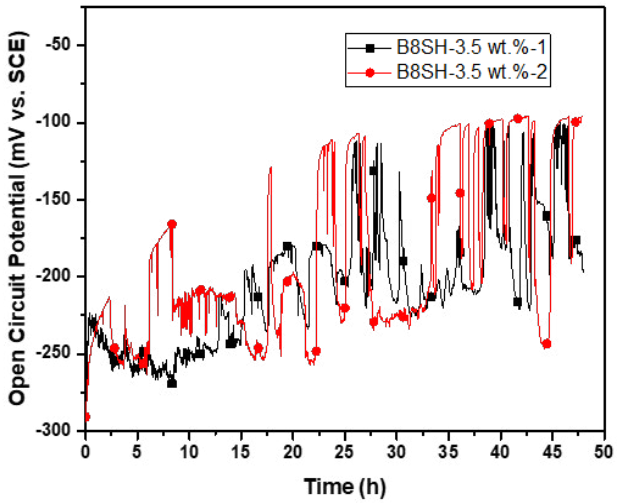


Figure 64: OCP vs. time of B8SH in 3.5 wt% NaCl solution; square and circle symbols are replicates 1, 2 respectively.



Appendix C – C PDP Graphs in 1.5 wt.% NaCl solution

Figure 65: Polarization curves in 1.5 wt% NaCl for 350AT (square), A325 type 1 carbon steel (red triangle), B8M (diamond), B8SH (star), galvanized steel (circle), and A490 (purple triangle).

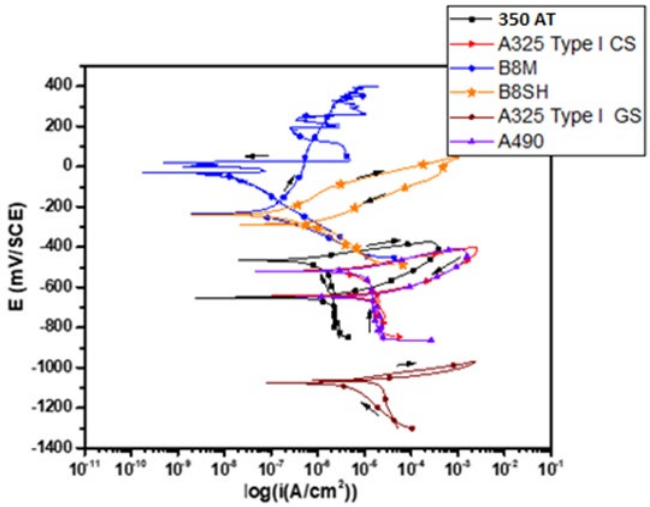


Figure 66: Polarization curves in 1.5 wt% NaCl solution for A1010 (square), B8M (circle), and B8SH (star).

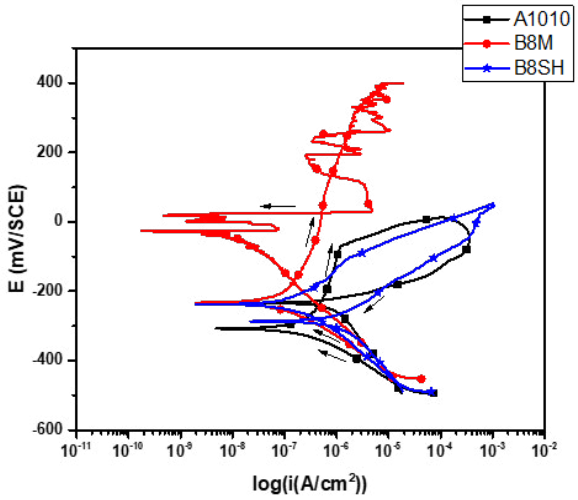
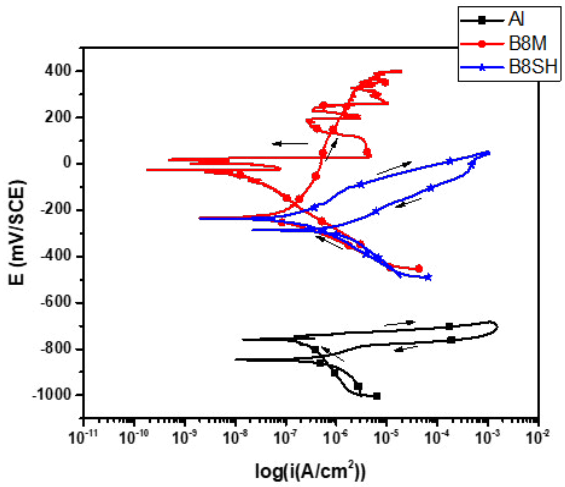


Figure 67: Polarization curves in 1.5 wt% NaCl for Al (square), B8M (circle), and B8SH (star).



CSA Group Research

In order to encourage the use of consensus-based standards solutions to promote safety and encourage innovation, CSA Group supports and conducts research in areas that address new or emerging industries, as well as topics and issues that impact a broad base of current and potential stakeholders. The output of our research programs will support the development of future standards solutions, provide interim guidance to industries on the development and adoption of new technologies, and help to demonstrate our on-going commitment to building a better, safer, more sustainable world.

CSA GROUP™

© 2022 His Majesty the King in Right of Canada, as represented by the National Research Council Canada. All Rights Reserved.